Dissertation

submitted to the

Combined Faculties for the Natural Sciences and for Mathematics

of the Ruperto-Carola University of Heidelberg, Germany

for the degree of

Doctor of Natural Sciences

presented by

Dipl.-Ing. (FH) für Biotechnologie Markus Johann Stemp

born in Freyung

Oral-examination: 19. November 2007

Analysis of Chaperone Function in Multi-domain Protein Folding

Referees: Prof. Dr. Felix Wieland

Prof. Dr. F. Ulrich Hartl

Most of the work was published in:

Agashe, V.R., Guha, S., Chang, H.C., Genevaux, P., Hayer-Hartl, M., **Stemp, M.**, Georgopoulos, C., Hartl, F.U. and Barral, J.M. (2004) Function of trigger factor and DnaK in multidomain protein folding: increase in yield at the expense of folding speed. *Cell*, **117**, 199-209.

Stemp, M.J., Guha, S., Hartl, F.U. and Barral, J.M. (2005) Efficient production of native actin upon translation in a bacterial lysate supplemented with the eukaryotic chaperonin TRiC. *Biol Chem*, **386**, 753-757.

Die Neugier steht immer an erster Stelle eines Problems,

das gelöst werden will.

Galileo Galilei
(1564-1642)

Danksagung

Die vorliegende Arbeit wurde in der Zeit von Juni 2002 bis Juli 2007 in der Abteilung Zelluläre Biochemie am Max-Planck-Institut für Biochemie in Martinsried angefertigt.

Mein besonderer Dank gilt **Prof. Dr. F. Ulrich Hartl** für die interessante und herausfordernde Themenstellung, die ausgezeichnete Betreuung und die guten wissenschaftlichen Arbeitsbedingungen in seiner Abteilung. Mein Dank gilt auch **Dr. Manajit Hayer-Hartl** für ihre hilfreichen Ratschläge und Anregungen.

Prof. Dr. Felix Wieland danke ich sehr herzlich für die Vertretung dieser Dissertation vor der Ruprecht-Karls-Universität Heidelberg.

Drs. Vishwas Agashe, **José Barral**, **Stephanie Etchells**, **Suranjana Guha** und **Katja Siegers** danke ich für ihre intensive Betreuung in den jeweiligen Teilprojekten, sowie die stete Diskussionsbereitschaft und die vielen wertvollen Anregungen. Stephanie Etchells und Katja Siegers danke ich außerdem für die sprachliche und inhaltliche Korrektur dieser Arbeit.

Weiterhin danke ich **allen momentanen und ehemaligen Mitarbeitern** der Abteilung Zelluläre Biochemie für die freundschaftliche Atmosphäre und die sehr gute Zusammenarbeit. Insbesondere danke ich **Annette**, **Carola**, **Heidi**, **Leslie**, **Niclas**, **Sarah**, **Sladjana** und **Xiaochun** für die vielen erheiternden Stunden im Laboralltag und die darüber hinaus entstandene Freundschaft. **Andrea**, **Bernd** und **Elisabeth** danke ich für ihre stete Hilfsbereitschaft und die oftmals gewährte Möglichkeit zur „bayrischen Dialektpflege".

Karoline Bopp und **Dr. Roland Wedlich-Söldner** danke ich für ihre Unterstützung bei der Elektronen- bzw. Fluoreszenzmikroskopie.

Ein großes Dankeschön geht auch an die **Freunde vom Gräfelfinger Anger**. Ihnen verdanke ich unzählige kurzweilige Stunden auf dem Rad oder in den Bergen sowie bei verschiedensten Aktivitäten in und um München.

Von ganzem Herzen aber danke ich meiner Familie. Der größte Dank richtet sich dabei an meine **Eltern Maria und Johann Stemp**, die mir immer mit Rat und Tat bei Seite stehen und mich seit Jahren in meiner Ausbildung unterstützen. Meiner **Freundin Katrin** danke ich ganz herzlich für ihr alltägliche Hilfe und Liebe, ohne die mir diese Arbeit sicher um ein Vielfaches schwerer gefallen wäre.

Table of Contents

I Zusammenfassung

Proteine sind die zentralen Bausteine des Lebens. Um ihre Funktion erfüllen zu können, ist es von entscheidender Bedeutung, dass neu synthetisierte Polypeptidketten innerhalb kurzer Zeit in ihre einzigartige dreidimensionale Struktur falten. Obwohl die zur korrekten Faltung benötigte Information in der linearen Abfolge der Aminosäuren eines Proteins enthalten ist, benötigen Proteine zur Faltung unter zellulären Bedingungen die Unterstützung von so genannten „Helferproteinen“, bekannt als molekulare Chaperone. Diese Gruppe von Proteinen hat die Eigenschaft, dass sie an neu synthetisierte nicht-native Proteine bindet und dadurch unproduktive Nebenreaktionen verhindert, die andernfalls zu Fehlfaltung oder Aggregation führen würden. Bei der *de novo* Faltung von Proteinen im Zytosol sind vorrangig zwei Klassen von Chaperonen beteiligt: die Hsp70-artigen Chaperone und die Chaperonine. Die Hsp70-artigen Chaperone stabilisieren in erster Linie die naszenten Ketten bis eine komplette, zur Faltung fähige, Domäne am Ribosom synthetisiert wurde. Die tonnenförmigen Chaperonine hingegen stellen physikalisch definierte Faltungskompartimente bereit, in denen Proteine oder Proteindomänen, abgeschirmt von den aggregationsfördernden Bedingungen des Zytosols, falten können. Die Faltung von eukaryontischen Proteinen, die im Durchschnitt komplexer aufgebaut sind als ihre prokaryontischen Vertreter, verläuft in bakteriellen Expressionssystemen häufig ineffizient. Dieses Phänomen stellte in der Vergangenheit eine generelle Limitierung bei der Herstellung rekombinanter Proteine dar.

In dieser Arbeit wurden mehrdomänige eukaryontische Proteine in zellfreien Translationssystemen synthetisiert, um den Einfluss einzelner Chaperone auf deren *de novo* Faltung zu untersuchen: Im Falle des eukaryontischen Enzyms Luziferase konnte gezeigt werden, dass dessen Faltung bei der Expression in einem Chaperon-dezimierten *Escherichia coli*-Lysat schnell und eng gekoppelt an die Translation erfolgt. Die Ausbeute an richtig gefaltetem Protein war allerdings sehr gering. Im Gegensatz dazu führte die Zugabe von

gereinigtem Triggerfaktor und DnaK/DnaJ/GrpE zum Lysat zu einer Ausbeutesteigerung an nativem Protein, wobei gleichzeitig die Faltung von Luziferase in Relation zur Translation erheblich verzögert wurde. Während das mehrdomänige bakterielle Protein β-Galaktosidase die endogene Chaperonmaschinerie optimal zu dessen Faltung nutzen kann (Agashe et al., 2004), ist die ansonsten im eukaryontischen Zytosol beobachtete und sehr effektive co-translationale Domänenfaltung von Luziferase nicht mit dem prokaryontischen Chaperonsystem kompatibel. Das lässt darauf schließen, dass bei der Kopplung von Translation und Proteinfaltung in pro- und eukaryontischen Zellen grundlegende Unterschiede bestehen.

Des Weiteren wurde das bakterielle Lysat, welches keine eukaryontischen Chaperone enthält, zur Bestimmung der Mindestanforderungen für die Faltung von neu synthetisiertem Aktin verwendet. Die *in vitro* Translation von Aktin in Anwesenheit verschiedener gereinigter Chaperone zeigte, dass einzig das eukaryontische Chaperonin TRiC für die *de novo* Faltung von Aktin ausreichend und absolut essentiell ist. Die native Konformation, des auf diese Weise produzierten Aktins, wurde durch dessen spezifische Bindung an DNase I und Aktinfilamentbildung nachgewiesen. Interessanter Weise erfolgte im TRiC-angereicherten Lysat die Aktinfaltung wesentlich langsamer als dies im eukaryontischen Zytosol der Fall ist. Lysate, die mit den bakteriellen Chaperonen GroEL/GroES bzw. DanK/DnaJ/GrpE ergänzt wurden, führten zwar zu größtenteils löslichem jedoch fehlgefaltetem Aktin.

Zusätzlich konnte gezeigt werden, dass TRiC durch den partiellen Einschluss von Domänen großer modularer Proteine zu deren domänenweisen Faltung beiträgt. Diese Schlussfolgerung basiert auf der Beobachtung, dass bei der Expression von mehrdomänigen Aktinfusionsproteinen *in vivo* und *in vitro* diese entweder in das Aktin-Zytoskelett von Hefen integrieren bzw. einen stabilen Komplex mit DNase I formen. Der Mechanismus, mit dem TRiC die Faltung von mehrdomänigen Proteinen bewerkstelligt, könnte dabei dem kürzlich veröffentlichten endoproteolytischen Abbau von einzelnen Proteindomänen durch das Proteasom ähnlich sein (Liu et al., 2003).

II Summary

Proteins are the central molecules of life. To become functionally active, newly synthesized polypeptide chains must fold into unique three-dimensional structures on a biologically relevant time scale. Although the information required for correct folding resides in the linear amino acid sequence of a protein, execution of the folding process under cellular conditions is critically dependent on the assistance of "helper proteins" termed molecular chaperones. This group of proteins shares the common function of binding to newly synthesized non-native proteins to prevent off-pathway reactions which otherwise would lead to misfolding and aggregation. Two major classes of chaperones, the Hsp70s and the chaperonins, have been implicated in *de novo* protein folding in the cytosol. While Hsp70s are primarily involved in stabilizing nascent chains until a complete domain has emerged from the ribosome and is competent for folding, the barrel-shaped chaperonins provide physically defined compartments inside which complete proteins or protein domains can fold unimpaired by aggregation. Proteins of eukaryotic origin which, on average, have a more complex architecture than their prokaryotic counterparts, often fold inefficiently upon expression in bacterial hosts. For many decades, this phenomenon placed great limitations on the recombinant production of proteins.

In the present study, eukaryotic multi-domain proteins were synthesized in cell-free translation systems in order to investigate the contribution of individual chaperones to their *de novo* folding: Upon expression under chaperone-depleted conditions in an *Escherichia coli* based lysate, the modular eukaryotic protein firefly luciferase was demonstrated to fold by a rapid default-pathway, tightly coupled to translation. However, only a minor fraction of the translated protein chains folded correctly. In contrast, supplementation of the lysate with purified trigger factor and DnaK/DnaJ/GrpE increased the amount of native protein, but markedly delayed firefly luciferase folding relative to translation. Interestingly, while the bacterial multi-domain protein β-galactosidase uses the endogenous chaperone machinery effectively (Agashe et

al., 2004), the efficient co-translational domain folding of firefly luciferase observed in eukaryotes is not compatible with the prokaryotic chaperone system. Thus, important differences between bacterial and eukaryotic cells seem to exist in the coupling of translation and folding.

Moreover, the bacterial lysate which did not contain any eukaryotic chaperones was further utilized to determine the minimum requirements for the folding of newly synthesized actin. By conducting *in vitro* translation reactions in the presence of purified components, the chaperonin TRiC was found to be the only eukaryotic chaperone absolutely necessary and sufficient for *de novo* actin folding. The actin thus produced bound DNase I and polymerized into filaments, hallmarks of its native state. Lysate supplementation with the bacterial chaperonin GroEL/GroES or the DnaK/DnaJ/GrpE chaperones led to mostly soluble actin, yet failed to facilitate its correct folding. Notably, actin folding in the TRiC-supplemented bacterial lysate occurred with slower kinetics when compared to the eukaryotic cytosol.

Additionally, TRiC was demonstrated to be capable of mediating the domain-wise folding of modular proteins by their partial encapsulation in the chaperonin cavity. This was based on the fact that upon expression of actin multi-domain fusion proteins both *in vivo* and *in vitro*, the proteins properly integrated into yeast cytoskeleton structures as well as formed stable complexes with DNase I. The mechanism of how TRiC might promote the folding of individual protein domains is thereby reminiscent of the domain-wise endoproteolytical degradation of proteins by the proteasome, as reported recently (Liu et al., 2003).

1 Introduction

Proteins are very diverse biomolecules and play crucial roles in virtually all biological processes. They are built from a repertoire of 20 different amino acids which are linked to each other by peptide bonds in order to form chains of various lengths. Proteins constitute the majority of the dry mass of a cell and fulfill a remarkable number of biological functions. Some proteins act as enzymes and are responsible for catalyzing thousands of chemical reactions involved in metabolism. Others provide structural building blocks or serve as transport and storage devices. Proteins are also involved in the control of cell division, differentiation of cells, their coordinated motion and the delivery of information between them.

1.1 From DNA to protein

1.1.1 Protein synthesis and structure

Inside the cell, the information for the synthesis of individual proteins is encoded in genes as part of double-stranded DNA. Prior to synthesis, the gene is transcribed into a linear single-stranded messenger RNA (mRNA), and in the case of eukaryotic cells, exported from the nucleus into the cytosol. There, ribosomes, large ribonucleotide complexes, translate the mRNA into its amino acid sequences in a vectorial manner. The newly synthesized polypeptide chain exits these complexes through the ribosomal exit tunnel and generally adopts its unique three-dimensional structure during and upon release. The process in which the linear sequence of amino acids is converted into a three-dimensional structure is called protein folding.

Amino acids consist of an amino group, a carboxyl group, a hydrogen atom, and a variable side chain, all of which are bonded to the central alpha carbon atom (Cα). Twenty kinds of side chains varying in size, charge, shape, hydrogen-bonding capacity, and chemical reactivity are commonly found in naturally occurring proteins. The α-carboxyl group of one amino acid is joined to

the α-amino group of another amino acid by a peptide-bond, forming a stable linear and unbranched backbone structure (Figure 1). By convention, the amino end is referred to as the beginning of a polypeptide chain.

The structure of proteins is typically described in terms of four hierarchical levels of organization: The linear arrangement of amino acids constituting the polypeptide chain is called the primary structure. The secondary structure refers to the localized organization of parts of a polypeptide chain due to the formation of stabilizing hydrogen bonds between certain residues. As a consequence, the backbone folds periodically into one of two geometric arrangements: an α-helix, which is a spiral rodlike structure, or a β-sheet, a planar structure consisting of alignments of two or more β-strands, which are generally short and fully extended segments of the backbone. The tertiary structure of a protein describes the overall conformation of a polypeptide chain, that is, the three-dimensional arrangement of all the amino acids organized in secondary structural elements. The stability of the tertiary structures is mostly attained by hydrophobic interactions between nonpolar side chains and, in some proteins, disulfide bonds. For proteins consisting of only a single polypeptide chain, tertiary structures are the highest level of organization. The final association of multiple polypeptide chains resulting in an active and functional unit is referred to as quaternary structure, mainly stabilized by all types of noncovalent interactions between the subunits.

1.1.2 The protein folding problem

In order to fulfill their biological functions, proteins have to acquire a specific and unique three-dimensional structure, the so called “native state”. All the information necessary to reach this energetically favored and most stable folded conformation of a protein is contained in its amino acid sequence, as shown by pioneering experiments of Christian Anfinsen (Anfinsen, 1973). He demonstrated that correct refolding of fully denatured ribonuclease into its native and enzymatically active conformation occurs spontaneously and without any further assistance in free solution. Even more striking was the observation

that this refolding process can take place on a biologically relevant time scale (Schechter et al., 1970).

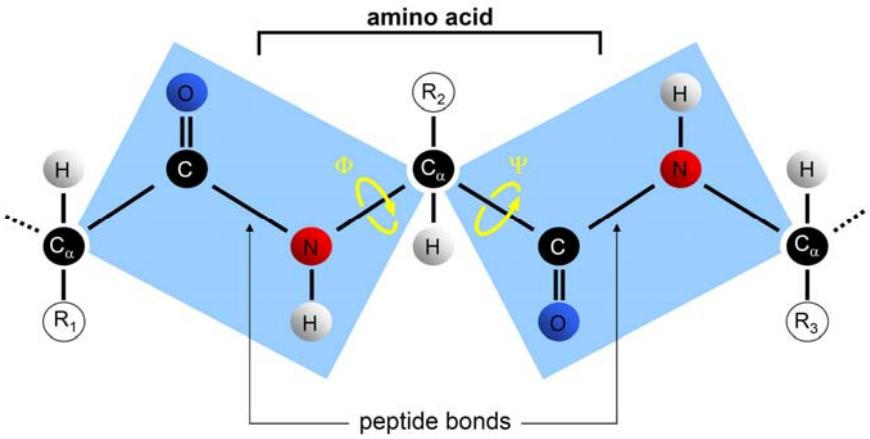

Figure 1: Individual amino acids in a protein are linked by peptide bonds.

Each amino acid has the same fundamental structure, differing only in the side chain, designated the R-group (R). The carbon atom to which the amino-, carboxyl-, and R-groups are attached is called the alpha carbon (Cα). Individual amino acids are linked by peptide bonds which are planar (blue shading) and do not allow rotation. Rotation within the polypeptide is only possible around the N-Cα and Cα-C bonds – their angles are described as psi (Ψ) and phi (Φ), respectively.

While the structures of amino acids are relatively simple and similar to one another, three-dimensional conformations of proteins are exceedingly complex. Theoretically, proteins have an incomparably high number of possible conformations due to the nearly free rotation around the bond connecting the Cα and the carboxyl carbon and the bond between the Cα and the amino group in their peptide backbone (Figure 1). The angles of these rotations are defined as the dihedral angles Ψ (psi) and Φ (phi). The peptide bond itself is planar, resulting from the partial double bond character, caused by the resonance of electrons rapidly moving between the oxygen and the nitrogen. Furthermore, steric repulsions between amino acid side chains are responsible for the exclusion of most of the theoretically existing Ψ and Φ pairs. In 1968, Ramachandran calculated the energy contained in various pairs of Ψ and Φ angles and found the two most stable pairs, termed the α and the β conformation (Ramachandran and Sasisekharan, 1968). These two pairs of angles are found to occur almost

exclusively in folded proteins, including the most prominent examples of secondary structure: α-helices and β-strands.

In order to get an idea of how long it would take a protein to reach its lowest-energy conformation through random folding, Levinthal computed the number of all theoretically possible conformations of a polypeptide containing 150 amino acids (Levinthal, 1969). The result for this particular protein was ~10^{300} possible conformations. Even if one assumes that each amino acid populates only the two lowest energy regions Ψ and Φ in the Ramachandran plot, there are still ~10^{30} main-chain conformations for a small protein with 100 residues. Based on the physical speed limit of ~10^{11} s^{-1} possible interconversions between main-chain conformations, it would take about 10^{11} years (longer than the lifetime of the universe!) to populate the full number of potential conformers (Dinner et al., 2000). This so called "Levinthal paradox" led to the conclusion that a protein cannot sample all the possible conformations during the process of folding. Rather, "folding is speeded and guided by the rapid formation of local interactions which then determine the further folding of the peptide. This suggests local amino acid sequences which form stable interactions and serve as nucleation points in the folding process"(Levinthal, 1969).

1.1.3 Protein folding mechanisms

As protein folding through random, unbiased adoption of all possible conformations would take "an eternity", it was a logical step to assume that there must be defined pathways to reduce the choices in folding. The search for a single, general mechanism of protein folding led to various proposals, all of which simplified the folding process by uncoupling the formation of secondary structure from that of tertiary structure (Daggett and Fersht, 2003).

The classical "nucleation-growth" mechanism (Wetlaufer, 1973) postulated that initially some neighboring amino acids form stable secondary structures, acting as nuclei from which native tertiary structure propagates in a stepwise manner. However, nucleation dropped from favor as it predicts the absence of folding intermediates, although the field of protein folding was

dominated by the study of folding intermediates at that time (Kim and Baldwin, 1982; Ptitsyn, 1987).

Therefore, alternative models became more attractive: one was the "framework" model (Ptitsyn and Rashin, 1975; Kim and Baldwin, 1982; Kim and Baldwin, 1990) together with the closely related "diffusion-collision" model (Karplus and Weaver, 1976). This model predicts that local elements of native secondary structure form independently and then diffuse until they collide, successfully adhere, and coalesce to result in the final native tertiary structure. The second model, the "hydrophobic collapse" model (Schellman, 1955; Kauzmann, 1959; Tanford, 1962; Baldwin, 1989), hypothesized that a protein rapidly collapses around its hydrophobic side chains so that folding can occur in a confined volume, thereby reducing the number of possible conformations during the process of folding to the native sate.

In the early 1990s, proteins were observed which folded by simple two-state kinetics without the formation of detectable intermediate structures (Jackson and Fersht, 1991). Others formed secondary and tertiary structure in parallel as they undergo hydrophobic collapse (Otzen et al., 1994). These findings led to the formulation of the "nucleation-condensation" mechanism (Fersht, 1997) which unites features of both the "hydrophobic collapse" and the "framework" mechanism.

Nowadays, the synergy of experimental data and protein folding simulations by molecular dynamics computations are beginning to describe folding and unfolding pathways at atomic-level resolution (Mayor et al., 2000; Fersht and Daggett, 2002; Vendruscolo and Dobson, 2005). Despite the tremendous progress within the last decade, these kinds of simulations are still limited to very small proteins and are not yet applicable to the large majority of proteins in the cell.

1.1.4 Protein folding energy landscapes

The "classical view" of protein folding along folding pathways has recently been replaced by the "new view" (Baldwin, 1995), the so-called "folding funnel" or "energy landscape" theory (Baldwin, 1995; Dill and Chan, 1997;

Dobson et al., 1998; Onuchic and Wolynes, 2004). Here, protein folding is described as a process of reaching a global minimum in free energy (satisfying Anfinsen's thermodynamic hypothesis) and doing so quickly (satisfying Levinthal's kinetic theory) by multiple down-hill routes on funnel-like energy landscapes (Figure 2).

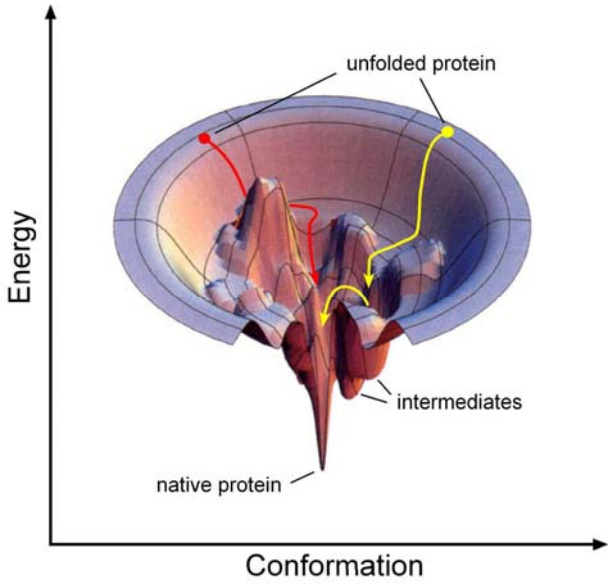

Figure 2: Energy landscape of a folding funnel.

Protein folding proceeds from an unfolded state of high energy towards a unique three-dimensional native structure where the energy level is lowest. In general, several folding pathways down the rugged energy landscape are possible. For instance, the red trajectory illustrates a fast track of folding whereas the yellow trajectory illustrates a slow track of folding in which a kinetically stable intermediate is populated, slowing down the folding process. Adapted from Dill and Chan (1997).

The distinction between a pathway and a funnel is that the former describes a one-dimensional route through the space of all configurations possible, whereas the latter delineates folding as a progressive reduction in dimensionality of the accessible conformational space, beginning from the many degrees of freedom available to denatured chains, down to the almost a complete lack of freedom of the native protein (Dill and Chan, 1997). Thus, in the funnel theory, folding can occur either on a sub-second timescale by reducing all potential conformations to a subset of thermodynamically favored local minima (Schultz, 2000) or undergo a slow trajectory through many unproductive transition states in a more or less

rugged energy landscape (Bryngelson et al., 1995; Onuchic et al., 1995; Wolynes et al., 1995). Kinetic traps arising close to the bottom of the folding funnel correspond to the accumulation of misfolded proteins. Despite the information gained from these models addressing some principles of folding kinetics, they are not yet recipes for predicting the defined three-dimensional structure from a given amino acid sequence (Dill and Chan, 1997).

1.1.5 Differences in protein folding *in vitro* and *in vivo*

The process of protein folding *in vitro* has been studied extensively over the last few decades in order to gain insights in how proteins fold inside living cells. Most of the initial *in vitro* refolding experiments utilized small, single-domain proteins that undergo cooperative and reversible folding reactions, since multi-domain proteins often refold very inefficiently due to aggregation. To investigate protein refolding, purified proteins are in general first unfolded in denaturants like guanidinium-hydrochlorid (6 M) or urea (8 M) and then rapidly diluted into aqueous solutions where refolding to the native state is allowed to occur spontaneously. In order to avoid protein aggregation during refolding, the experiments are usually performed in simple buffer systems and under optimized conditions (very low protein concentrations as well as optimal pH, salt, and temperature).

Compared to *in vitro* protein refolding under idealized conditions, folding inside the cell is much more complex. Here, protein folding must be achieved in a highly crowded and dynamic environment that favors protein misfolding and aggregation (Figure 3). The total concentration of proteins and RNA in the cytosol of an *Escherichia coli* (*E. coli*) cell has been estimated to be in the range of 300-400 mg/ml (Zimmerman and Trach, 1991). Thus, a significant proportion of the cellular volume is already physically occupied by the large amount of mutually impenetrable macromolecules and is therefore inaccessible for other molecules. This phenomenon, designated as "excluded volume effect" or "macromolecular crowding" (Ellis, 2001; Minton, 2001), is also responsible for significant increases in the affinities and rate constants of many cellular reactions by several orders of magnitude. Thus, macromolecular crowding can result,

among other effects, in an increased propensity of folding protein molecules to aggregate (Zimmerman and Minton, 1993; Ellis and Hartl, 1996; Minton, 2000).

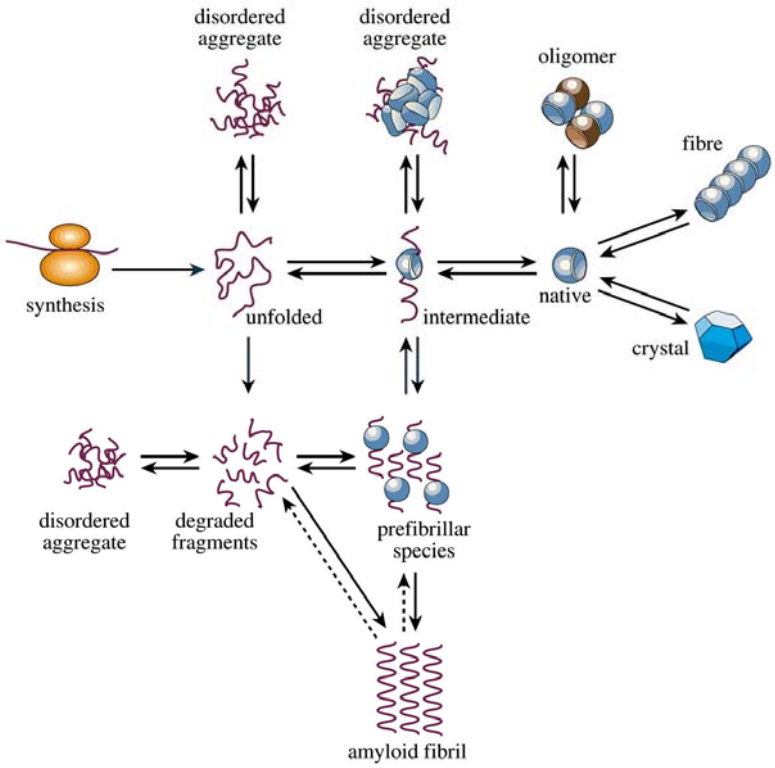

Figure 3: Folding states accessible to a protein after synthesis on the ribosome.

Upon synthesis on the ribosome, proteins are assumed to fold from a largely disordered unfolded state through a partially structured intermediate into their final globular native conformation. Native proteins can act as monomers, oligomers or assemble into highly ordered fibres and crystals, whilst preserving their overall structure. Instead, unfolded and partially folded proteins mostly form aggregated species that are frequently disordered. Exceptions are the so-called amyloid fibrils, which are thought to form through a nucleation growth mechanism, utilizing partially folded soluble precursor proteins as seeds. Adapted from Vendruscolo and Dobson (2005).

Another major difference between protein refolding out of denaturant and folding *in vivo* is that in the cell folding is tightly coupled to the vectorial synthesis of polypeptide chains (N-terminus to C-terminus) on the ribosome. Thus, the folding information encoded in the amino acid sequence becomes available sequentially and not all at once, as is the case during *in vitro* refolding. Since stable folding requires the presence of at least a complete protein domain of ~100-300 residues, nascent chains remain unfolded until the entire sequence of

such a folding competent unit has been synthesized and emerged from the ribosomal exit tunnel (Jaenicke, 1991). In eukaryotes, the rate of chain elongation was estimated to be approximately 4 amino acids per second (Thulasiraman et al., 1999). Hence, the synthesis of a complete domain takes more than a minute. During this time, nascent chains expose hydrophobic amino acid residues and segments of unstructured polypeptide backbone which are normally buried in the interior of a native protein and are thus susceptible to aggregation. This propensity to aggregate is thought to be greatly increased by the high local concentration of identical nascent chains synthesized on neighboring ribosomes in a polysome (Ellis and Hartl, 1996). In order to minimize off-pathway reactions during *de novo* protein folding, nascent chains either have to fold co-translationally or need to be stabilized in a nonaggregated, folding-competent conformation until post-translational folding of a complete chain is possible (Netzer and Hartl, 1998).

1.1.6 Protein misfolding and diseases

Protein folding and unfolding belong to the most important mechanisms to generate and abolish cellular activities. Given the enormous complexity of the protein folding process, as described above, it is not surprising that the failure to fold correctly, or to remain correctly folded, will inevitably lead to malfunctioning in living systems and therefore to diseases (Thomas et al., 1995). The so-called "protein misfolding diseases" include pathological states in which impairment in the folding of a certain protein is accompanied by a reduction in the available amount of native protein normally necessary to fulfill its proper function. This reduction can, among other effects, result from an increased probability for misfolded proteins to be degraded by the quality control system of the endoplasmatic reticulum, as it is the case in cystic fibrosis (Amaral, 2004), or the improper trafficking of a protein to the site where it is needed, as it occurs in early-onset emphysema (Lomas and Carrell, 2002). The largest group of misfolding diseases, however, is associated with the conversion of proteins or protein fragments from their normally soluble form into insoluble, highly organized amyloid fibrils or plaques (Chiti and Dobson, 2006) (Figure 3).

Depending on the disease involved, such deposits can accumulate in a variety of organs including liver, spleen and brain (Dobson, 1999). The quantity of these aggregates can thereby range between an almost undetectable level and several grams to kilograms in certain manifestations of systemic amyloidosis. In recent years, most attention has been focused on the group of neurodegenerative diseases, associated with the formation of brain lesions, including Alzheimer's disease, Parkinson's disease, the polyglutamine-expansion diseases such as Huntington's disease, as well as the prion diseases such as Creutzfeldt-Jakob disease (Barral et al., 2004). Interestingly, despite the native forms of the proteins involved in the respective diseases being quite different (they range from globular proteins to mostly unstructured polypeptides), the fibrils in which they appear in the disease state have many similar characteristics (Sunde and Blake, 1997). For instance, all the fibrillar structures have very similar morphologies (long and unbranched), as evidenced by electron microscopy, and show a characteristic "cross-β" X-ray diffraction pattern. Furthermore, they all show specific optical properties on binding of special dye molecules, like Congo red, which have been utilized in diagnostics for more than a century (Dobson, 2004).

In addition to the misfolding diseases described above, large-scale genome sequencing projects revealed mutations being responsible for a variety of inherited human diseases, such as McKusick-Kaufman Syndrome (MKKS) and Bardet-Biedel type 6 Syndrome (BBS6) (Slavotinek et al., 2000; Stone et al., 2000). Interestingly, a detailed analysis of the open reading frames harboring these mutations discovered heat shock proteins or proteins with similarities to this class of proteins which assist other proteins in folding, the so called molecular chaperones (Barral et al., 2004). Furthermore, these findings indicate that defects in the folding machinery can be directly associated with a variety of severe human diseases.

1.2 Molecular Chaperones

Over the past 15 years, intense research efforts have demonstrated that efficient folding of newly synthesized proteins necessitates a complex cellular machinery of molecular chaperones (Ellis and Hemmingsen, 1989; Gething and Sambrook, 1992; Buchner, 1996; Hartl, 1996; Ellis and Hartl, 1999; Frydman, 2001; Hartl and Hayer-Hartl, 2002). The term "molecular chaperone" was originally coined to describe the specialized function of nucleoplasmin, a nuclear protein that promotes chromatin assembly by preventing improper interactions between histones and DNA (Laskey et al., 1978). This specific usage of the term was later generalized by John Ellis (Ellis, 1987).

A key property, common to all chaperones, is their mediation of folding by minimizing improper interactions within and between molecules. To fulfill this function, molecular chaperones transiently bind to structural elements of non-native polypeptide chains, such as exposed hydrophobic residues and unstructured backbone regions, which are normally buried inside the globular structure of native proteins. Binding and release of substrate polypeptides by chaperones is often regulated in a complex ATP-dependent manner and may occur several times until folding is completed. Importantly, chaperones contribute neither steric information to the folding process nor are they part of the final native structure of the folded protein (Agashe and Hartl, 2000). Furthermore, chaperones do not catalyze or accelerate folding reactions in a classical sense, but rather increase the number of molecules that are on a productive folding pathway. Instead, real folding catalysts are peptidyl-prolyl *cis-trans* isomerases (PPIases) and protein disulfide isomerases (PDIs), which specifically catalyze rate-limiting steps in the folding process, such as the isomerization of peptide bonds preceding prolyl residues (Schmid et al., 1993) and the rearrangement of disulfide bonds (Freedman et al., 1994), respectively.

Molecular chaperones are distributed ubiquitously across the boundaries of all three kingdoms of life and can fulfill their functions inside living cells over a wide temperature range. Although constitutively expressed under normal growth conditions, many chaperones are greatly upregulated upon

exposure to elevated temperatures or other conditions of stress, such as starvation and exposure to toxins (Lindquist, 1986; Lindquist and Craig, 1988; Morimoto, 1998). Therefore, molecular chaperones are also referred to as "stress proteins" or "heat shock proteins" (Hsp). At present, more than 25 different protein families are described as molecular chaperones, but not all of them are stress proteins. The most prominent chaperones belong to five sequence-related families and were initially classified according to their sequences and apparent molecular masses (in kDa): Hsp60, Hsp70, Hsp90, Hsp100 and the small heat shock proteins (sHsp).

In addition to protein folding and refolding, molecular chaperones are also involved in many other cellular processes, such as protein degradation, targeting and signal transduction (Hartl, 1996; Ellis and Hart, 2000).

1.2.1 Pathways of chaperone mediated protein folding in the cytosol

In living cells, a multitude of molecular chaperones is required to mediate the correct folding of newly synthesized proteins into their unique three-dimensional structures. In order to fulfill this challenging task, chaperones are thought to be organized in complex chaperone networks (Figure 4). Although individual differences in *de novo* protein folding exist, the essential principles of these networks are conserved among eubacteria and eukarya. Chaperones initially interact with nascent chains during their biogenesis and the polypeptides are then conveyed between functionally cooperating chaperones that complete their folding to the native sate (Young et al., 2004).

Cytosolic protein folding generally starts with the interaction of nascent chains emerging at the peptide exit tunnel with ribosome-associated factors: these are trigger factor (TF; 1.2.2) in prokaryotes and the nascent chain-associated complex (NAC) in eukaryotes. Notably, some eukaryotes like *Saccharomyces cerevisiae* (*S. cerevisiae*) feature an additional ribosome associated complex, called RAC (ribosome-associated complex), which consists of Ssz (a member of the Hsp70 family) and zuotin (a Hsp40 homolog). All these factors, although structurally unrelated, are associated with the large ribosomal subunit and are believed to guide proteins to their correct folding pathway.

Upon completion of translation and release from this first set of ribosome-bound factors, the majority (>60% of total) of small proteins are thought to fold rapidly and without further assistance. Longer polypeptide chains (~10-20% of total) subsequently interact with a second class of nascent chain-binding chaperones, the classical Hsp70 proteins (1.2.3). These chaperones, not associated with the ribosome themselves, bind to short hydrophobic sequences of nascent chains thereby preventing their aggregation during elongation. Moreover, Hsp70 proteins together with their respective co-chaperones of the Hsp40 family are able to assist in both co-translational folding, while the nascent chain is still associated with the ribosome, and post-translational folding, once the protein is released.

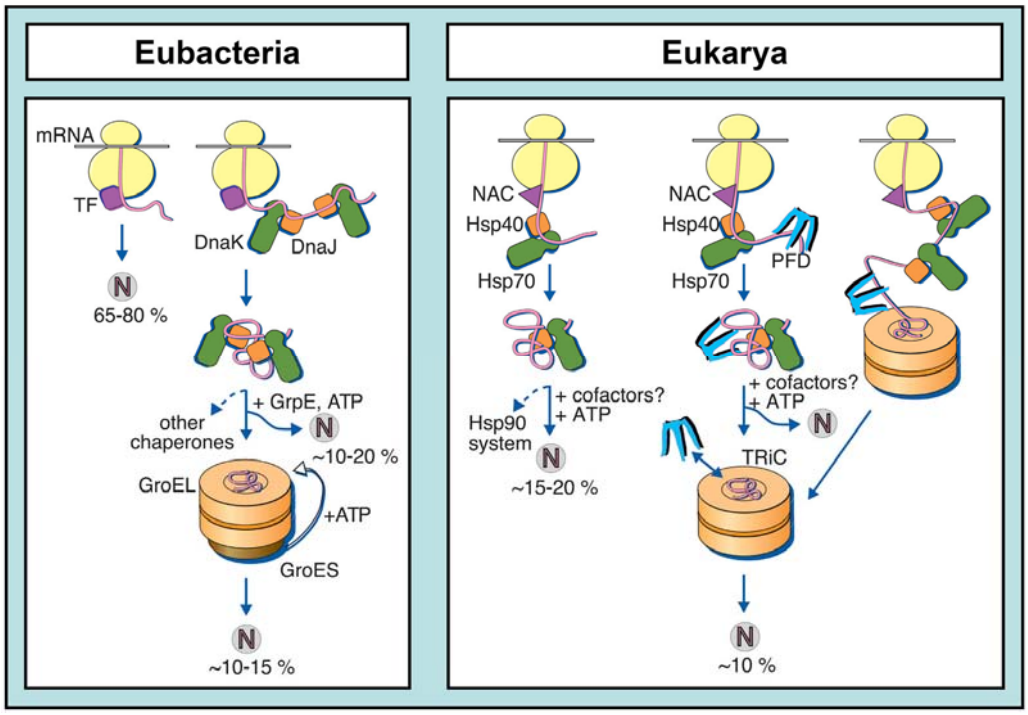

Figure 4: Models for chaperone-assisted folding of newly synthesized proteins in the cytosol of eubacteria and eukarya.

N: native protein, TF: trigger factor, NAC: nascent-chain associated complex, PFD: prefoldin, DnaK/DnaJ: Hsp70/Hsp40 chaperone system in the bacterial cytosol, GroEL/GroES: bacterial chaperonin, TRiC: eukaryotic chaperonin. Detailed information is provided in the text. Adapted from Hartl and Hayer-Hartl (2002).

Furthermore, a fraction of slow-folding and aggregation-sensitive proteins (~10-15% of total) require transfer to a protected folding environment provided by the central cavity of the multimeric chaperonins bacterial GroEL or the eukaryotic TRiC (1.2.4 and 1.3). Notably, TRiC mediated protein folding in the eukaryotic cytosol is facilitated in close cooperation with an additional factor, termed prefoldin (PFD), which directly binds to nascent chains and does not exist in bacteria.

Finally, the correct folding of another, diverse subset of eukaryotic polypeptides (including transcription factors and regulatory kinases) strongly depends on the successive transfer from the Hsp70/40 system to chaperones of the Hsp90 family. Folding of these proteins is performed in a cooperative process between both chaperone systems, regulated by several cofactors.

Despite the fact that proteins fold quite efficiently along individual folding pathways in bacteria and eukaryotes, the predominant folding mechanism for complex multi-domain proteins in both cytosols appear to be fundamentally different. Whereas folding of these proteins in bacteria occurs mostly post-translationally, folding of similar complex polypeptides in eukaryotes is generally facilitated in a co-translational manner. Although it was proposed that the shift from a post-translational to a co-translational folding mechanism must have occurred during evolution (the so called "folding shift hypothesis"; Netzer and Hartl, 1997), it is not yet clear, whether the ability to support co-translational folding has been lost (or reduced) by prokaryotes or acquired by eukaryotes.

Thus, the reduced efficiency of co-translational folding in prokaryotes might be a valid explanation for the low abundance of multi-domain proteins in these organisms (~13% of total compared to ~38% in eukaryotes; Netzer and Hartl, 1998), and why modular proteins of eukaryotic origin tend to misfold and form inclusion bodies upon expression in bacterial hosts (Marston, 1986; Baneyx, 1999).

1.2.2 Trigger factor: a ribosome-associated chaperone

Trigger factor (TF), initially discovered as an *E. coli* protein facilitating protein export into the periplasmic space (Crooke and Wickner, 1987), is now known to be one of the first bacterial chaperone to meet nascent chains as they emerge from the ribosome exit tunnel (Valent et al., 1995; Hesterkamp et al., 1996; Scholz et al., 1997; Valent et al., 1997).

1.2.2.1 TF structure and localization at the ribosome

E. coli TF (the *tig* gene product) is a 48 kDa protein composed of three individual domains (Figure 5A, bottom): The N-terminal ribosome-binding domain, containing the highly conserved and essential ribosome binding signature GFRxGxxP (aa 43-50), is exclusively responsible for the specific binding of TF to the ribosomal proteins L23 and L29 located in close proximity to the polypeptide exit tunnel (Hesterkamp et al., 1997; Kramer et al., 2002). Importantly, TF binding to the ribosome has been shown to be essential for its interaction with nascent chains and is markedly reduced upon mutation of its ribosome binding signature motif (Kramer et al., 2002). The second domain in sequence exhibits a catalytic activity as a peptidyl-prolyl *cis/trans* isomerase (PPIase). Its contribution to *de novo* protein folding still remains unclear, since it is not essential for TF function *in vivo* (Genevaux et al., 2004; Kramer et al., 2004a). The C-terminal domain, comprising virtually half of the TF molecule, displays no sequence homology to any other protein (Hesterkamp and Bukau, 1996). Recent studies using a photo-crosslinking approach demonstrated this domain to be directly involved in substrate binding (Lakshmipathy et al., 2007). Furthermore, deletion of the C-terminal domain drastically reduced the chaperone activity of TF *in vitro* and *in vivo* (Kramer et al., 2004b; Merz et al., 2006).

In 2004, Ferbitz *et al.* solved the crystal structure of *E. coli* TF, as well as the ribosome binding domain of TF in complex with ribosomes of archaeal origin (Ferbitz et al., 2004). As depicted in Figure 5A (top panel), TF adopts a fairly elongated structure which was proposed to resemble the shape of a "crouching dragon". Thereby, the "tail" is formed by the N-terminal ribosome binding

domain, whereas the PPIase domain constitutes the "head". The C-terminal domain is positioned in the middle of the three-dimensional structure, forming two "arms" and the back of the molecule. The result of this crescent TF structure is a large cavity, located between the tail and the arms of the protein. This so-called "cradle" is highly enriched in hydrophobic side chains and therefore supposedly the contact region for emerging nascent chains from the ribosome.

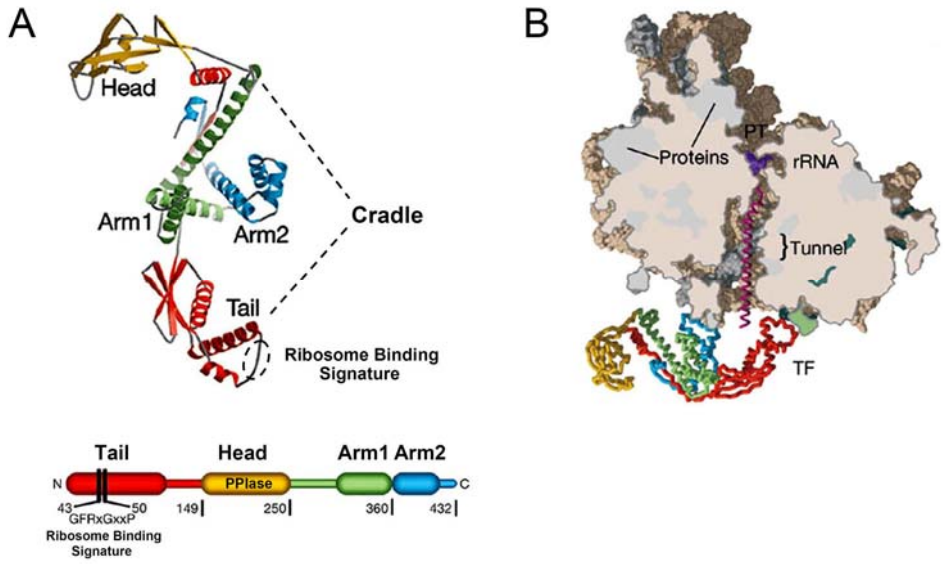

Figure 5: Structure of *E. coli* TF.

(A) Top: ribbon diagram of the extended TF structure. Bottom: domain arrangement comprising the N-terminal ribosome-binding domain (Tail), the central PPIase domain (Head) and the C-terminal domain (Arm1 and Arm2). Domain borders and the ribosome-binding signature (residues 43-50) are indicated. **(B)** Model of full-length TF bound to the large ribosomal subunit of *Haloarcula marismortui* shown as slice along the peptide exit tunnel containing a modeled nascent chain (magenta), extruding from the peptidyl transferase center (PT). In all parts, the ribosome-binding "tail" is shown in red, the PPIase "head" in yellow and "arm1" and "arm2" in green and blue, respectively. Adapted from Ferbitz et al. (2004).

A model of full-length TF bound to the L23 protein of an archaeal ribosome suggests TF to hunch over the polypeptide exit of the ribosome, exposing the hydrophobic inner surface of the cradle towards the area where the nascent chain exits the ribosome (Figure 5B). A similar orientation was shown for the N-terminal domain of *Deinococcus radiodurans* TF in complex with its cognate 50S subunit (Baram et al., 2005; Schlunzen et al., 2005). Interestingly, recent protease

protection studies utilizing model proteins such as firefly luciferase reported the cradle to form a shielded folding environment for nascent chains at the ribosome (Hoffmann et al., 2006; Tomic et al., 2006).

1.2.2.2 Role of TF in protein folding

The formation of a 1:1 complex between TF and vacant ribosomes is a prerequisite for its interaction with nascent chains emerging from the polypeptide exit tunnel (Kramer et al., 2002; Patzelt et al., 2002; Maier et al., 2003). Since TF function is ATP-independent, the chaperone does not actively assist protein folding through regulated cycles of substrate binding and release. Instead, TF was for a long time thought to mainly bind to short nascent chains (Valent et al., 1995; Hesterkamp et al., 1996), mediated by sequences enriched in hydrophobic amino acids (Patzelt et al., 2001), in order to prevent early aggregation events. Recently, TF interactions were also reported for longer nascent chains (Hoffmann et al., 2006; Tomic et al., 2006). Additionally, Kasier et al. demonstrated that TF interaction with ribosomes and newly synthesized polypeptide chains occurs in a dynamic reaction cycle which involves all three functional domains of the chaperone (Kaiser et al., 2006). Upon release from TF, active folding of newly synthesized proteins can then be facilitated by the ATP-driven chaperones, located further downstream in the folding pathway. So far, a role of TF in post-translational folding has not yet been shown, but would be consistent with the observation that only approximately half the TF molecules are ribosome associated (Bukau et al., 2000) and that TF is able to bind unfolded proteins *in vitro* (Scholz et al., 1997).

TF and DnaK (the main bacterial Hsp70 system) have been shown to have overlapping chaperone function in stabilizing nascent chains in a state competent for subsequent folding (Deuerling et al., 1999; Teter et al., 1999). Although not physically tethered to the ribosomes itself, DnaK is known to bind nascent chains during translation while these are still attached to the ribosome (Teter et al., 1999). In *E. coli* cells lacking TF (Δ*tig*), DnaK can function as an effective substitute in chaperoning nascent chains during translation, reflected in an increased amount of this particular chaperone being transiently associated

with ribosome bound nascent chains. Furthermore, the simultaneous deletion of the genes encoding for TF and DnaK severely diminishes the viability of *E. coli* cells at temperatures above 30 °C and results in the accumulation of misfolded and aggregated proteins, including a number of large multi-domain proteins (Deuerling et al., 1999; Teter et al., 1999; Genevaux et al., 2004). Interestingly, recent results have demonstrated that some bacterial cells can cope with this loss of viability by the accumulation of suppressor mutations, when first grown at 20 °C and gradually adapted to higher temperatures (Genevaux et al., 2004; Vorderwulbecke et al., 2004). Moreover, the growth defect can also be complemented by overproduction of SecB (a chaperone involved in protein translocation) and GroEL/GroES, utilized as backup system for TF and DnaK (Ullers et al., 2004; Vorderwulbecke et al., 2004).

1.2.3 The Hsp70 chaperone system

The members of the Hsp70 family are highly conserved ATPases found in the cytosol of prokaryotes, eukaryotes and some archaea, as well as within most eukaryotic organelles (Craig et al., 1993; Hartl, 1996; Hartl and Hayer-Hartl, 2002). Hsp70s act on their substrates by a mechanism of binding and release, usually in a cofactor dependent manner, and play an essential role in a variety of cellular processes under both stress- and non-stress conditions. Among those, assisting in *de novo* protein folding and the prevention of aggregation are probably the most important ones. Additionally, they are also involved in protein targeting and membrane translocation, the dissociation of large aggregates, and protein degradation (Hartl, 1996; Bukau and Horwich, 1998).

1.2.3.1 Hsp70 structure and reaction cycle

Hsp70 chaperones typically consist of two major functional domains, a highly conserved N-terminal ATPase domain (44 kDa) and a less conserved C-terminal peptide binding domain (25 kDa). In the case of DnaK, crystal structures of both individual domains, but not of the entire molecule have been determined (Zhu et al., 1996; Harrison et al., 1997). Interestingly, the ATPase domain turned out to have a fold similar to that of monomeric actin, consisting of

two structural lobes with a deep nucleotide-binding cleft between them (Flaherty et al., 1991). The peptide binding domain is divided into a β-sandwich subdomain, comprising the peptide-binding cleft, and an α-helical extension that functions as a lid for substrate enclosure (Zhu et al., 1996).

The ATP-regulated cycle of substrate binding and release is best understood for the bacterial DnaK, its Hsp40 co-chaperone DnaJ, and the nucleotide exchange factor GrpE (Bukau and Horwich, 1998; Naylor and Hartl, 2001). During this cycle, DnaK alternates between two different structural states, dependent on the phosphorylation state of the nucleotide bound (Figure 6).

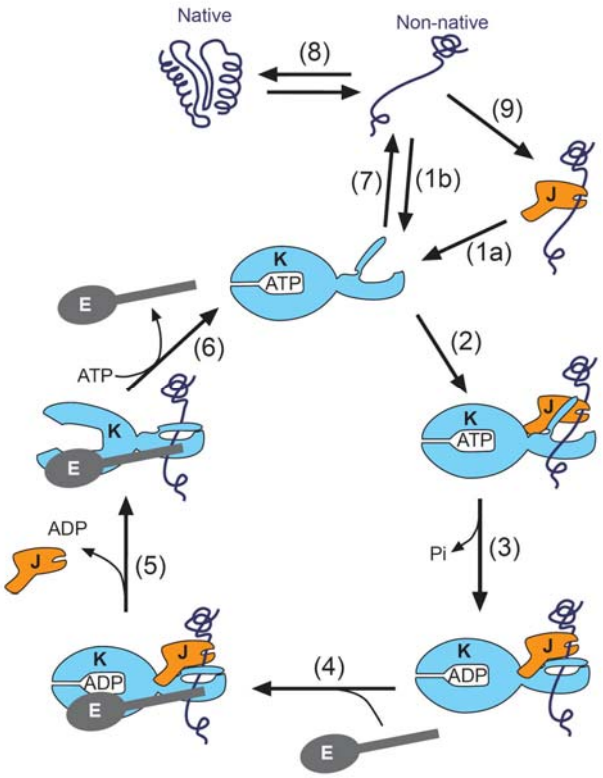

Figure 6: Chaperone cycle of the bacterial Hsp70 chaperone system DnaK, DnaJ and GrpE.

The cycle starts with the association of non-native substrate proteins with either DnaJ (J) (1a) or DnaK (K) in the ATP-bound open conformation (1b). DnaJ and substrate protein (2) then stimulate the ATP-hydrolysis of DnaK (3), resulting in the closure of its substrate binding pocket. The interaction of GrpE (E) with DnaK (4) efficiently promotes the exchange of bound ADP (5) for ATP (6). This results in the opening of the substrate binding cleft and the exchange of substrate proteins (7). The released protein can then either fold towards the native state (8) or rebind to DnaJ (9) or DnaK (1b). Adapted from Naylor and Hartl (2001).

In the ATP-bound state, the lid over the peptide-binding cleft is in an open conformation and substrate binding and release is allowed to occur rapidly. In the ADP-bound form, the binding pocket is closed and substrates are bound with high affinity. Cycling of DnaK between its different nucleotide-bound states is regulated by the cofactors DnaJ and GrpE (Szabo et al., 1994). Upon substrate binding of DnaK in the ATP-bound state, interaction with DnaJ stimulates the ATPase activity of DnaK, thus facilitating tight peptide capture (Mayer et al., 2000). Importantly, DnaJ is itself a chaperone which can bind unfolded polypeptides and subsequently present them to the ATP-bound state of DnaK (Langer et al., 1992a; Rudiger et al., 2001). Substrate release from DnaK requires the exchange of bound ADP for ATP, catalyzed by the nucleotide exchange factor GrpE (Harrison et al., 1997). Furthermore, rebinding of ATP not only dissociates the DnaK:substrate complex but also resets DnaK to its initial low substrate affinity state completing the reaction cycle.

Although the bacterial and eukaryotic Hsp70 systems have similar functional properties (Figure 4), a GrpE-like nucleotide exchange factor homolog is absent in the eukaryotic cytosol. Such a factor may be dispensable as the rate-limiting step in the ATPase cycle of eukaryotic Hsp70 is normally not the dissociation of ADP but rather the hydrolysis of ATP itself (Hohfeld et al., 1995).

1.2.3.2 Hsp70 substrates and folding mechanism

Hsp70 proteins are known to recognize exposed hydrophobic amino acid side chains within an accessible polypeptide backbone, structural features which are common to most nascent chains and proteins in their non-native states. Nevertheless, there has been some controversy regarding the *in vivo* role of DnaK. This was based on the fact that, under non-stress conditions, deletion of DnaK in a certain wild-type *E. coli* strain is lethal, whereas in others it is not (Hesterkamp and Bukau, 1998; Teter et al., 1999). Importantly, DnaK is absolutely essential for cell viability under heat stress conditions (Bukau and Walker, 1989). Furthermore, downstream of TF, DnaK has been shown to interact transiently with a variety of nascent and newly synthesized polypeptides (~15% of total; Figure 4), preferentially in the size range of 30-75 kDa (Teter et al., 1999). For

some proteins, the half-life of DnaK transit has been determined to be <1 min, consistent with the rapid protein folding upon completion of synthesis. The extent of DnaK binding to nascent chains is modulated by TF since in Δ*tig* cells the fraction of nascent polypeptides interacting with DnaK increases more than twofold and is markedly enriched in short chains (Deuerling et al., 1999; Teter et al., 1999). Additional depletion of DnaK in Δ*tig* cells results in the aggregation of many large, newly synthesized proteins (Deuerling et al., 1999), arguing for DnaK to play an important role in facilitating the post-translational folding of complex multi-domain proteins, which do not fit into the central cavity of the GroEL chaperonin (size exclusion: ~60 kDa). Similar to DnaK, mammalian Hsp70 was also shown to act co-translationally on a large subset of newly synthesized polypeptides, including a variety of multi-domain proteins (Frydman et al., 1994; Thulasiraman et al., 1999).

The binding motif of putative Hsp70 target peptides was determined to be ~4-8 amino acids in length and of preferentially hydrophobic character (Flynn et al., 1991; Rudiger et al., 1997). It was predicted to occur, on average, every 36 residues in every polypeptide and is normally buried in the interior of a folded protein (Bukau and Horwich, 1998).

From a mechanistic point of view, folding of an Hsp70-bound protein can only occur upon its release from the chaperone stabilized state. Once this has happened, the protein is given the chance to either fold spontaneously, to rebind to Hsp70 or to be transferred to another chaperone. *In vitro*, proteins can undergo multiple rounds of binding and release, as shown for the 62 kDa model protein firefly luciferase (Szabo et al., 1994). It is also possible that folding of especially large and complex proteins is mediated by binding and release of several Hsp70 molecules acting on individual domains of the protein.

1.2.4 The chaperonins

The chaperonins (Hemmingsen et al., 1988) are a ubiquitous family of sequence-related and essential proteins which form large, multimeric, bi-toroidal structures enclosing a central cavity in each ring (Hartl, 1996; Bukau and Horwich, 1998; Carrascosa et al., 2001; Frydman, 2001). Characteristically,

ATP-regulated folding of complete proteins (or protein domains) is facilitated inside the sequestered space of these cavities, unimpaired by aggregation with other non-native proteins of the cellular environment (Martin et al., 1993; Spiess et al., 2004). Chaperonins are divided into two subgroups which are similar in architecture but distantly related in sequence: Group I chaperonins are found in the bacterial cytosol (GroEL) and in eukaryotic organelles of endosymbiotic origin (Cpn60 in chloroplasts and Hsp60 in mitochondria). They function in close cooperation with cofactors of the Hsp10 family (GroES in bacteria, Cpn10 in chloroplasts, and Hsp10 in mitochondria). Group II chaperonins exist in archaea (thermosome) and the eukaryotic cytosol (TRiC) whose function is independent of an Hsp10-like cofactor.

Since the focus of this study mostly concerns TRiC, only a brief overview of the best characterized group I chaperonin system GroEL/GroES from *E. coli* will be given. GroEL is a homo-tetradecamer of nearly 800 kDa, composed of two identical back-to-back stacked seven-membered rings (Braig et al., 1994) (Figure 7A). Each ~60 kDa subunit consists of an equatorial ATP-binding, an intermediate, and an apical substrate-binding domain. In order to fold substrates efficiently, GroEL requires the cofactor GroES, a dome-shaped homo-heptameric ring of ~10 kDa subunits (Hunt et al., 1996).

GroEL/GroES mediated protein folding is an alternating process involving the encapsulation of unfolded or partially folded substrate proteins under the GroES lid on either side of the GroEL cylinder (Hayer-Hartl et al., 1995; Bukau and Horwich, 1998). Folding starts with the binding of a substrate polypeptide to the apical domains, exposing hydrophobic surfaces, at the free end of a GroEL/GroES complex (Figure 7B). This step is closely followed by the binding of ATP and GroES at the interacting GroEL toroid, resulting in substrate encapsulation. Upon GroES binding, GroEL undergoes major conformational changes (Xu et al., 1997) leading to cavity enlargement and a shift in its surface to a predominantly hydrophilic lining (Lin and Rye, 2006). Enclosed in this so-called "Anfinsen cage", single proteins up to ~60 kDa are given the chance to fold unimpaired by aggregation (Ellis, 2006). After ATP hydrolysis (~10-15 s), ATP binding to the opposite ring of GroEL results in the release of GroES and the

substrate protein. Proteins that have not acquired their native state are recaptured and subjected to another round of folding.

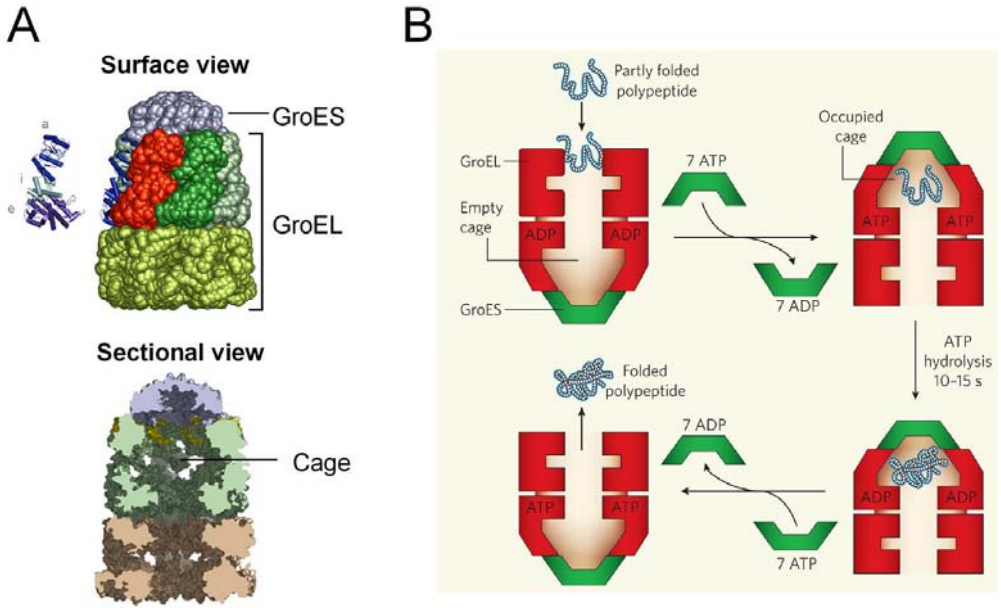

Figure 7: The chaperonin system GroEL/GroES of *E. coli*.

(A) Top: Space-filling model of the GroEL/GroES complex. The secondary structure of one subunit in the upper GroEL ring is shown and separately depicted with the apical (*a*), intermediate (*i*) and equatorial (*e*) domains highlighted. Bottom: Cross-section of the chaperonin complex, illustrating the central cage in the upper ring. Adapted from Lin and Rye (2006). **(B)** Simplified reaction cycle of protein folding in the GroEL/GroES cage. Substrate binding to the free GroEL-ring is closely followed by binding of ATP and GroES, resulting in substrate enclosure. During ATP-hydrolysis (10-15 s), the protein is given the chance to fold. After binding of ATP to the opposite ring, GroES and the substrate are released from the chaperonin. Adapted from Ellis (2006).

Whereas GroEL interacts with almost any non-native model protein *in vitro* (Coyle et al., 1997), only ~10% of newly translated polypeptides in *E. coli* interact with the chaperonin under normal growth conditions (Ewalt et al., 1997) (Figure 4). Recently, GroEL substrates where shown to preferentially consist of βα-barrel domains, including many essential proteins for cell viability (Houry et al., 1999; Kerner et al., 2005). Noteworthy, GroEL is also able to assist the folding of large proteins which cannot be encapsulated by the co-chaperonin GroES (Chaudhuri et al., 2001).

1.3 TRiC: the eukaryotic group II chaperonin

Among the chaperonins, the eukaryotic group II chaperonin TRiC (TCP1 ring complex; also termed CCT for chaperonin containing TCP1) is the most complex, not only with regard to its hetero-oligomeric subunit composition but also with respect to its function in protein folding (Gutsche et al., 1999; Carrascosa et al., 2001).

1.3.1 Structure and subunit composition

Unlike GroEL, which is a homo-oligomer, each of the two TRiC toroids consists of eight different, albeit homologous subunits, ranging between 50-60 kDa in size (Frydman et al., 1992; Gao et al., 1992; Lewis et al., 1992). The individual subunits (TRiC α, β, γ, δ, ε, ζ, η, and θ) display ~30% identity to one another and are thought to be organized in a unique arrangement within each ring (Liou and Willison, 1997; Miller et al., 2006). Interestingly, whereas in all organisms and tissues studied, the eight subunits are encoded by unique genes, a tissue-specific ζ2-subunit was identified in mammalian testis (Kubota et al., 1997). Notably, TRiC is not inducible by heat-shock (Lewis et al., 1992). The endogenous chaperonin concentrations were estimated to be ~0.5 μM in mammalian cells (Thulasiraman et al., 1999) and ~0.3 μM in yeast (Siegers et al., 1999), respectively.

Crystal structure analysis of the thermosome, the archaeal group II chaperonin from *Thermoplasma acidophilum* and homolog of TRiC, revealed domain folds of the individual subunits to be similar to that of GroEL (Ditzel et al., 1998). This observation is consistent with a high degree of sequence conservation in the equatorial (ATPase) domain and the intermediate domain between group I and group II chaperonins (Kim et al., 1994). No significant sequence similarity could be detected in the apical (substrate binding) domains of both groups. In fact, a direct comparison of thermosome and GroEL apical domains revealed an additional α-helical protrusion which is strictly conserved among group II chaperonins (Figure 8A), but is absent in group I chaperonins (Klumpp et al., 1997). These protrusions are thought to play an important role in

substrate binding and controlling access to the central cavity, independent of a GroES-like cofactor. Unfortunately, so far no high-resolution structure of the entire TRiC complex has been solved. However, the overall structure of TRiC, determined by cryoelectron microscopy (cryo-EM) (Llorca et al., 1999b; Llorca et al., 2000), is very similar to that of other group II chaperonins (Ditzel et al., 1998; Nitsch et al., 1998). It shows a barrel-shaped double-ring cylinder (150 Å x 160 Å) with every subunit interacting with only one subunit of the opposite ring (Llorca et al., 1999b) (Figure 8B, top panel), contrary to the staggered subunit arrangement observed in group I chaperonins (Braig et al., 1994). Closure of the chaperonin cavity was demonstrated to be ATP dependent and is accomplished by a ~70° clockwise rotation of the apical domains (Llorca et al., 1999b; Llorca et al., 2001), similar to an iris-like mechanism (Figure 8B, bottom panel).

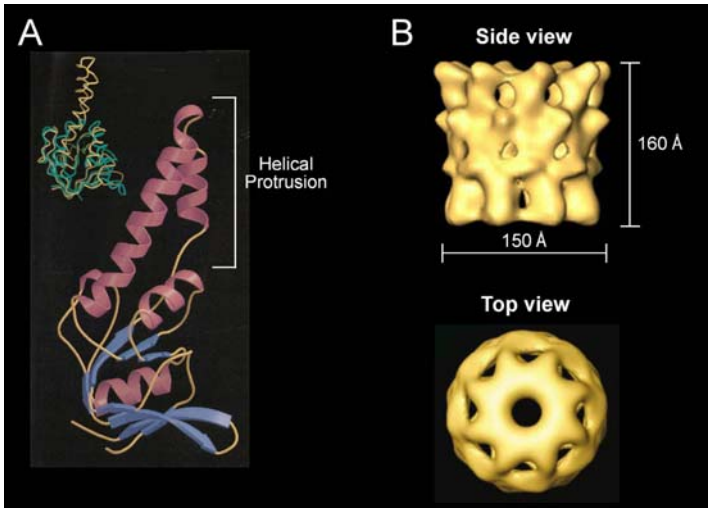

Figure 8: Structural properties of group II chaperonins.

(A) Apical domain of the thermosome α-subunit. The insert depicts a structural comparison with the corresponding domain of GroEL (green), illustrating the additional α-helical protrusion (yellow) present in the apical domain of group II chaperonins. Adapted from Klump et al. (1997). **(B)** Three-dimensional reconstruction of the eukaryotic chaperonin TRiC. Top: Side view of the apo-TRiC complex in the open conformation. Adapted from Llorca et al. (2000). Bottom: Top view of the AMP-PNP-TRiC complex in the closed conformation. Adapted from Llorca et al. (2001).

1.3.2 Mechanism of TRiC mediated protein folding

The mechanism by which group II chaperonins mediate folding of their substrate proteins is very poorly defined. Recent structural and biochemical data suggest a mechanism, similar to that of group I chaperonins, although differences exist. Similar to GroEL, folding is proposed to occur inside the central cavity and involves at least two different conformational stages of the chaperonin (Llorca et al., 2001; Meyer et al., 2003). In the nucleotide free or ADP-bound state, the apical domains of TRiC are in an open conformation exposing the substrate binding sites. On the other hand, binding of ATP results in lid-closure and substrate encapsulation. Importantly, unlike for GroEL, lid-closure is not solely triggered by ATP binding but instead requires the presence of an ATP-transition state, engaged during nucleotide hydrolysis (Meyer et al., 2003). How exactly ATP-hydrolysis triggers protein folding is not yet clear. One model suggests sequential anti-clockwise conformational changes in the apical domains of TRiC to actively convert bound substrate proteins from a largely unfolded towards a more compact (native) state (Lin and Sherman, 1997; Llorca et al., 2001) (Figure 9B). In contrast to folding by mechanical pushing, a recent model proposes distinct binding properties in individual subunits at different states of the chaperonin to be responsible for folding (Spiess et al., 2006). Surprisingly, although confinement of substrate proteins was shown to be essential for TRiC-assisted folding (Meyer et al., 2003), the substrates are not liberated into the central cavity but instead remain bound to the chaperonin apical domains until their release (Llorca et al., 2001). Finally, negative inter-ring cooperativity (Kafri et al., 2001) and lid-closure in only one ring of TRiC after incubation with an ATP-transition state analog (Meyer et al., 2003) strongly argue for a "two-stroke mechanism" of the chaperonin.

1.3.3 TRiC substrates

TRiC was initially found to facilitate the folding of the cytoskeletal proteins actin and tubulin *in vitro* (Gao et al., 1992; Yaffe et al., 1992). Subsequently, the crucial role of TRiC for the folding of these proteins could also be demonstrated *in vivo*. Temperature-sensitive mutations in the genes encoding

for individual TRiC subunits displayed cytoskeletal phenotypes in *S. cerevisiae*, including defects in actin and tubulin assembly as well as aberrant budding patterns (Chen et al., 1994; Ursic et al., 1994). Therefore, TRiC was for a long time assumed to be a highly specialized chaperone exclusively responsible for the folding of cytoskeletal proteins (Lewis et al., 1996).

This view changed upon the identification of new TRiC substrates, including firefly luciferase (Frydman et al., 1994), Gα-transducin (Farr et al., 1997), cyclin E (Won et al., 1998), and the Von Hippel-Lindau tumor suppressor protein VHL (Feldman et al., 1999). It was even proposed that the substrate specificity of TRiC for actin and tubulin was based on an artifact, resulting from the high abundance of these proteins in cell extracts. Hence, other putative chaperonin substrates have possibly been overlooked. This would be in line with the high affinity of TRiC for cytoskeletal proteins (Melki and Cowan, 1994) and the observation that *in vivo* ~50-60% of the chaperonin capacity is devoted to the folding of actin and tubulin (Siegers et al., 2003). However, a pulse-chase analysis in mammalian cells revealed TRiC to interact with a broader range of proteins than the ones previously cited (Thulasiraman et al., 1999). Approximately 9-15% of the total synthesized proteins, mostly ranging from 30 to 60 kDa in size, were shown to associate transiently with the chaperonin (Figure 4). Notably, chaperonin interactions were also demonstrated for several proteins of 100-120 kDa which clearly exceed the ~50 kDa size limit of the central cavity determined for group II chaperonins (Ditzel et al., 1998). More recently, proteomic analyses of protein complexes in yeast identified a new set of TRiC-associated proteins, the so-called "WD40-repeat proteins" (Ho et al., 2002). For several of these proteins, folding was demonstrated to be critically dependent on the chaperonin, thus, providing evidence for the first class of structurally defined TRiC substrates (Camasses et al., 2003; Siegers et al., 2003). WD40-repeat proteins are characterized by the content of four or more copies of a 40-60 amino acid long sequence motif ending with the conserved dipetide tryptophan-aspartate (WD). Their common fold is defined as a β-propeller and consists entirely of anti-parallel β-strands (Smith et al., 1999). Interestingly, the interaction of TRiC with protein domains enriched in β-strands was also noted for several

other TRiC substrates, including the well characterized tumor suppressor protein VHL (Feldman et al., 2003). Based on these results it is tempting to speculate that β-strands constitute a possible chaperonin-recognition motif and that TRiC plays a role in folding of β-sheet-containing domains or participates in their stabilization during *de novo* synthesis (Spiess et al., 2004).

1.3.4 TRiC-substrate interaction

By analogy to group I chaperonins, substrate recognition by TRiC is believed to occur at the apical domains of individual subunits. However, the nature and exact location of substrate binding sites are still undefined. One hypothesis suggested the flexible α-helical protrusions to contain the substrate binding site (Klumpp et al., 1997; Heller et al., 2004). However, these protrusions seem not to be essential as their deletion in an archaeal chaperonin did not impair substrate binding efficiency (Iizuka et al., 2004). Based on cryo-EM and evolutionary analyses, binding sites were also proposed to reside in the region lining the inner face of the cavity, consisting mostly of charged and polar amino acids (Pappenberger et al., 2002; Gomez-Puertas et al., 2004). Finally, recent data suggest substrate binding to be facilitated by hydrophobic interactions in an α-helical region (Spiess et al., 2006), analogous to the binding site defined in the distal region of the GroEL apical domains (Sigler et al., 1998; Chen and Sigler, 1999). Although quite diverse, all mentioned substrate binding sites are not mutually exclusive. Instead, given the sequence diversity in the apical domains of TRiC, it is feasible that different subunits recognize different types of motifs in a substrate protein, including hydrophobic as well as polar sites (Rommelaere et al., 1999; Hynes and Willison, 2000; Spiess et al., 2004). Additionally, this may provide TRiC with the versatility of fine-tuning its interactions with certain proteins, in a manner not possible for homo-oligomeric group I chaperonins.

The specific interactions between actin and individual TRiC subunits were initially investigated by cryo-EM analyses (Llorca et al., 1999a; Llorca et al., 2000). Thereby, actin was shown to bind across the chaperonin cavity by interacting with apical domains of two TRiC subunits via the tips of its two subdomains (Figure 9B). Moreover, actin:TRiC complexes were found in either of

two different 1:4 arrangements: TRiC δ-TRiC β and TRiC δ-TRiC ε, based on the proposed clockwise subunit orientation within the ring (Llorca et al., 1999a).

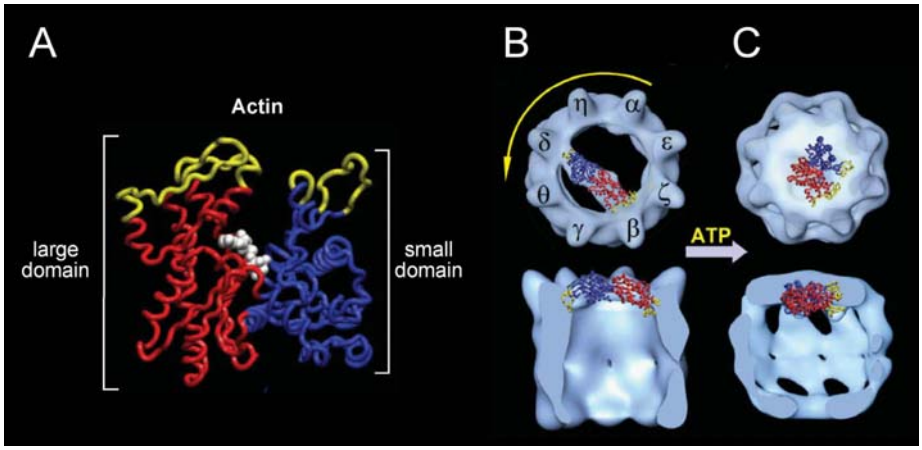

Figure 9: Interaction between actin and TRiC.

(A) Atomic structure of actin (Kabsch et al., 1990). The two topological domains of actin, historically named the large and small domain, are colored in red and blue. The putative TRiC-binding site on the tip of both domains is highlighted in yellow. **(B)** Three-dimensional reconstruction of the TRiC:actin complex in the nucleotide-free, open conformation. Top: top view; bottom: side, cut view. **(C)** Three-dimensional reconstruction of the TRiC:actin complex in the presence of ATP, generating the closed chaperonin conformation where folding occurs. The actin molecule in (B) and (C) has been colored as in (A). The yellow arrow indicates the sequential conformational change in the TRiC subunits induced by ATP binding, as proposed by Lin and Sherman (1997). The subunit arrangement within one ring of the chaperonin is depicted according to Liou and Willison (1997). Adapted from Gomez-Puertas et al. (2004).

Thus, unlike for GroEL, actin binding to TRiC was proposed to be both subunit-specific and geometry-dependent. Interestingly, in both bound orientations, actin was observed opened up across its nucleotide-binding cleft, presumably in a quasi-native and nucleotide-free state. The importance of the opening of the actin molecule during its interaction with TRiC was confirmed by an actin mutant, G150P, located in the hinge region between the small and large domains (Figure 9A). This point-mutation was proposed to block the opening of the actin molecule, hence, the interaction with the two sides of the TRiC cavity and consequently prevents its folding (McCormack et al., 2001). In contrast, recent photo-crosslinking studies demonstrated TRiC to contact newly synthesized actin with multiple chaperonin subunits while the chain emerges form the ribosomal tunnel (Etchells et al., 2005). Additionally, the interactions between the

polypeptide substrate and the chaperonin were suggested to be highly dynamic and to follow a preferred "interaction pathway", depending on the chain length of the substrate protein.

1.3.5 Role of TRiC in protein folding both *in vitro* and *in vivo*

Shortly after its discovery, TRiC was demonstrated to be the only chaperone necessary and sufficient to mediate refolding of actin and tubulin upon dilution from denaturant (Tian et al., 1995). After several cycles of folding, the native product was generated with a half-time of approximately 15-30 min. Strikingly, these proteins cannot be folded by group I chaperonins such as GroEL or Cpn60, even after multiple rounds of binding and release in an ATP-dependent manner and regardless of the presence or absence of their respective co-chaperonins (Tian et al., 1995). Interestingly, the interaction between TRiC and its substrate proteins was shown to differ considerably during refolding and the situation engaged throughout *de novo* synthesis (Frydman and Hartl, 1996). When chemically denatured actin was allowed to refold in a eukaryotic cell lysate, the protein partitioned freely between the Hsp70/40 system, the bulk cytosol, and the chaperonin TRiC. In contrast, during *in vitro* translation, Hsp70/40 and TRiC were sequentially recruited to the elongating actin chain, similar to the mechanism shown for firefly luciferase (Frydman et al., 1994), in order to protect it from exposure to the bulk cytosol during folding (Frydman and Hartl, 1996).

Subsequently, a hetero-oligomeric chaperone complex, termed Prefoldin (PFD) or GimC (for genes involved in microtubule biogenesis complex), was shown to participate in the maturation pathway of cytoskeletal proteins (Geissler et al., 1998; Vainberg et al., 1998). PFD (~90 kDa in size) consists of six subunits and has a unique quaternary structure resembling that of a jellyfish (Siegert et al., 2000). The distal regions of the six α-helical coiled-coil tentacles emanating from a β-barrel body are partially unwound and expose hydrophobic residues responsible for substrate binding. *In vitro*, PFD was shown to bind nascent (or non-native) actin chains in an ATP-independent manner and promotes their transfer to TRiC for folding (Vainberg et al., 1998; Hansen et al., 1999). In the

yeast cytosol, PFD and TRiC were proposed to form an integrated "folding compartment" which functions in close cooperation with the translation machinery and facilitates the post-translational completion of actin folding sequestered from the bulk cytosol (Siegers et al., 1999). Interestingly, single PFD-deletions resulted in reduced speed and efficiency of actin folding with non-native chains being released into the cytosol. Moreover, actin folding *in vivo* was determined to proceed with an apparent half-time of ~1 min and most likely requires only a few chaperonin cycles. Thus, *de novo* folding is at least 20-times faster than chaperonin-assisted actin refolding out of denaturant (see above).

Recently, photo-crosslinking experiments confirmed the co-translational interaction of TRiC with nascent chains, as proposed earlier (Frydman et al., 1994; Dobrzynski et al., 1996; Frydman and Hartl, 1996; McCallum et al., 2000; Etchells et al., 2005). Hence, these data do no longer support the theory of TRiC binding its substrate proteins in a strictly post-translational manner (Hansen et al., 1999). However, the exact mechanism of how TRiC is recruited to nascent chains and whether further components (*e.g.* Hsp70/40 and PFD) are necessary to assist in this process remains to be elucidated. Given these findings and the structural divergence of group II compared to group I chaperonins, TRiC is suggested to mediate the co-translational folding of multi-domain proteins which are too large for their entire encapsulation (Young et al., 2004). Thus, discrete protein domains might be folded upon their sequestration in the central cavity, whilst the rest of the protein remains outside and extends through a gap in the apical domains (Frydman et al., 1994; Llorca et al., 2001). A TRiC mediated domain-wise folding of proteins in the eukaryotic cytosol (Netzer and Hartl, 1997) would be in line with the large proteins (100-120 kDa in size) observed to transiently associate with the chaperonin (Thulasiraman et al., 1999).

1.4 Cell-free protein synthesis

Cell-free protein synthesis is a concept that is decades old and was already utilized to decipher the mechanism coupling the information stored in polynucleotides to the production of functional proteins in living cells (Nirenberg and Matthaei, 1961). Later, cell-free systems became a useful technique for

investigating the function of chaperones in the context of *de novo* protein synthesis, as mentioned previously (1.2.1).

Cell-free systems are generally prepared from crude cell extracts, containing all the enzymes and factors necessary for protein synthesis. For increased efficiency, the lysates are additionally supplemented with essential nucleotides, amino acids, salts and energy-regenerating systems. Nowadays, the most commonly used systems are derived from *E. coli* extracts (S30 fraction: soluble fraction when centrifuged at 30,000 *g*), rabbit reticulocyte lysates (RRL) and wheat germs (WG). Cell-free protein translation is routinely performed by programming such extracts with either mRNA (uncoupled reaction) or DNA (coupled transcription-translation reaction), following incubation in the test-tube. In addition to the gene of interest, the DNA template must contain specific regulatory elements including promoter, ribosomal binding site, start codon, and transcription/translation termination regions. Typically, standard *in vitro* translations (performed in small scale batch reactions) yield several micrograms of a particular protein and are suitable for the expression of a variety of different protein families.

Compared to the limitations faced by using traditional cell-based protein expression methods, cell-free protein synthesis offers a wide range of possible applications. Firstly, cell-free systems provide a simple and robust tool to rapidly convert genes into proteins, thereby leaving room for various application specific modifications. Since access to these systems is not restricted by a cell wall, reaction supplementation with additives and rapid sampling is feasible at any desired time. In this regard, synthesis conditions for each individual protein can be adjusted and controlled by the addition of particular helper molecules (*e.g.* molecular chaperones or crowding agents) to provide a defined environment supporting correct protein folding. Furthermore, cell-free translation systems are applicable to modifications which are usually not physiologically tolerated by living cells. This includes the incorporation of non-natural amino acids as well as the functional expression of toxic and/or unstable proteins. Upon supplementation with microsomes, RRL and WG are even capable of accomplishing several co- and post-translational modifications such as

phosphorylation, glycosylation or signal peptide cleavage. In recent years, improvements to cell-free protein synthesis resulted in milligram quantities of functional protein, thus, making these systems more suitable for protein consuming applications like NMR and X-ray crystallography. In summary, *in vitro* protein synthesis is a powerful technology, which contributes to a wide range of scientific and biotechnological questions.

1.5 Aim of the study

In vivo, a substantial fraction of newly synthesized proteins requires the assistance of molecular chaperones for efficient folding (Hartl and Hayer-Hartl, 2002). Despite the evolutionary conservation of the major chaperone families, eukaryotic multi-domain proteins often fold with low yield upon recombinant expression in bacterial hosts (Baneyx and Mujacic, 2004). In view of the biotechnological interest in the production of recombinant proteins, the examination of this particular phenomenon is of great importance, since the folding requirements for each protein are quite distinct.

The primary goal of this research project was to determine the role of molecular chaperones in the folding of modular eukaryotic proteins upon *in vitro* translation in an *E. coli*-based cell-free transcription/translation system. The well studied eukaryotic multi-domain proteins firefly luciferase and cytoskeletal actin served as model proteins. Importantly, correct folding of these proteins can be directly monitored by using an enzymatic luciferase assay or the interaction of actin with specific actin binding partners (*e.g.* DNase I and phalloidin), respectively. To accomplish the aims of this study, the bacterial lysate was supplemented with purified chaperones of bacterial (*e.g.* TF, DnaK/DnaJ/GrpE, and GroEL/GroES) or eukaryotic (TRiC) origin, and their effect on efficiency and mechanism of *de novo* folding of luciferase and actin analyzed.

Secondly, the eukaryotic chaperonin TRiC was examined with regard to a possible domain-wise folding mechanism, suggested previously (Frydman et al., 1994). Therefore, various N- and C-terminal actin-fusion proteins, conceivably too large for complete encapsulation in the TRiC folding cage, were generated and served as multi-domain model substrates for chaperonin assisted folding.

Upon expression of these modular proteins in *S. cerevisiae*, their ability to fold correctly and to integrate into endogenous actin cytoskeleton structures (cortical patches and actin cables) was examined. Additionally, the native state of actin within the fusion proteins was assessed by binding to DNase I upon *in vitro* translation in a eukaryotic cell-free system.

2 Materials and Methods

2.1 Materials

2.1.1 Laboratory equipment

Abimed (Langenfeld, Germany): Gilson Pipetman (2 to 1000 µl).

Amersham Pharmacia Biotech (Freiburg, Germany): ÄKTA Explorer; SMART-System; chromatography columns: Mono-Q, HiTrap-Heparin, HiTrap-Chelating, Superdex 200, Superose 6; resins: CNBr-activated Sepharose 4B, Sephadex-G50, Source 30-Q; electrophoresis power supplies: EPS200, EPS600.

Amicon (Beverly, MA, USA): concentration chambers: Centriprep, Centricon.

Avestin (Mannheim, Germany): EmulsiFlex C5 homogenizer.

Beckmann (Munich, Germany): centrifuges: Avanti J-25, Avanti J-20 XP, J-6MI, GS-6R; ultracentrifuges: Optima TLX, Optima LE-80K; DU 640 UV/VIS Spectrophotometer.

Berthold (Bad-Wildbad, Germany): luminometer Lumat LB 9507.

Biometra (Göttingen, Germany): T3 PCR-Thermocycler.

Bio-Rad (Munich, Germany): electrophoresis chambers: MiniProtean 2 and 3, Sub-CellGT; electrophoresis power supply Power PAC 300; GelAirDryer; Micro BioSpin desalting columns.

Eppendorf (Hamburg, Germany): centrifuges: 5415C, 5417R; Thermomixer Comfort.

Fuji (Tokyo, Japan): Phosphoimager FLA-2000; ImageReader LAS-3000.

Getinge (Getinge, Sweden): autoclave.

Heraeus (Hanau, Germany): incubator B12.

Hoefer Scientific Instruments (San Francisco, USA): SemiPhore blotting transfer unit.

Kinematica AG (Littau, Switzerland): Polytron PT3100 tissue homogenizer.

Mettler Toledo (Gießen, Germany): balances: AE160, AG285, PB602.

Millipore (Eschborn, Germany): deionization system MilliQ plus PF; Millex-HA filters (0.22 µm); vacuum filtration unit (0.22 µm).

MWG BiotechAG (Göttingen, Germany): gel documentation system BioCapt.

New Brunswick Scientific (Nürtingen, Germany): orbital shaker and incubator Innova 4430.

Raytest (Straubenhardt, Germany): AIDA gel imaging software version 3.5.

SA-Instruments (New Jersey, USA): fluorescence spectrometer Fluorolog-3.

Savant (New York, USA): Speedvac DNA110.

WTW (Weilheim, Germany): pH-Meter pH538.

Zeiss (Jena, Germany): microscopes: Standard25, fluorescence microscopes: Axiovert200, Axio ImagerA.1 equipped with Metamorph 6.3 software.

Philips (Amsterdam, Netherlands): electron microscope CM20.

2.1.2 Chemicals

Chemicals and biochemicals used in this work were of *pro analysi* grade and purchased from Fluka (Deisenhofen, Germany), Calbiochem (Bad Soden, Germany), Merck (Darmstadt, Germany), Sigma-Aldrich (Steinheim, Germany), Roth (Karlsruhe, Germany), and Roche (Mannheim, Germany) unless stated otherwise.

Amersham Pharmacia Biotech (Freiburg, Germany): western blotting detection systems: ECL, X-ray film; gel filtration HMW und LMW calibration kit; native electrophoresis HMW calibration kit; radiolabeled amino acids: [^{35}S]-Met.

BioMol (Hamburg, Germany): IPTG, HEPES.

BioRad (Munich, Germany): ethidiumbromide; Bradford Protein-Assay.

Clontech (Mountain View, USA): herring testes carrier DNA.

Difco (Heidelberg, Germany): Bacto tryptone, Bacto yeast extract, Bacto agar, Bacto peptone, Bacto yeast nitrogen base without amino acids.

Fermentas (St. Leon-Rot, Germany): GeneRuler 1kb DNA Ladder.

Invitrogen (Karlsruhe, Germany): protein marker for SDS PAGE.

Molecular Probes (Eugene, USA): rhodamine phalloidin.

National Diagnostic (Hessle, England): Protogel (AA:BA=30:0.8).

New England Biolabs (Frankfurt a. Main, Germany): restriction enzymes; calf intestinal alkaline phosphatase (CIP); T4 DNA ligase; prestained protein marker for SDS PAGE.

Promega (Mannheim, Germany): Luciferase Assay System; Pfu DNA polymerase; TNT Coupled Reticulocyte Lysate System.

Qiagen (Hilden, Germany): QIAprep Plasmid Mini and Midi kits; QIAquick PCR purification and gel extraction kit; Ni-NTA agarose.

Roche (Mannheim, Germany): RTS *in vitro* translation systems: RTS 100 *E. coli* HY Kit, RTS 100 Wheat Germ CECF Kit.

Schleicher & Schuell: protran nitrocellulose transfer membrane; fluted paper filter 595-1/2 (270 mm).

2.1.3 Media and buffers

Media and buffers were prepared with demineralized water and autoclaved or sterile filtered unless stated otherwise. Concentrations are given in (v/v) for liquids and (w/v) for solids, respectively.

2.1.3.1 Media

LB medium: 10 g/l tryptone, 5 g/l yeast extract, 5 g/l NaCl, (+15 g/l agar for solid medium).

YPD medium: 10 g/l yeast extract, 20 g/l peptone, 20 g/l glucose, (+20 g/l separately autoclaved agar for solid medium).

SC-*Drop-out* medium: 6.7 g/l yeast nitrogen base without amino acids, 20 g/l glucose, 2 g/l Drop-out mix, (+15 g/l agar for solid medium).

***Drop-out* mix:** 0.5 g adenine hemisulfate, 0.2 g *para*-aminobenzoic acid, 4 g leucine, and 2 g alanine, arginine, asparagine, aspartic acid, cysteine, glutamine, glutamic acid, glycine, histidine, inositole, isoleucine, lysine, methionine, phenylalanine, proline, serine, threonine, tryptophan, tyrosine, uracil, valine, respectively. For selective reasons, media lacking uracil, tryptophan, histidine or leucine were used for strains prototrophic for these amino acids.

Carbon sources: 20% glucose; 20% raffinose; 20% galactose. All solutions were sterile filtered and added separately to the autoclaved media to the final concentrations indicated.

2.1.3.2 Buffers and stock solutions

PBS: 137 mM NaCl, 2.7 mM KCl, 8.4 mM Na_2HPO_4, 1.5 mM KH_2PO_4, pH 7.4.

PonceauS: 0.2% PonceauS, 3% trichloracetic acid.

TAE: 40 mM Tris-Acetate, 1 mM EDTA, pH 8.0.

TBS: 50 mM Tris, 150 mM NaCl, pH 7.5.

TBS-T: 0.1% Tween20 in TBS.

All other buffers and solutions were prepared as convenient stock solutions and either autoclaved or filter sterilized before usage, if applicable.

2.1.4 Bacterial and yeast strains

2.1.4.1 E. coli strains

Strain	Genotype	Reference
BL21(DE3)	*B F- dcm ompT hsdS(r_{B-} m_{B-}) gal (DE3)*	Novagene
DH5αF′	*F'/endA1 hsdR17(r_K-m_K+) supE44 thi-1 recA1 gyrA ($Na1^r$) relA1 D(lacZYA-argF)$_{U169}$(m80lacZDM15)*	Novagene

2.1.4.2 Yeast strains

Strain	Genotype	Reference
YPH499	*MATa ura3-52 lys2-801^{amber} ade2-101^{ochre} trp1Δ63 his3Δ200 leu2Δ1*	(Sikorski and Hieter, 1989)
Δ*reg* (KSY355)	*MATa ura3-52 lys2-801^{amber} ade2-101^{ochre} trp1Δ63 his3Δ200 leu2Δ1 Δreg1::loxP*	Katja Siegers

2.1.5 Plasmids and Oligonucleotides

2.1.5.1 Plasmids

Plasmid	Description	Reference
pET3a luciferase	firefly luciferase (FL) for expression in S30 and RRL lysate	Suranjana Guha
pET3a TFwt	trigger factor wild type (TF) for expression in BL21(DE3)	Suranjana Guha
pET3a TFmt	trigger factor FRK/AAA mutant ($TF_{FRK/AAA}$) for expression in BL21(DE3)	Suranjana Guha
pJMBiA1	yeast actin for expression in S30 and RRL lysate	José M. Barral
pRSET6a mouse actin	mouse β-actin for expression in BL21(DE3), S30 and RRL	(Siegers et al., 1999)
pCHAct-L16-cGFP	yeast actin-L16[a)]-GFP (AG) in pCHORF-L16-cGFP vector for expression in S30 and RRL lysate	(Chang et al., 2005)
pMS BA	BFP-L16[b)]-yeast actin (BA) for subcloning	this work
pMS BG	BFP-L15[c)]-GFP (BG) for expression in S30 and RRL lysate	this work
pMS GA	GFP-L18[d)]-yeast actin (GA) for expression in S30 and RRL lysate	this work
pMS BAG	BFP-L16[b)]-yeast actin-L16[a)]-GFP (BAG) for expression in S30 and RRL lysate	this work
pMS BA-TEV	BFP-L16TEV[e)]-yeast actin (BA-TEV) for subcloning	this work
pMS BTAG	BFP-L16TEV[e)]-yeast actin-L16[a)]-GFP (BTAG) for expression in S30 and RRL lysate	this work

pMS BTAG-G150P	BFP-L16TEV[e)]-yeast actinG150P-L16[a)]-GFP (BTAG-G150P) for expression in S30 and RRL lysate	this work
pMS CAG	mCherry-L16[b)]-yeast actin-L16[a)]-GFP (CAG) for expression in S30 and RRL lysate	this work
pMS LA	firefly luciferase-L17[f)]-yeast actin (LA) for subcloning	this work
p415 yeast actin	yeast actin for expression in yeast	Hung-Chun Chang
p415GAL1 GFP	GFP for expression in yeast	(Chang et al., 2005)
p415 BAG	BFP-L16[b)]-yeast actin-L16[a)]-GFP (BAG) for expression in yeast	this work
p415 BTAG	BFP-L16TEV[e)]-yeast actin-L16[a)]-GFP (BTAG) for expression in yeast	this work
p415 BTAG-G150P	BFP-L16TEV[e)]-yeast actinG150P-L16[a)]-GFP (BTAG-G150P) for expression in yeast	this work
p415 CAG	mCherry-L16[b)]-yeast actin-L16[a)]-GFP (CAG) for expression in yeast	this work
p415 CG	mCherry-L15[c)]-GFP (CG) for expression in yeast	this work
p415 GA	GFP-L18[d)]-yeast actin (GA) for expression in yeast	this work
p415GAL1Act-L16-cGFP	yeast actin-L16[a)]-GFP (AG) in p415GAL1ORF-L16-cGFP vector for expression in yeast	(Chang et al., 2005)
p415 LA	firefly luciferase-L17[f)]-yeast actin (LA) for subcloning	this work
pIVEX1.3WG CAG	mCherry-L16[b)]-yeast actin-L16[a)]-GFP (CAG) for expression in WG	this work
pIVEX1.3WG CG	mCherry-L15[c)]-GFP (CG) for expression in WG	this work

The linkers in all fusion proteins were designed according to the L16-linker described previously (Chang et al., 2005). Minimal differences in length and amino acid sequences are due to the restriction endonuclease sites used for cloning. Amino acids identical in all linkers are highlighted in gray:

[a)] L16: TSGSAASAAGAGEAAA
[b)] L16: SGSAASAAGAGEAAAH
[c)] L15: SGSAASAAGAGEAAA
[d)] L18: GASGSAASAAGAGEAAAH
[e)] L16TEV: SGSAASAAGAG***ENLYFQG***EAAAH (***ENLYFQG:*** TEV protease cleavage site)
[f)] L17: ASGSAASAAGAGEAAAH

Construction of **pMS GA**: The coding region of GST in pCHGFP-L16-GST (Hung-Chun Chang) was excised with *Nde* I and *Nhe* I restriction endonucleases and replaced by the coding region of yeast actin from pCHAct-L16-cGFP excised with *Nde* I and *Spe* I.

Construction of **pMS BA**: The coding region of BFP was amplified by PCR (primer #1 and #2) from pGEMEX2BFP (Heim et al., 1994) and inserted into pMS GA at the *Xba* I and *Not* I restriction endonuclease sites, replacing GFP.

Construction of **pMS BAG**: The coding region of GFP (including parts of yeast actin and the linker region) from pCHAct-L16-cGFP was excised with *Kpn* I and *Dra* III restriction endonucleases and inserted into pMS BA.

Construction of **pMS BG**: The coding region of yeast actin from pMS BAG was excised with the double cutting *Not* I restriction endonuclease. The resulting backbone was religated.

Construction of **p415 BAG**: The coding region of BA from pMS BAG was excised with *Xba* I and *Spe* I restriction endonucleases and inserted into p415GAL1Act-L16-cGFP, replacing yeast actin.

Construction of **pMS CAG and p415 CAG**: The coding region of mCherry was amplified by PCR (primer #3 and #4) from pRSETB mCherry (Shaner et al., 2004) and inserted between *Xba* I and *Nde* I restriction endonuclease sites in pCHAct-L16-cGFP and p415GAL1Act-L16-cGFP, respectively.

Construction of **pIVEX1.3WG CAG**: The coding region of CAG was amplified by PCR (primer #5 and #6) from p415 CAG and inserted into pIVEX1.3WG (Roche) at the *Nco* I and *Sal* I restriction endonuclease sites by partial digestion.

Construction of **pIVEX1.3WG CG** and **p415 CG**: The coding region of yeast actin from pIVEX1.3WG CAG and p415 CAG, respectively, was excised with the double cutting *Not* I restriction endonuclease. The resulting backbone was religated.

Construction of **p415 GA**: The coding region of yeast actin was at first excised from pMS GA and inserted into pCHLuc-L16-cGFP (Chang et al., 2005) at the *Not* I and *Dra* III restriction endonuclease sites (replacing GFP) resulting in pMS LA. Secondly, actin was amplified by PCR (primer #7 and #8) from pMS LA and inserted into p415GAL1Luc-L16-cGFP (Chang et al., 2005) at the *Not* I and *Nhe* I restriction endonuclease sites (replacing GFP) resulting in p415 LA. Thirdly, the coding region of actin was excised with *Not* I and *Sal* I restriction endonucleases from p415 LA and inserted into p415GAL1nGFP-L16-Luc (Chang et al., 2005), replacing firefly luciferase.

Construction of **pMS BA-TEV**: The coding region of BFP was amplified by PCR (primer #1 and #9) from pMS BA and inserted back into the same plasmid at the *Xba* I and *Not* I restriction endonuclease sites. Thereby, a TEV protease cleavage site (ENLYFQG) was introduced into the linker between BFP and yeast actin.

Construction of **pMS BTAG** and **p415 BTAG**: The coding region of BA-TEV was amplified by PCR (primer #1 and #10) from pMS BA-TEV and inserted between

Xba I and *Spe* I restriction endonuclease sites in pMS BAG and p415 BAG, respectively.

Generation of **pMS BTAG-G150P** and **p415 BTAG-G150P** was performed by site-directed mutagenesis using pMS BTAG and p415 BTAG as template plasmids. PCR reactions were carried out in presence of primer #11 and #12, respectively.

2.1.5.2 Oligonucleotides

Primer	Sequence	Direction
#1 BFPup2	5´ CTA GTC TAG AAA TAA TTT TGT TTA ACT TTA AGA AGG AGA TAT ACA TAC CAT GAG TAA AGG AGA AGA ACT TTT C 3´	forward
#2 BFPdn	5´ TTT TCC TTT TGC GGC CGC TTC GCC AGC ACC AGC AGC GGA GGC AGC GGA TCC ACT TTT GTA TAG TTC ATC CAT GCC ATG 3´	reverse
#3 LimChf	5´ C TAG TCT AGA AAT AAT TTT GTT TAA CTT TAA GAA GGA GAA TTC ATG GTG AGC AAG GGC GAG GAG GAT AAC 3´	forward
#4 mChLir	5´ GGG AAT TCC ATA TGC GCG GCC GCT TCG CCA GCA CCA GCA GCG GAG GCA GCG GAT CCA CTC TTG TAC AGC TCG TCC ATG CCG CCG GTG 3´	reverse
#5 CAGf	5´ CAT GCC ATG GTG AGC AAG GGC GAG 3´	forward
#6 CAGr	5´ TCC GCG GCC GCT ATG GCC GAC GTC GAC GGT ATC GAT AAG CTT TAG 3´	reverse
#7 LiyAf2	5´ AGG AGC GGC CGC GCA TAT GGA TTC 3´	forward
#8 yAr2	5´ CTA GCT AGC ACC GAA ACA CTT GTG GTG AAC G 3´	reverse
#9 B-TEV-Ar	5´ TTT TCC TTT TGC GGC CGC TTC GCC CTG AAA ATA CAG GTT TTC GCC AGC ACC AGC AGC GGA GGC AG 3´	reverse
#10 yASper	5´ GG ACT AGT GAA ACA CTT GTG GTG AAC 3´	reverse
#11 G150Pf	5´ CT TCC GGT AGA ACT ACT CCA ATT GTT TTG GAT TCC GGT G 3´	forward
#12 G150Pr	5´ C ACC GGA ATC CAA AAC AAT TGG AGT AGT TCT ACC GGA AG 3´	reverse

2.1.6 Antibodies

Antibody	Species	Reference
Primary Antibodies		
anti-Actin	mouse, monoclonal	Amersham N350
anti-Act1p	rabbit, polyclonal	Katja Siegers
anti-Adh1p	rabbit, polyclonal	Katja Siegers
anti-CCTα	rat, monoclonal	StressGen CTA-191
anti-GFP	mouse, monoclonal	Roche 1 814 460

Secondary Antibodies		
anti-mouse IgG-HRP	goat, polyclonal	Sigma A4416
anti-rabbit IgG-HRP	goat, polyclonal	Sigma A9169
anti-rat IgG-HRP	rabbit, polyclonal	Sigma A5795

2.1.7 Proteins

2.1.7.1 Special enzymes

Invitrogen (Karlsruhe, Germany): TEV protease.
Roche (Mannheim, Germany): Benzonase, creatine kinase, DNase I, RNase A.
Sigma-Aldrich (Steinheim, Germany): apyrase, lysozyme, firefly luciferase.

2.1.7.2 Chaperones

The following chaperones (purified according to the protocol referenced) were obtained from the laboratory collection of the Department of Cellular Biochemistry, Max Planck Institute of Biochemistry:

DnaK (Jordan and McMacken, 1995) with modifications,
DnaJ (Zylicz et al., 1985),
GrpE-$(His)_6$,
GroES (Hayer-Hartl et al., 1996),
GroEL (Hayer-Hartl et al., 1994) with modifications.

2.2 Molecular biology methods

All experimental methods used throughout this work were performed according to "Molecular Cloning" (Sambrook et al., 1989) unless stated otherwise.

2.2.1 Plasmid purification

A single *E. coli* colony containing the plasmid of interest was inoculated in LB medium (supplemented with the appropriate antibiotic) and shaken overnight at 37 °C. Plasmid DNA was purified using the QIAprep Plasmid kits according to the manufacturer's protocol.

2.2.2 DNA analytical methods

DNA concentrations were measured by UV absorption spectroscopy at λ=260 nm. An optical density of OD_{260}=1 corresponds to approximately 50 µg/ml double stranded DNA and 31 µg/ml oligonucleotides, respectively.

Agarose gel electrophoresis was performed with 1-2% TAE-buffered agarose gels (TAE, 2.1.3.2) supplemented with 10 µg/ml ethidiumbromide. Size fractionation of DNA fragments was carried out at 80-100 V in TAE buffer. Prior to electrophoresis, loading buffer (6x loading buffer: 60% glycerol, 0.25% bromphenol blue, 0.25% xylene cyanol FF) was added to the DNA samples to a 1x concentration.

Primers were purchased from Metabion (Martinsried, Germany), DNA sequencing was performed by Medigenomix GmbH (Martinsried, Germany) or Sequiserve (Vaterstetten, Germany).

2.2.3 PCR amplification

DNA was amplified using PCR (polymerase chain reaction) according to a standard protocol. Modifications in the reaction setup and the running conditions were made when necessary.

Typical PCR reaction:

DNA template	<0.2 µg/50 µl
Primers	0.5 µM each
dNTPs	200 µM each
Pfu DNA Polymerase	3 U/50 µl
Polymerase buffer	1x
DMSO	10%

Typical PCR cycling conditions (30 cyles):

Initial denaturation	95 °C for 2 min
Cycle denaturation	95 °C for 30-60 s
Annealing	50-55 °C for 30-60 s
Extension	72 °C for 2-6 min (2 min/kb of DNA)
Final extension	72 °C for 10 min
Pause	4 °C indefinite

Following the PCR reaction, the amplified DNA was purified using the QIAquick PCR purification and gel extraction kit.

2.2.4 DNA restriction digestions and ligations

DNA restriction digestions were performed according to the product instructions of the respective enzymes. Typically, a 20 µl preparative reaction containing the purified PCR product or plasmid DNA, 0.1 mg/ml BSA and 1 µl of each restriction enzyme in the appropriate reaction buffer was used. In order to avoid religation, dephosphorylation of vector DNA cohesive ends was carried out using calf intestinal alkaline phosphatase (CIP) following subsequent purification with QIAquick PCR purification and gel extraction kit according to the manufacturer's instructions.

DNA ligations were performed in the presence of T4 DNA ligase. Typically, for a 10 µl reaction containing 1 µg DNA consisting of dephosphorylated vector DNA and an insert fragment in a molar ratio between 1:3 and 1:10, 1 µl T4 DNA ligase (400 U/µl) and 1x ligase buffer was used. The ligation was carried out for 1 h at 25 °C or, for increased efficiency, overnight at 16 °C. The complete reaction was used to transform chemically competent *E. coli* DH5α cells.

2.2.5 Preparation and transformation of competent *E. coli* cells

Competent *E. coli* DH5α cells for standard cloning reactions were prepared as described (Nishimura et al., 1990). In brief, a 50 ml culture, inoculated with 0.5 ml of an *E. coli* DH5α overnight culture, was grown in medium A (LB medium supplemented with 10 mM $MgSO_4$ and 0.2% glucose) to mid-logarithmic phase of growth. The cells were kept on ice for 10 min and then pelleted at 1,500 *g* for 10 min at 4 °C. After the cells were gently resuspended in 0.5 ml of prechilled medium A, 2.5 ml of storage solution B (36% glycerol, 12% PEG-7500, 12 mM $MgSO_4$ added to LB medium and filter sterilized) was added and mixed well without vortexing. Cells were divided in 50 µl aliquots and stored at -80 °C.

For transformations, competent cells were thawed on ice, immediately mixed with 1 µl plasmid DNA or 10 µl of a ligation reaction and incubated on ice for 30 min. Cells were then subjected to a heat shock at 42 °C for 45 s and immediately chilled on ice for 2 min. 800 µl of prewarmed LB medium was

added and upon phenotypical expression for 60 min at 37 °C, the transformation reaction was plated on selective LB-agar plates and incubated at 37 °C overnight or until colonies had developed.

2.2.6 Site-directed mutagenesis

Plasmid DNA, encoding the gene of interest, was isolated from *E. coli* DH5α (supporting *dam* methylation of DNA) as described (2.2.1). The template DNA was amplified using PCR in the presence of complementary primers containing the mutation to be introduced. In contrast to a regular PCR reaction, the extension temperature was reduced to 69 °C and only 12-15 reaction cycles were performed. After reaction completion, the parental DNA was digested by *Dpn I* (20 U/50 µl PCR reaction, 1 h at 37 °C), an endonuclease specific for methylated DNA. Finally, 1 µl of the reaction was transformed in competent *E. coli* DH5α cell and the mutation of the isolated plasmid DNA confirmed by DNA sequencing.

2.2.7 Yeast culture methods

All experimental yeast techniques were performed according to "Yeast Protocols" (Evans, 1996) unless stated otherwise.

2.2.7.1 Cultivation of yeast cells

S. cerevisiae strains were grown in YPD or synthetic complete SC-*Drop-out* medium (2.1.3.1) at 30 °C on agar plates or in liquid culture. For short term storage, cells were streaked on agar plates and stored at 4 °C. For long term storage, liquid cultures were mixed in a 1:1 ratio with 50% glycerol and stored at -80 °C.

The yeast strains used throughout this study contained a point mutation in the *ade2-101* gene, thus, the media used for cultivation were additionally supplemented with 0.01% adenine.

2.2.7.2 Transformation of yeast cells

Yeast transformations were performed with modifications to the protocol described (Gietz et al., 1992). In brief, 1-2 ml of exponentially growing cells (OD_{600}~1.0) were pelleted at 2,500 *g* for 3 min and washed with TE/LiAc (made fresh from 10x stock solutions: 10x TE [0.1 M Tris, 10 mM EDTA, pH 7.5] and 10x LiAc [1 M LiAc]). Cells were resuspended in 100 µl TE/LiAc and mixed thoroughly with 50 µg of denatured herring sperm carrier DNA, 1 µg transforming DNA and 300 µl of a 40% PEG solution (40% PEG 4000, 1x TE, 1x LiAc, made fresh from stocks of sterile 50% PEG, 10x TE, and 10x LiAc). After incubation at 30 °C for 30 min with gentle agitation, cells were subjected to heat shock for 15 min at 42 °C and subsequently pelleted at 4,500 *g* for 1 min. Transformation reactions were plated on selective agar plates and incubated at 30 °C until colonies developed.

2.2.7.3 Lysis of yeast cells

For the preparation of yeast crude protein extracts under denaturing conditions approximately 2 OD_{600} units of cells were harvested (2,000 *g* for 5 min at 4 °C) and washed with H_2O. The pellet was resuspended in H_2O and incubated with 240 mM NaOH and 1% β-mercaptoethanol for 15 min on ice. TCA was added to a final concentration of 6.5% and incubated for 10 min on ice. The denatured proteins were pellet by centrifugation (20,000 *g* for 30 min at 4 °C) and the pellet resuspended in HU-buffer (8 M urea, 5% SDS, 200 mM Tris (pH 6.8), 0.1 mM EDTA, 1% bromphenol blue). Prior to loading on SDS gels, samples were incubated at 65 °C for 10 min.

For the preparation of cytosolic extracts under native conditions, an appropriate amount of yeast cells was harvested (2,000 *g* for 5 min at 4 °C) and resuspended in 250 µl glass-bead lysis buffer (PBS, 5 mM EDTA, EDTA-free Complete protease inhibitors, 10 µM Antipain, 10 µM Leupetin, 1 µM Aprotinin, 0.3 µM Trypsin-inhibitor, 0.4 µM Pepstatin, 10 µM Chymostatin, 0.5% Tween20). Cell lysis was performed by agitation with glass-beads for 6x 30 s at 4 °C. Upon lysis, beads were washed twice with 250 µl yeast lysis buffer and combined with

the crude lysate. Non-lysed cells were separated from the lysate by centrifugation (2,000 *g* for 5 min at 4 °C).

2.3 Protein biochemical methods

2.3.1 Protein analytical methods

2.3.1.1 Determination of protein concentrations

Protein concentrations of complex protein mixtures and cell lysates were determined spectrophotometrically at λ=595 nm using Bradford reagent (Bradford, 1976) and BSA calibration curves.

Concentrations of purified proteins were determined on the basis of the Beer-Lambert law and their theoretical extinction coefficients at λ=280 nm (Gill and von Hippel, 1989), as calculated by the ProtParam tool at the ExPASy proteomics server (http://www.expasy.ch) unless mentioned otherwise. Molar concentrations of chaperones are expressed for the native state oligomers.

2.3.1.2 SDS-polyacrylamide gel electrophoresis (SDS-PAGE)

SDS-PAGE was performed using a discontinuous buffer system under denaturing and reducing conditions (Laemmli, 1970). Typically, gels were poured with a 5% polyacrylamide stacking gel on top of a 9-15% polyacrylamide separating gel, depending on the required resolution. SDS sample buffer was added to the protein samples to a 1x concentration. Prior to loading, samples were boiled at 95 °C for 5 min following a short centrifugation step at 20,000 *g* for 2 min. Electrophoresis was carried out at a constant current of 30 mA/gel in running buffer.

Stacking gel: 5% acrylamide/bisacrylamide (30:0.8), 130 mM Tris (pH 6.8), 0.1% SDS, 0.1% TEMED, 0.1% ammonium persulfate.

Separating gel: 9-15% acrylamide/bisacrylamide (30:0.8), 0.75 M Tris (pH 8.8), 0.1% SDS, 0.1% TEMED, 0.05% ammonium persulfate.

4x SDS sample buffer: 240 mM Tris (pH 6.8), 8% SDS, 40% glycerol, 1.4 M β-mercaptoethanol, 0.02% bromphenol blue.

Running buffer: 50 mM Tris-Base, 380 mM glycine, 0.1% SDS.

Coomassie stain: 0.1% Coomassie Brilliant Blue R250, 30% methanol, 10% acetic acid.

Destain solution: 30% methanol, 10% acetic acid.

SDS gels not intended for further immunodetection analysis were fixed and stained in Coomassie stain. Unspecific background stain was removed by incubation in destaining solution. Radiolabeled proteins were visualized and quantified by phosphoimaging (Fuji FLA-2000) and AIDA software.

2.3.1.3 Bis-Tris native polyacrylamide gel electrophoresis (native-PAGE)

The discontinuous native gel system utilized was performed essentially as described (Schagger and von Jagow, 1991). Gels were composed of two layers (5.5% polyacrylamide on top of 12.5%). The cathode buffer consisted of 50 mM Tricine and 15 mM Bis-Tris (pH 7.0). The anode buffer contained 50 mM Bis-Tris (pH 7.0). Reaction mixtures were adjusted with native gel loading buffer to final concentrations of 50 mM Bis-Tris (pH 7.0), 5% glycerol, 2 mM DTT, 0.01% bromphenol blue. The gels were initially run at 150 V for 45 min followed by 300 V at 4 °C until the dye front migrated to the bottom of the gel. Proteins were visualized as mentioned previously (2.3.1.2).

2.3.1.4 Western blot analysis of SDS-PAGE gels

Western blotting was carried out in a semi-dry blotting unit. Upon separation by SDS-PAGE, proteins were transferred to nitrocellulose membranes by applying a constant current of ~1 mA/cm^2 gel size in 25 mM Tris, 192 mM glycine, 20% methanol for 1.5 h.

Prior to blocking the membranes with 5% skim milk powder in TBS (2.1.3.2) for 1 h, transfer efficiency was verified by PonceauS (2.1.3.2) staining. The membranes were then incubated with primary antibodies (diluted to a suitable concentration in 5% milk-TBS) for 1 h at RT or overnight at 4 °C, followed by the incubation with HRP-conjugated secondary antibodies (diluted 1:1000 in milk-TBS) for 1 h at RT. Extensive washing between the incubation steps was performed with TBS-T (2.1.3.2).

Immunodetection was carried out with the ECL system and exposure to X-ray films or the ImageReader (Fuji LAS-3000), followed by quantitative image analysis with AIDA software, if required.

2.3.1.5 Dot blot analysis

Dot blots were performed for fast and qualitative protein detection in column fractions during protein purification. Typically, 2-5 µl of each fraction were applied to a nitrocellulose membrane and air-dried for 10 min. Immunodetection was carried out as described for western blotting analysis of SDS-PAGE gels (2.3.1.4) with the exception that all incubation times were reduced to half.

2.3.2 TCA precipitation of proteins

Protein solutions were concentrated by TCA precipitation, when necessary. Therefore, the protein sample was mixed 1:1 with 25% TCA and incubated for 15 min on ice. The precipitated proteins were pelleted by centrifugation (20,000 *g* for 15 min at 4 °C). After washing twice with acetone (-20 °C), pellets were resuspended in SDS sample buffer and boiled at 95 °C for 5 min.

2.3.3 Protein purification

All protein purification steps were performed at 4-8 °C unless stated otherwise.

2.3.3.1 Purification of TRiC from bovine testis

The eukaryotic chaperonin TRiC was purified according to the protocol described by Ferreyra and Frydman (2000) with modifications. Fresh bovine testes (~200 g) were skinned, cut up in small pieces and subsequently homogenized using a Polytron tissue homogenizer in an equal volume of buffer A (50 mM HEPES pH 8.0, 2 mM EGTA, 10 mM NaCl, 5 mM $MgCl_2$, 10% glycerol, 2 mM DTT, 1 mM PMSF, EDTA-free Complete protease inhibitors). The homogenate was incubated with 5 U/ml Benzonase for 30 min and clarified by centrifugation (40,000 *g* for 45 min followed by 130,000 *g* for 1 h). The

supernatant was passed through a fluted filter paper and subsequently applied to a 250 ml Source 30-Q column equilibrated in buffer B (20 mM HEPES pH 8.0, 2 mM EDTA, 5 mM $MgCl_2$, 10% glycerol, 2 mM DTT). Elution was carried out by an NaCl gradient (0-300 mM) in buffer B. TRiC-containing fractions were pooled after identification by dot blot analysis with an antibody specific for the α-subunit of TRiC (anti-CCTα, 2.1.6). The NaCl concentration of this pool was adjusted to 200 mM prior to loading on a 20 ml HiTrap Heparin column equilibrated in buffer C (20 mM HEPES pH 7.4, 2 mM EDTA, 5 mM $MgCl_2$, 10% glycerol, 2 mM DTT) containing 200 mM NaCl. TRiC-containing material was eluted by an NaCl gradient (200-700 mM) in buffer C. TRiC fractions were pooled, diluted with buffer C to reach an NaCl concentration of 50 mM and applied to a 20 ml Mono-Q column equilibrated in buffer C containing 50 mM NaCl. After protein elution with a NaCl gradient (50-500 mM) in buffer C, TRiC-containing fractions were concentrated with Centriprep devices (MWCO 100,000 kDa) and passed through a HiLoad Superdex 200 column (XK 16/60) equilibrated in 20 mM HEPES pH 7.4, 1 mM $MgCl_2$, 100 mM NaCl, 10% glycerol, 1 mM DTT. Fractions eluting at ~900 kDa were pooled and concentrated (as above) to ~25 mg/ml, aliquoted and snap-frozen in liquid nitrogen. The protein yield was determined by Bradford analysis and was typically ~8 mg *per* 100 g of starting material. SDS-PAGE followed by Coomassie blue staining revealed TRiC purity to be >95%. Functionality of the TRiC complex was assessed by an actin refolding assay as described in section 2.4.4.

2.3.3.2 Purification of Trigger Factor

TF and $TF_{FRK/AAA}$ (residues $_{44}FRK_{46}$ were replaced by alanines) were purified according to the protocol described by Hesterkamp et al. (1997) with modifications. *E. coli* BL21(DE3) cells harboring the expression vector pET3a encoding the C-terminally His_6-tagged wild-type or FRK/AAA TF mutant were grown to OD_{600}~0.5 in LB medium (supplemented with 100 µg/ml ampicillin). Expression was induced with 1 mM IPTG for 3 h at 37 °C. Cells were harvested by centrifugation (4,000 *g* for 1 h) and resuspended in buffer D (25 mM KPi pH 8.0, 300 mM NaCl, 10 mM imidazole, 10% glycerol) containing 0.5%

TritonX-100 and EDTA-free Complete protease inhibitors. The suspension was frozen in liquid nitrogen and thawed before incubation with lysozyme (0.5 mg/ml) for 30 min. Following Benzonase treatment (5 U/ml) for 30 min on ice, cell debris was removed by centrifugation for 30 min at 100,000 *g*. The supernatant was applied to a 15 ml Ni-NTA agarose column equilibrated in buffer D. After a washing step with buffer D containing 20 mM imidazole, protein elution was performed with 250 mM imidazole in buffer D. Fractions containing trigger factor were pooled and diluted with buffer E (20 mM HEPES pH 7.4, 1 mM DTT, 10% glycerol) to reach a final NaCl concentration of 50 mM. The diluted protein solution was loaded on an 8 ml Mono-Q column equilibrated in buffer E containing 50 mM NaCl. Protein elution was achieved by applying a shallow NaCl gradient from 50-500 mM in buffer E. Trigger factor containing fractions were pooled and dialyzed against 20 mM HEPES pH 7.4, 100 mM NaCl, 1 mM DTT, 10% glycerol. Protein aliquots were snap-frozen in liquid nitrogen and stored at -80 °C. The accurate protein concentration of trigger factor samples was determined at 280 nm (theoretical extinction coefficient ε=15,930 $M^{-1}cm^{-1}$).

2.3.3.3 Purification of mouse β-actin

E. coli BL21(DE3) cells transformed with the bacterial expression vector pRSET6a encoding mouse β-actin (Siegers et al., 1999) were grown to OD_{600}~0.5 in LB medium (supplemented with 100 µg/ml ampicillin). Expression of actin was induced with 1 mM IPTG for 3 h at 37 °C. Cells were harvested by centrifugation (2,000 *g* for 15 min) and the resulting pellets resuspended in lysis buffer (50 mM Tris pH 7.4, 100 mM NaCl, 10 mM $MgCl_2$, 1 mM DTT, EDTA-free Complete protease inhibitors). Lysis was performed by freeze-thawing and incubation with 2 mg/ml lysozyme for 20 min. The lysate was incubated with 5 U/ml Benzonase for 30 min and clarified by centrifugation (22,000 *g* for 45 min). The pellet was washed extensively with IB-buffer (10 mM Tris pH 7.4, 150 mM NaCl, 1 mM EDTA, 0.1% SDS, 1.0% TritonX-100) followed by wash buffer (50 mM Tris pH 7.4, 100 mM NaCl, 1 mM DTT). The remaining actin inclusion bodies were resuspended in 20 mM Tris pH 7.4, 8 M urea, 2 mM DTT. SDS-PAGE followed by Coomassie blue staining revealed actin purity to be

>95%. Protein concentration of denatured mouse β-actin was determined at 280 nm (theoretical extinction coefficient ε=42,320 $M^{-1}cm^{-1}$). This material was used as a protein standard for quantitative western blotting.

2.3.3.4 Enrichment of the actin fusion protein CAG from yeast

YPH499 *S. cerevisiae* cells were transformed with the yeast expression vector p415 encoding the C-terminally His_6-tagged CAG actin-fusion protein and grown to OD_{600}~0.3 in SC-Leu medium. Expression was induced with 2% galactose for 24 h at 30 °C. Cells were harvested by centrifugation (4,000 *g* for 30 min) and lysed in PBS, 300 mM NaCl, 5% glycerol, 1% TritionX-100, EDTA-free Complete protease inhibitors, 1 mM PMSF, 10 mM imidazole using an EmulsiFlex high-pressure homogenizer according to the manufacturer's instructions. The lysate was cleared by centrifugation (40,000 g for 1 h) and the supernatant applied to a HiTrap metal-chelating column (pre-charged with Ni^{2+}-ions) and equilibrated in buffer F (PBS, 5% glycerol, 300 mM NaCl) containing 10 mM imidazole. The column was washed with a gradient of 10-50 mM imidazole in buffer F and the protein eluted with 500 mM imidazole in buffer F. CAG-containing fractions were concentrated with Centriprep devices (MWCO 30,000 kDa) and passed through a 120 ml HiLoad Superdex 200 column equilibrated in PBS containing 5% glycerol. Detection of CAG in the fractions was performed by SDS-PAGE and Coomassie blue staining followed by a concentration step as described above. Purity of the enriched CAG sample was estimated to be ~50% corresponding to ~0.5 µM CAG when compared to a purified standard protein of known concentration. Protein aliquots were snap-frozen in liquid nitrogen and stored at -80 °C.

2.3.4 Protein synthesis using *in vitro* transcription/translation systems

In vitro translations were performed from plasmids with a T7 promoter. For protein expression in a prokaryotic model system the coupled RTS *E. coli* 100 HY transcription/translation system from a bacterial S30 lysate (S30) was utilized. As a eukaryotic expression system the TNT coupled system from

rabbit reticulocyte lysate (RRL) or the coupled RTS 100 Wheat Germ CECF kit (WG) was used. S30 and RRL translation reactions were typically run for 1 h at 30 °C. WG reactions were carried out for 24 h at 24 °C and 900 rpm in the CECF two-chamber device. The specific activity of [^{35}S]-Met was identical in all reactions. For analysis of soluble and insoluble material, the reactions were centrifuged (22,000 *g* for 30 min at 4 °C) to separate supernatant and pellet fractions. For kinetic experiments, reactions were run for longer periods, as indicated. Unless indicated otherwise, chaperones were added to S30 translations in the following concentrations: TRiC: 5 μM; TF: 5 μM; DnaK/DnaJ/GrpE (KJE): 10, 2 and 6 μM; and GroEL/ES (EL/ES): 1 and 2 μM. Chaperones added to the bacterial S30 lysate were buffer-exchanged into RTS reconstitution buffer (Roche) by passing them through Micro BioSpin desalting columns, when necessary.

2.4 Biochemical and biophysical methods

2.4.1 Luciferase activity assay

Firefly luciferase (FL) activity measurements were performed with the Luciferase Assay System according to the manufacturer's protocol. Translation aliquots were diluted 100-fold into stopping buffer (25 mM Tris-Phosphate buffer pH 7.4, 2 mM CDTA, 2 mM DTT, 1% TritonX-100, 1 mg/ml BSA) before measuring activity in a luminometer. Relative specific activities were calculated by normalizing activity values with relative band intensities of full-length protein upon SDS-PAGE and phosphoimaging analysis (2.3.1.2).

2.4.2 Firefly luciferase refolding assay

In vitro FL refolding was assayed using the method of Terada (Terada et al., 1997) with the following modifications: native FL was denatured in 50 mM HEPES pH 7.4, 5 mM DTT, 6 M GdnHCl at 30 °C for 30 min at a concentration of 10 μM and subsequently placed on ice. To begin refolding, FL was diluted 100-fold into unsupplemented *E. coli* S30 lysate and in lysates supplemented with either TF (5 μM) or KJE (10, 2, 6 μM) or all of the above. At given time points, aliquots were removed and luciferase activity was measured as described (2.4.1).

In all experiments, the refolding yield was expressed as a percent of the native enzyme control.

2.4.3 Post-translational folding assay for firefly luciferase

Firefly luciferase S30 translations were stopped after 22 min by adding RNase A (50 µg/ml). FL activity was measured immediately before and at regular intervals after RNase A addition up to 60 min. The resulting activities were normalized by setting the initial value before RNase A addition to unity. Chaperone concentrations in afore mentioned reactions were as above (2.4.2). Apyrase was added to 10 U/ml final.

2.4.4 Actin refolding assay

Radiolabeled denatured mouse β-actin was prepared as follows: actin was synthesized in the S30 translation system supplemented with [^{35}S]-Met according to the manufacturer's instructions. After completion of the reaction, actin was pelleted by centrifugation (22,000 *g* for 30 min at 4 °C) and resuspended in an equal volume of urea-containing buffer (20 mM Tris pH 7.5, 10 mM DTT, 7.5 M urea). The denatured actin (~4 µM) was diluted 100-fold into dilution buffer (20 mM MOPS pH 7.4, 2.5 mM $MgCl_2$, 1 mM DTT, 0.2 mM $CaCl_2$, EDTA-free Complete protease inhibitors, 1 mM PMSF) containing 1 µM TRiC. The sample was then divided into four equal aliquots (I-IV). Aliquot (I) was diluted into SDS-sample buffer and later run on a 12% SDS-PAGE for accurate determination of the total amount of actin in the refolding reaction. Whereas aliquot (II) and (III) both received an ATP-regenerating system (1 mM ATP, 8 mM creatine phosphate, 50 µg/ml creatine kinase); aliquot (III) additionally received DNase I (2 µM). Aliquot (II) and (III) as well as the remaining, untreated control aliquot (IV) were then incubated for 1 h at 30 °C. Refolding reactions were stopped by dilution into native Bis-Tris gel loading buffer (supplemented with 15 mM CDTA). The reaction products were run on native PAGE as described previously (2.3.1.3). Actin bands on SDS- and native PAGE were quantified using phosphoimaging and AIDA software. The percentage of refolded actin was determined by comparing the total amount of synthesized

actin on the SDS-PAGE with the material bound to DNase I on the native PAGE (indicated by a mobility shift).

2.4.5 DNase I mobility shift assay

Supernatants from S30 and RRL translation reactions were diluted 5-fold into DNase I-containing buffer (20 mM MOPS pH 7.4, 10 U/ml apyrase, 1 mM DTT, EDTA-free Complete protease inhibitors, 1 mM PMSF, 5 µM DNase I) and incubated for 30 min at 30 °C. To ensure complete translation termination, the dilution buffer for S30 and RRL translations additionally received 200 µg/ml chloramphenicol or 200 µM cycloheximide, respectively. DNase I-bound actin was analyzed by its mobility shift on native PAGE and quantified as described (2.3.1.3).

2.4.6 DNase I binding assay

DNase I was crosslinked to CNBr-activated Sepharose 4B according to the manufacturer's protocol. RRL reactions were carried as described previously (2.3.4). After a 90 min, reactions were treated with 10 U/ml apyrase for 2 min at 30 °C following incubation with 500 U/ml TEV-protease for 30 min at 30 °C, if required. The reactions were then diluted into 400 µl glass-bead lysis buffer (2.2.7.3) and the actin bound to 40 µl of DNase I-beads (1:1 suspension in PBS) during a 2 h incubation at 4 °C (Lazarides and Lindberg, 1974). Prior to protein elution with SDS sample buffer, the beads were essentially washed as described (Ewalt et al., 1997). Protein analysis was performed using SDS-PAGE and phosphoimaging.

Yeast Δ*reg* cells expressing actin fusion proteins (3 h at 30 °C in SC-Leu, supplemented with 2% glucose and 2% galactose) were lysed with glass beads in presence of 0.36 mM cycloheximide and 10 U/ml apyrase, as described (2.2.7.3). After removal of non-lysed cells, TEV-cleavage (500 U/ml) of actin fusion proteins was carried out for 30 min at 30 °C. After centrifugation (20,000 *g* for 10 min at 4 °C), actin in the supernatant was bound to 60 µl of DNase I-beads (1:1 suspension in PBS) and analyzed as described above.

2.4.7 Determination of actin folding kinetics in S30 and RRL

Two identical S30 and two identical RRL translations were set up as described (2.3.4) and the appearance of total actin as well as actin bound to DNase I was followed over time, as reported above (2.4.5). At the time of mid-logarithmic protein translation in the different translation systems (at 30 min and 60 min for S30 and RRL, respectively), one out of the two translation reactions was stopped by addition of RNase A (100 µg/ml), and monitoring continued for 1 h. The final values of total as well as folded actin protein of untreated reactions were set to 100%. Time points of RNase A addition were set to the equivalent percentage values at the same time point as in untreated reactions.

2.4.8 Fluorescence microscopy analysis

Samples from RTS reactions were incubated with 10 µM rhodamine-phalloidin (rPh) for 30 min at 37 °C, transferred to a microscope slide and air-dried to bind proteins to the glass surface. Upon removal of excess rPh by washing with PBS, actin filaments (F-actin) were analyzed by fluorescence microscopy (Axiovert200 equipped with filter set 15, an AxioCAM HRm digital camera and Axiovision 3.1 software).

For fluorescence microscopy analyses in yeast, Δ*reg* cells were grown to OD_{600}~0.5 in SC-Leu (containing 2% glucose) and protein expression induced with 0.5% galactose for 3 h at 30 °C. Fixation of the cells was performed by adding 3.7% formaldehyde into the medium, following incubation for 30 min on a rotor (Adams and Pringle, 1991). After washing the cells twice with PBS, the pellet was resuspended in 40 µl PBS, 0.3 µM rPh, 0.1% TritonX-100 and incubated in the dark for 10 min. The stained cells were washed with PBS and visualized by UV-illumination in an Axio ImagerA.1 fluorescence microscope (equipped with filter sets 15 and 38) and a CoolSnap HQ digital camera. To compare the location of rPh stained actin patches with those resulting from GFP-labeled actin fusion proteins, images from the red and green emission channels were merged with Metamorph 6.3 software.

2.4.9 Fluorescence measurements

Emission spectra of purified proteins or proteins translated *in vitro* and diluted into PBS were acquired at 25 °C on a Fluorolog-3 fluorescence spectrometer. GFP fluorescence was measured at an excitation wavelength of 397 nm and emission spectra were collected from 450 to 575 nm. mCherry was excited at 585 nm and the emission was recorded from 595 to 700 nm. Band passes were set to 5 nm for all measurements.

2.4.10 Quantitation of rPh-stained F-actin

Actin was translated in the presence of 5 µM TRiC as described previously (2.3.4). The reaction was stopped after 60 min by the addition of RNase A (100 µg/ml). After incubation for 60 min at 37 °C with rPh (10 µM), the reaction was passed through a Sephadex-G50 size exclusion column equilibrated in F-actin stabilizing buffer (2 mM Tris pH 7.4, 1 mM ATP, 0.5 mM DTT, 0.2 mM $CaCl_2$, 150 mM KCl, 2 mM $MgCl_2$) to separate rPh-labeled actin filaments from free dye. Fractions were collected and the fluorescence was measured at 540/572 nm (Excitation/Emission).

2.4.11 Electron microscopy

For negative staining, the protein sample was adsorbed onto a carbon-coated copper grid (400x100 mesh) made hydrophilic by glow discharge for 1 min. After removal of excess liquid by wicking to filter paper, staining was performed by incubation on a drop of 2% uranyl acetate for 1 min. The preparations were inspected in a Philips CM20 electron microscope.

3 Results

3.1 Role of trigger factor and DnaK in multi-domain protein folding

In the cell, a large number of newly translated proteins are dependent on the assistance of molecular chaperones to acquire their native state on a biologically relevant time scale (Ellis, 1987; Bukau et al., 2000; Frydman, 2001; Hartl and Hayer-Hartl, 2002). Interestingly, although the major chaperone families have been conserved throughout evolution, complex modular proteins of eukaryotic origin often fold with low efficiency upon recombinant expression in bacteria (Baneyx, 1999). Differences between bacterial and eukaryotic chaperones regarding their functional coupling to the translation process might contribute to this phenomenon (Netzer and Hartl, 1997; Netzer and Hartl, 1998; Hartl and Hayer-Hartl, 2002).

This part of the work was performed in close collaboration with Drs. Vishwas Agashe and Suranjana Guha.

3.1.1 Misfolding of eukaryotic firefly luciferase in *E. coli* lysate

To investigate the effects of bacterial chaperones on the folding of modular eukaryotic proteins upon translation in an *E. coli*-based cell-free translation system, firefly luciferase (FL) was chosen as a model eukaryotic multi-domain protein. FL from the North American beetle *Photinus pyralis* is a two-domain protein of 62 kDa in size. Its structure has been solved to 2 Å resolution, showing a large N-terminal domain and a smaller C-terminal domain (Conti et al., 1996). FL catalyzes the oxidation of the heterocyclic compound luciferin with molecular oxygen in the presence of ATP and Mg^{2+}. This reaction is very rapid and results in the emission of yellow-green light, which makes FL an ideal candidate for protein folding studies. FL is naturally located in specialized peroxisomes of the firefly and its uptake into the organelle is thought to occur after folding in the cytosol (McNew and Goodman, 1996). Importantly, the apparent folding rate of FL is strongly affected by the folding environment.

Refolding of fully denatured FL in the absence of cellular factors is exceedingly slow, reaching equilibrium after days (Herbst et al., 1998). This is due to kinetically trapped species imposed by intramolecular misfolding (Herbst et al., 1998; Frydman et al., 1999). Refolding in the presence of the *E. coli* Hsp70 system DnaK, DnaJ, and GrpE (KJE) takes only ~10-15 min (Szabo et al., 1994). GroEL does not support FL refolding but can mediate its transfer to DnaK (Buchberger et al., 1996). In striking contrast, newly synthesized FL in eukaryotic cell lysates is fully active within seconds upon completion of synthesis (Kolb et al., 1994), resulting from co-translational folding assisted by the Hsp70/40 chaperone system and the cytosolic chaperonin TRiC (Frydman et al., 1994; Frydman et al., 1999).

In order to gain more information about the role of chaperones in the early stages of protein synthesis, FL was expressed to similar levels in bacterial (*E. coli*) and eukaryotic (*S. cerevisiae*) cells (Figure 10, left side). Upon expression in yeast, essentially all of the synthesized FL protein was soluble and enzymatically active. In contrast, expression of FL in *E. coli* revealed only 40% soluble and 5-10% active protein, respectively. Size exclusion chromatography analysis of soluble FL from *E. coli* showed that ~30-40% of the protein was monomeric but not functional. The remaining ~60-70% were found in higher molecular weight fractions, forming oligomeric structures (H.-C. Chang: personal communication). Expression of FL in coupled transcription/translation lysates of rabbit reticulocytes (RRL) and *E. coli* (S30) confirmed these findings (Figure 10, right side). These lysates support efficient protein synthesis (up to ~200 µg/ml *per* hour), but represent dilute cytosol preparations with low levels of endogenous chaperones (3.1.2). The translation reactions were typically run for 1 h at 30 °C in the presence of radiolabeled [^{35}S]-Met following separation of soluble and insoluble material by centrifugation. Quantitation of the radioactively labeled FL bands upon SDS-PAGE analysis revealed FL translated in RRL to be ~100% soluble (Figure 10, top panel). FL activity of total synthesized protein was estimated to be approximately 55%. In contrast, the specific activity of FL translated in the S30 lysate was only ~5%, with ~45% of the

protein being in the soluble state. Thus, intramolecular misfolding followed by aggregation accounts for the low specific activity of bacterially expressed FL.

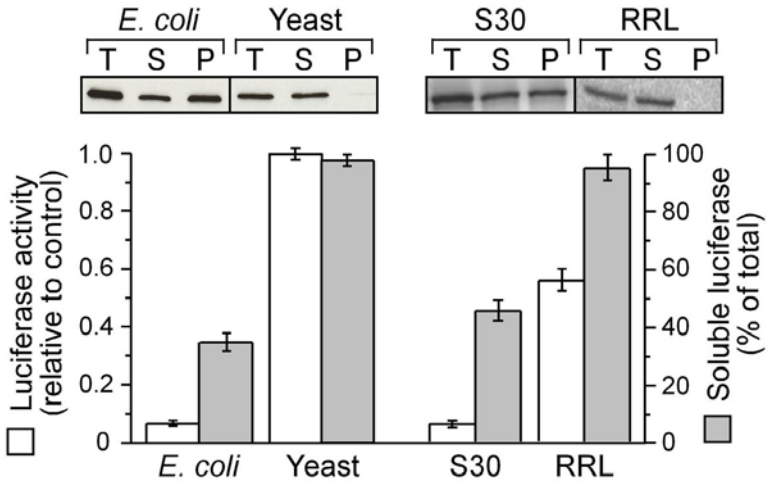

Figure 10: Folding of FL is inefficient in bacteria compared to eukaryotes.

FL was expressed to similar levels *in vivo* in *E. coli* and *S. cerevisiae* (Agashe et al., 2004) and *in vitro* in *E. coli* (S30) and rabbit reticulocytes lysate (RRL) translation reactions. Top panel: Distribution of FL protein upon fractionation of total cell extracts (T) into soluble (S) and pellet fractions (P) by centrifugation. Bottom panel: FL relative activities (white bars) and amount of soluble FL in % of total (gray bars). The specific activity in yeast was set to 1.

3.1.2 Cooperative effect of TF and DnaK on folding

In general, misfolding of FL in the bacterial cytosol can result either from the lack of specific eukaryotic factors or the presence of inhibitory prokaryotic factors, or a combination of both. As shown in the past, TF and DnaK have partially overlapping functions in *de novo* protein folding in *E. coli* cells (Teter et al., 1999; Deuerling et al., 2003). Therefore, the contribution of TF and DnaK to FL folding in the *in vitro* S30 translation lysate was analyzed. The *in vivo* concentration of TF and DnaK under standard growth conditions in *E. coli* cells are ~40 µM and ~50 µM, respectively (Lill et al., 1988; Hesterkamp and Bukau, 1998). In contrast, the S30 lysate used throughout this study represents a highly diluted cytosol with final concentrations of both TF and DnaK of ~0.5 µM as determined by quantitative western blotting (Agashe et al., 2004). In order to determine whether these residual amounts of TF and DnaK were still able to

successfully promote protein folding *in vitro*, refolding experiments of FL were performed (Figure 11).

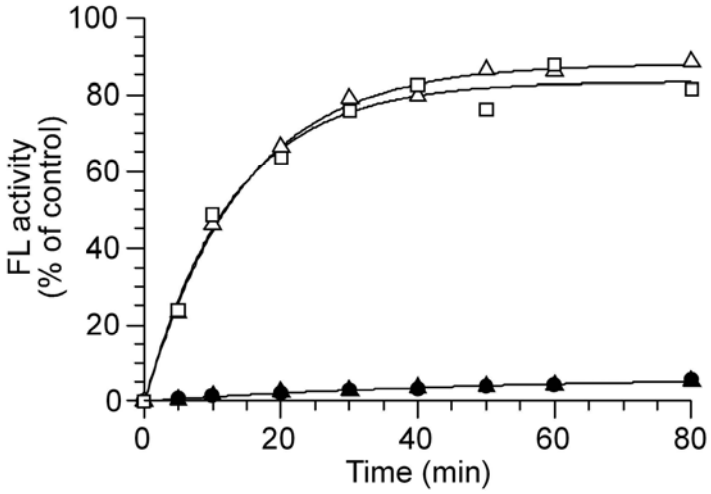

Figure 11: Refolding of chemically denatured FL.

Time course of refolding of chemically denatured FL (final concentration: 100 nM upon 100-fold dilution from 6 M GdnHCl) in unsupplemented bacterial S30 lysate (no chaperones, ●) and in lysates supplemented with TF (5 μM, ▲), KJE (10, 2, 6 μM, △), and TF with KJE (□) at 30 °C. The refolding yield is expressed as percent of a native enzyme control.

Interestingly, ATP-dependent refolding of purified chemically denatured FL, diluted into the S30 lysate, was only ~10% efficient. In contrast, refolding in the S30 lysate upon supplementation with the purified bacterial Hsp70 chaperone system KJE (10, 2, and 6 μM) occurred with a half-time of ~10 min and resulted in 80-90% native FL (Figure 11 and 12A). This effect was irrespective of the presence of TF (5 μM) (Figure 11 and 12A). Importantly, TF alone was not able to refold FL above background level. Together, the refolding efficiency of FL out of denaturant solely depends on the presence of KJE and cannot be further increased by the addition of TF.

Next, the S30 lysate was supplemented with different combinations of purified bacterial chaperones (Figure 12A) and their effect on the specific activity of FL during *de novo* synthesis analyzed. In contrast to the results obtained for FL refolding (Figure 11), the sole addition of TF to the S30 lysate increased the specific activity of newly translated FL 2- to 3-fold (Figure 12B), while the

solubility improved from ~40% to ~60%. When the same experiment was performed in an S30 lysate that had been immunodepleted of DnaK to further reduce the DnaK concentration, TF had no effect (Agashe et al., 2004: Supplemental Figure S3). Thus, TF action is strongly dependent on the residual amounts of DnaK present in the lysate. Surprisingly, addition of purified KJE alone was without effect on FL activity, even though FL is maintained in an almost completely soluble state under these conditions (Figure 12B). Adding TF and KJE together resulted in a ~4-fold increase in specific activity. These findings lead to the assumption that, during *de novo* folding of FL, TF and KJE must cooperate in order to increase its folding efficiency while refolding of FL out of denaturant is TF independent (Figure 11). Thus, TF is critical in maintaining FL nascent chains competent for folding by the KJE system.

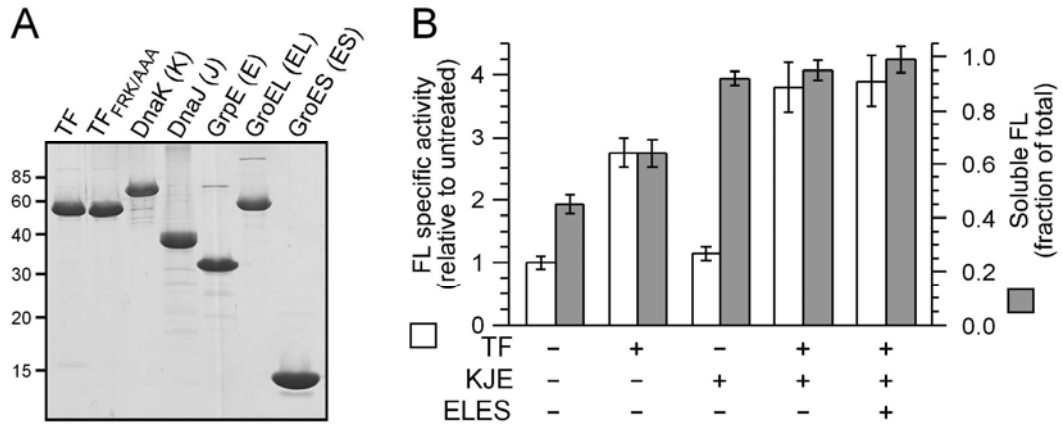

Figure 12: Effect of purified chaperones on folding yields of FL during translation.

(A) SDS-PAGE analysis of purified *E. coli* chaperones: Trigger factor wild-type (TF) and FRK/AAA-mutant ($TF_{FRK/AAA}$), DnaK (K), DnaJ (J), GrpE (E), and the chaperonin GroEL (EL) with its co-chaperone GroES (ES). **(B)** Expression of FL in S30 translation reactions with and without chaperone supplementation, as indicated (TF, 5 µM; KJE, 10, 2, and 6 µM; ELES, 1 and 2 µM). Specific FL activities after 1 h translation at 30 °C (white bars) are shown relative to the unsupplemented lysate (set to 1). Protein solubility (gray bars) is given as a fraction of total protein in the presence or absence of added chaperones, as indicated.

However, the 4-fold increase in activity upon *de novo* synthesis of FL in the presence of TF and KJE (~20%, compared to ~5% in the unsupplemented S30 lysate; Figures 10 and 12B) is lower than the yield obtained from FL refolding

(80-90% in presence of KJE alone; Figure 11). This finding suggests that TF functions inefficiently in stabilizing ribosome bound FL in a conformation productive for the interaction with DnaK. Moreover, a folding yield of ~20% with essentially all translated protein appearing in the soluble fraction indicates, that, similar to FL expression in *E. coli*, a large fraction of the protein must be in a misfolded sate. As expected, supplementation of the S30 lysate with purified GroEL/GroES (ELES; Figure 12A) at physiological concentrations (1 and 2 μM) in addition to TF and KJE did not further improve the yield of FL folding (Figure 12B).

3.1.3 Chaperone enforced shift in folding mechanism

As mentioned previously, refolding of denatured FL in the presence of the bacterial Hsp70 system takes approximately 10-15 min (Figure 11 and Szabo et al., 1994), whereas FL translated in a eukaryotic system is fully active within seconds upon completion of synthesis (Kolb et al., 1994).

In order to find out whether the differences in FL folding efficiencies observed in eukaryotic and prokaryotic systems are based on different folding mechanisms, kinetics of FL translation and folding in the unsupplemented (chaperone diminished) S30 lysate were compared to those in RRL. In the latter system, folding of FL is assisted by mammalian Hsp70/40 and TRiC (Frydman et al., 1994). Surprisingly, despite the marked difference in folding yield (~5% in unsupplemented S30 *versus* ~60% in RRL; Figure 10), in both systems FL activity appeared virtually concurrently with the production of full-length protein (Figure 13A), indicative of the occurrence of co-translational folding. Further kinetic experiments were performed to test whether TF and KJE affect the mechanism of FL folding when present during translation at concentrations closer to physiological levels (3.1.2). Indeed, when TF (5 μM) was added to the S30 lysate, the kinetics of FL folding showed a significant deceleration (Figure 13B), indicative of a shift towards a post-translational mode of folding. Increasing amounts of added TF (up to 15 μM) did not cause a further delay in folding (S. Guha: personal communication). Importantly, upon addition of TF to the reaction, the speed of translation was not affected (Figure 13B).

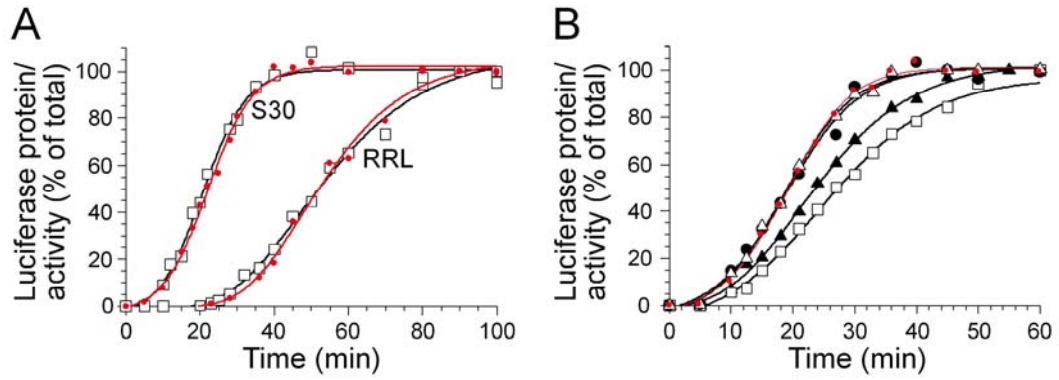

Figure 13: TF and KJE delay folding relative to translation *in vitro*.

(A) Apparent co-translational folding of FL in *E. coli* (S30) and rabbit reticulocytes (RRL) translation reactions. Appearance of full-length protein (●) and activity (□) were followed with time. Final values were set to 100%. **(B)** Appearance of FL activity during S30 translation in the absence of added chaperones (●) and presence of added KJE (10, 2, 6 μM, △), TF (5 μM, ▲) or a combination of both (□). The appearance of full-length FL in all translations was identical and is represented in red.

Deceleration in FL folding was not observed when KJE was added in the absence of TF. However, concurrent with the increase in folding yield (Figure 12B), the post-translational component of folding became even more pronounced when the reaction was supplemented with TF and KJE together (Figure 13B). Thus, TF and the DnaK-system seem to cooperate in order to assure a post-translational folding mechanism. In contrast, the rapid folding observed in the unsupplemented S30 lysate apparently represents a co-translational but highly inefficient default-pathway.

3.1.4 Shift in folding mechanism requires co-translational action of TF and DnaK

A hallmark of co-translational folding is the immediate stop of the appearance of native, active protein after translation termination (Figure 14). In contrast, proteins following a post-translational folding mechanism typically continue to form native protein after translation is inhibited. This effect is due to the specific interaction of chaperones with the nascent polypeptide chain upon its release from the ribosome in order to mediate proper folding. The time necessary for post-translational completion of folding is thereby strongly dependent on the protein and the folding environment.

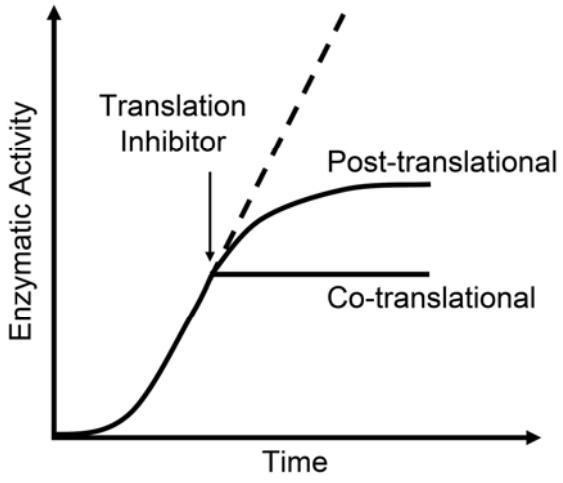

Figure 14: Co- *versus* post-translational protein folding model data.

After a short lag phase, due to ribosome loading with mRNA, the appearance of enzymatically active protein in a coupled transcription/translation reaction *in vitro* typically occurs linear over time. Upon termination of protein synthesis by a translation inhibitor, the appearance of folded protein either stops concomitantly with translation termination (indicative for a co-translational folding mechanism) or increases further over time (indicative for a post-translational folding mechanism).

To see whether the delay in folding caused by TF and KJE is dependent on the co-translational action of these chaperones, FL was translated in the S30 lysate. The appearance of FL activity was followed over time after the reaction was stopped by the addition of RNase A (an efficient translation inhibitor for both prokaryotic and eukaryotic systems), 22 min after translation initiation. Inhibition of translation in the unmodified S30 lysate was not followed by any further increase in FL activity (Figure 15; also see Figure 11), consistent with the virtually concurrent appearance of full-length protein and enzyme activity, reported previously (Figure 13A). In contrast, supplementation of the lysate with TF together with KJE resulted in a more than 2-fold increase of FL activity upon inhibition of translation (Figure 15). The kinetics for the post-translational appearance of FL activity ($t_{1/2}$~10 min) was in good agreement to those observed for the ATP-dependent, KJE-mediated refolding of denatured FL (Figure 11; Szabo et al., 1994). Depletion of ATP by apyrase concomitant with RNase A addition eliminated the post-translational phase, consistent with an ATP requirement for DnaK function (Figure 15). Although the sole addition of TF

showed a similar post-translational folding phase, the increase of FL activity was less pronounced when compared to the lysates supplemented with both TF and KJE. Addition of a triple-mutant form of TF, $TF_{FRK/AAA}$ (Figure 12A), defective in ribosome binding (Kramer et al., 2002), did not result in post-translational FL folding (Figure 15) or an increase in FL folding efficiency (data not shown).

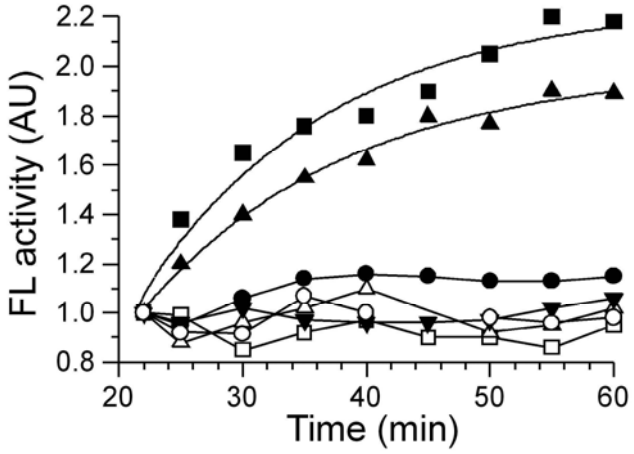

Figure 15: Co-translational actin of TF and KJE changes the mechanism of FL folding.

Post-translational changes in FL activity were followed after translation inhibition with RNase A (22 min after initiation). S30 lysate without added chaperones (○) and with chaperones added at the beginning of translation: TF (5 µM, ▲) and $TF_{FRK/AAA}$ (5 µM, ▼), KJE (10, 2, 6 µM, △), TF and KJE (■), TF together with KJE and apyrase (□). In another reaction, TF and KJE were added together with RNase A at the time of stopping translation (●).

Thus, binding of TF to the ribosome is a prerequisite for both the switch in FL folding from a co- to a post-translational mechanism (Figure 13) and the resulting gain in FL activity seen with wild-type TF (Figure 12B). Strikingly, addition of TF and KJE after the translation was stopped with RNase A failed to produce any post-translational folding phase. These findings were corroborated by the lack of a post-translational folding phase upon translation of FL in a DnaK-immunodepleted lysate, which contained TF from the beginning and received KJE after the translation was inhibited (S. Guha: personal communication). Hence, the co-translational action of TF and KJE, preventing misfolding or aggregation, is essential for productive, post-translational folding of FL.

Taken together, folding of the multi-domain protein FL in a chaperone-diminished S30 lysate occurs by a fast and co-translational default mechanism which is limited by misfolding and aggregation of the nascent chains. Although lysate supplementation with TF and KJE counteracts this off-pathway folding, directing nascent polypeptides to a post-translational folding route, the mechanistic shift applied cannot substitute for the efficient co-translational folding of FL in the eukaryotic system (Frydman et al., 1994).

3.2 TRiC-assisted folding of actin upon bacterial translation

The inability of the bacterial cytosol to support efficient folding of eukaryotic proteins results, among other factors, from the presence of incompatible molecular chaperones, as described for FL (3.1 and Agashe et al., 2004). On the other hand, certain eukaryotic proteins, such as actin, are known to have specific chaperone requirements for efficient folding. *In vivo* folding and *in vitro* refolding of actin is strictly dependent on the eukaryotic chaperonin TRiC (Tian et al., 1995; Siegers et al., 1999). Although architecture and mechanism of TRiC function are thought to be similar to those of bacterial GroEL, the bacterial chaperonin cannot mediate actin folding. Indeed, recombinant expression of actins from multiple species (including *Dictyostelium discoideum*, *S. cerevisiae* and rabbit) in *E. coli* results in the generation of non-native species that aggregate into inclusion bodies (Frankel et al., 1990).

Therefore, this part of the study focuses on the minimum chaperone requirements for the production of substantial amounts of native actin upon synthesis in the bacterial S30 lysate.

3.2.1 Purified TRiC is active and does not affect *in vitro* translation efficiency of S30 lysates

In order to investigate the effect of TRiC on actin translation rates during *de novo* synthesis in the bacterial S30 lysate, the chaperonin was purified from bovine testes with the following modifications of the protocol published by Ferreyra and Frydman (2000): Only four chromatographic steps were necessary to obtain >95% pure TRiC (Figure 16A), in contrast to six steps and an

ammonium sulfate precipitation in the published protocol (2.3.3.1). The modifications applied did not lead to a decrease in the overall yield of purified material: routinely ~8 mg of purified TRiC *per* 100 g of starting material were obtained. Characterization of the purified chaperonin complex by analytical gel filtration analysis resulted in a single homogenous peak eluting at the appropriate size of ~900 kDa, indicative of TRiC being pure and fully assembled (Figure 16B).

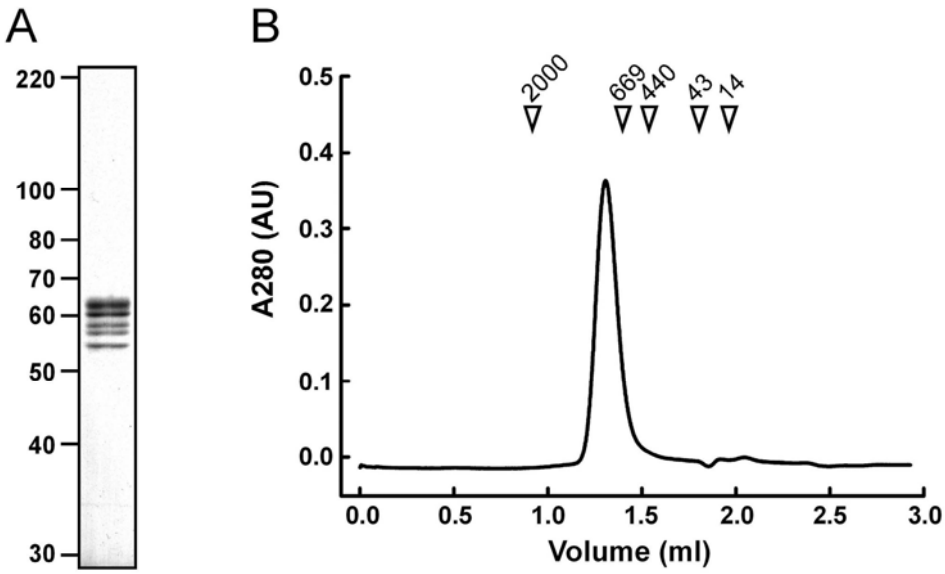

Figure 16: Characterization of purified TRiC from bovine testes.

(A) SDS-PAGE analysis of TRiC purified from bovine testes according to the protocol of Ferreyra and Frydman (Ferreyra and Frydman, 2000) with modifications (2.3.3.1). **(B)** Absorption profile of the purified TRiC complex applied to an analytical Superose 6 gel filtration column (SMART system). Arrows indicate the position of marker proteins (in kDa).

Examination of purified TRiC samples by negative stain electron microscopy revealed particles extremely regular in size and shape (Figure 17). The predominant view was of ring-shaped structures with a central stain-filled hole. Aggregates or individual subunits resulting from disassembled TRiC complexes were not observed. These findings are consistent with previously reported electron microscopy analyses of large barrel shaped double ring complexes, including TRiC and ELES (Frydman et al., 1992; Langer et al., 1992b).

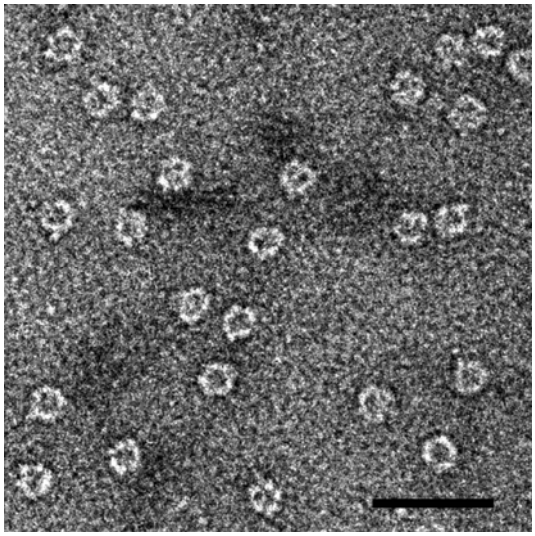

Figure 17: Electron micrograph of negatively stained TRiC.

Purified TRiC was negatively stained with uranyl acetate and examined by electron microscopy on a carbon coated copper grid. Size bar = 50 nm. Image was recorded by Karoline Bopp, Department of Molecular Structural Biology, MPI of Biochemistry).

To test whether TRiC purified by this method was active, its ability to refold actin upon dilution from denaturant was examined. Denatured radiolabeled actin (~4 μM) was diluted 100-fold into buffer containing TRiC (1 μM) in the absence and presence of ATP and DNase I. The resulting complexes were analyzed by native PAGE and phosphoimaging (Figure 18A). Throughout this study, generation of native monomeric actin (G-actin) was monitored by its characteristic mobility on native PAGE and the shift in position of this band upon formation of a binary complex with DNase I (Hansen et al., 1999). In the absence of ATP, most of the material was stably bound to TRiC, whereas actin was released upon incubation with ATP (Figure 18A). The released actin was native, since it was able to form a stable complex with DNase I, as evidenced by the shift associated with the decreased mobility of this complex upon native PAGE analysis. Quantitation of the band corresponding to native actin demonstrated that TRiC purified by this method was able to refold ~50% of the diluted actin within a 1 h incubation at 30 °C (Figure 18B), a similar amount to that reported previously (Gao et al., 1992).

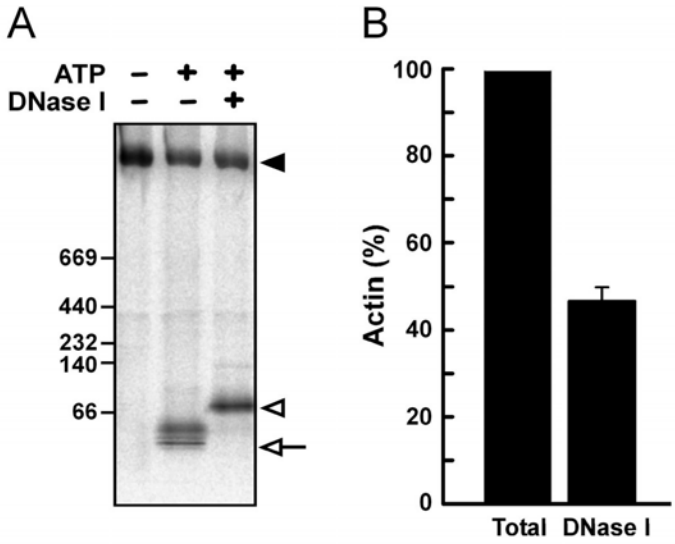

Figure 18: TRiC assisted actin refolding.

(A) Native PAGE of TRiC assisted actin refolding upon dilution from denaturant. All reactions were performed in the presence of TRiC. Supplementation with ATP and DNase I is indicated above the panel. Filled arrowhead: actin:TRiC complex; empty arrowhead: actin:DNase I complex; empty arrow: native monomeric actin (G-actin). **(B)** Quantitation of phosphoimaging results: G-actin bound to DNase I (DNase I) as assessed in (A) relative to the total amount of denatured actin (Total) used for refolding.

The bacterial S30 translation lysate used in this work is designed to produce large quantities of recombinantly expressed protein (~200 µg/ml *per* hour; 3.1). To make sure that supplementation of the bacterial lysate with purified TRiC did not lead to any detrimental effects on translation, the amount of total actin synthesized in translation reactions in absence and presence of 5 µM TRiC (the amount used throughout this study; Figure 21) were compared by quantitative immunoblotting (Figure 19). Importantly, the addition of purified TRiC to the S30 lysate had no effect on the actin translation efficiency, which typically resulted in the production of ~175 µg/ml (~4 µM) *per* hour when compared to purified actin standard protein (2.3.3.3).

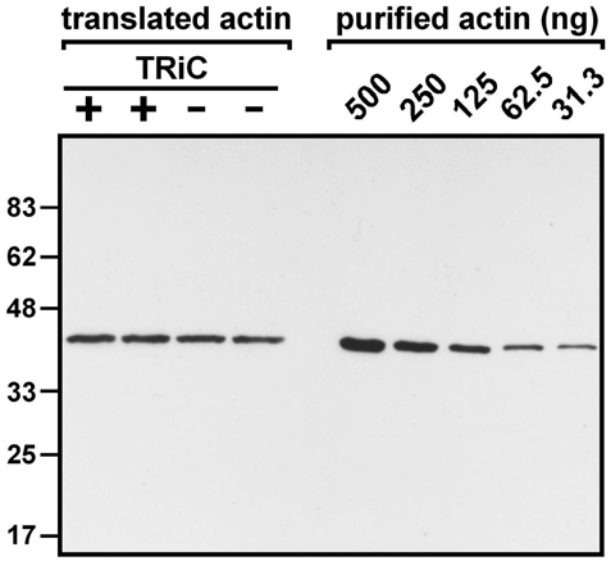

Figure 19: Supplementation of bacterial lysates with purified TRiC did not affect translation efficiency.

Quantitative immunoblotting of translated actin protein (42 kDa). Left: duplicate experiments of actin translations (1 µl of total reaction) in absence or presence of TRiC (5 µM), as indicated. Right: actin standard protein purified from inclusion bodies of *E. coli* (2.3.3.3).

3.2.2 TRiC is capable to assist the folding of newly synthesized actin

Next, the effect of TRiC on the behavior of actin synthesized in the S30 lysate was characterized. Actin translation reactions, supplemented with [^{35}S]-Met, were performed in the absence and presence of TRiC (5 µM) and subsequently centrifuged to separate soluble and insoluble fractions (2.3.4). In absence of TRiC, quantitation of the corresponding actin bands upon SDS-PAGE analysis revealed ~90% of synthesized actin to be in the insoluble fraction. In contrast, lysate supplementation with TRiC turned approximately 80% of the translated actin into soluble protein (Figures 20A and 20B). The supernatants of these reactions were incubated with DNase I and the actin:DNase I complexes examined by native PAGE (Figures 20B and 20C; 2.4.5). Only the reaction supplemented with TRiC resulted in material that formed complexes with DNase I (Figure 20C). Quantitation revealed that ~40% of the total actin synthesized in the presence of TRiC bound to DNase I in form of monomeric

G-actin (a similar amount was present as F-actin, but incapable of binding to DNase; 3.2.5).

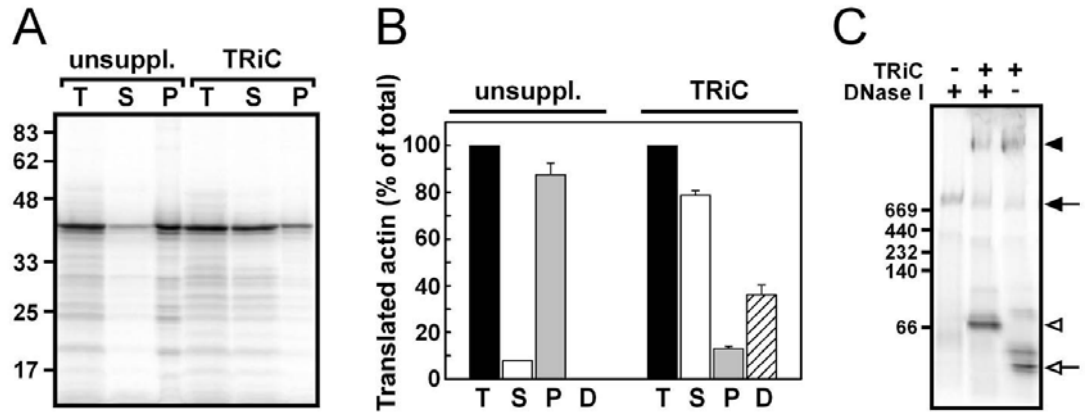

Figure 20: TRiC supplementation of a bacterial translation lysate results in the production of native actin.

(A) SDS-PAGE of total (T), supernatant (S) and pellet (P) fractions of actin (42 kDa) produced in unsupplemented and TRiC-supplemented bacterial S30 translation reactions, as indicated. **(B)** Phosphoimaging quantitation of actin translations as shown in (A) as well as DNase I-bound native actin (D) as assessed in (C). **(C)** Native PAGE of actin synthesized in absence and presence and of TRiC (5 μM), as indicated. After translations were stopped, DNase I was added to the supernatants of the reactions. Filled arrowhead: actin:TRiC complex; filled arrow: actin:GroEL complex (determined by comparing the mobility of a complex between purified GroEL and actin, data not shown); empty arrowhead: actin:DNase I complex; empty arrow: native actin.

In order to determine the optimal TRiC concentration required for the folding of the substantial actin quantities synthesized in this lysate, translation reactions with increasing concentrations of TRiC were performed. The amount of actin capable of binding to DNase I was examined by native PAGE, as described above (Figure 21A). The yield of DNase I-bound actin (~40%) did not increase at concentrations >5 μM, which correlated well with the observed actin solubility (Figure 21B). Therefore, a concentration of 5 μM TRiC was used in subsequent experiments.

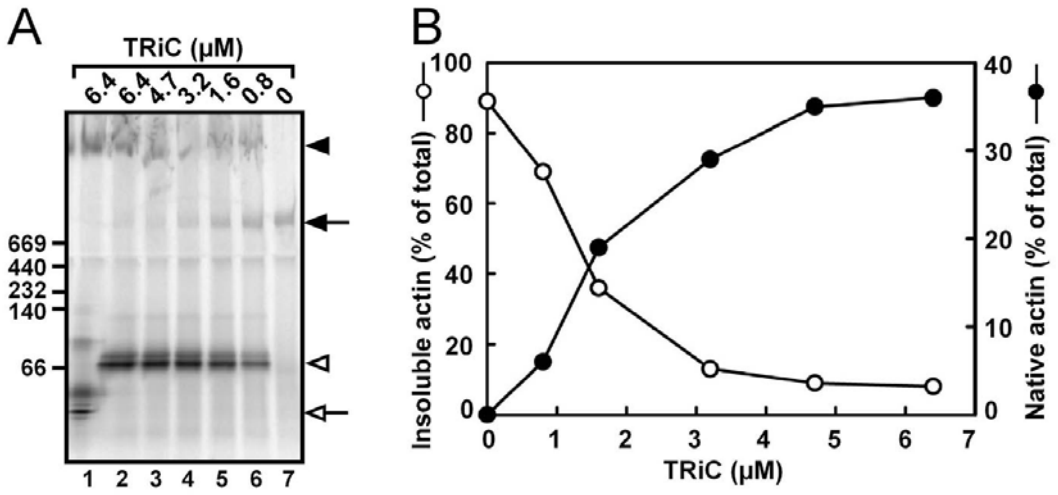

Figure 21: Titration of purified TRiC added to the bacterial translation lysate.

(A) Native PAGE of actin S30 translations performed in presence of increasing amounts of supplemented TRiC (indicated above the panel). Reactions in lanes 2-6 received DNase I, as indicated. Symbols are as in Figure 20C. **(B)** Phosphoimaging quantitation of the actin:DNase I band as assessed in (A) (filled circles) and the material remaining in the pellet fraction as assessed by SDS-PAGE analysis (empty circles and data not shown).

3.2.3 Bacterial chaperones are not able to fold actin nascent chains

It is well known that recombinant expression of actin in *E. coli* cells results in the formation of insoluble aggregates (Frankel et al., 1990). Moreover, the bacterial S30 translation lysate used in this study represents a dilute cytosol preparation functionally-depleted of endogenous chaperones and thus unable to support the efficient folding of the eukaryotic multi-domain protein FL, as mentioned previously (3.1).

In order to examine the effects of bacterial chaperones on actin solubility and folding during *de novo* synthesis in the S30 lysate, translation reactions were supplemented with purified ELES (1 and 2 μM) and the major nascent chain binding chaperones TF (5 μM) and KJE (10, 2 and 6 μM) (Figures 22A and 12A). Addition of these chaperones did not affect translation rates when compared to unsupplemented lysate (Figure 22A). The reactions were centrifuged to separate soluble and insoluble material and examined as before (Figures 22A and 22B).

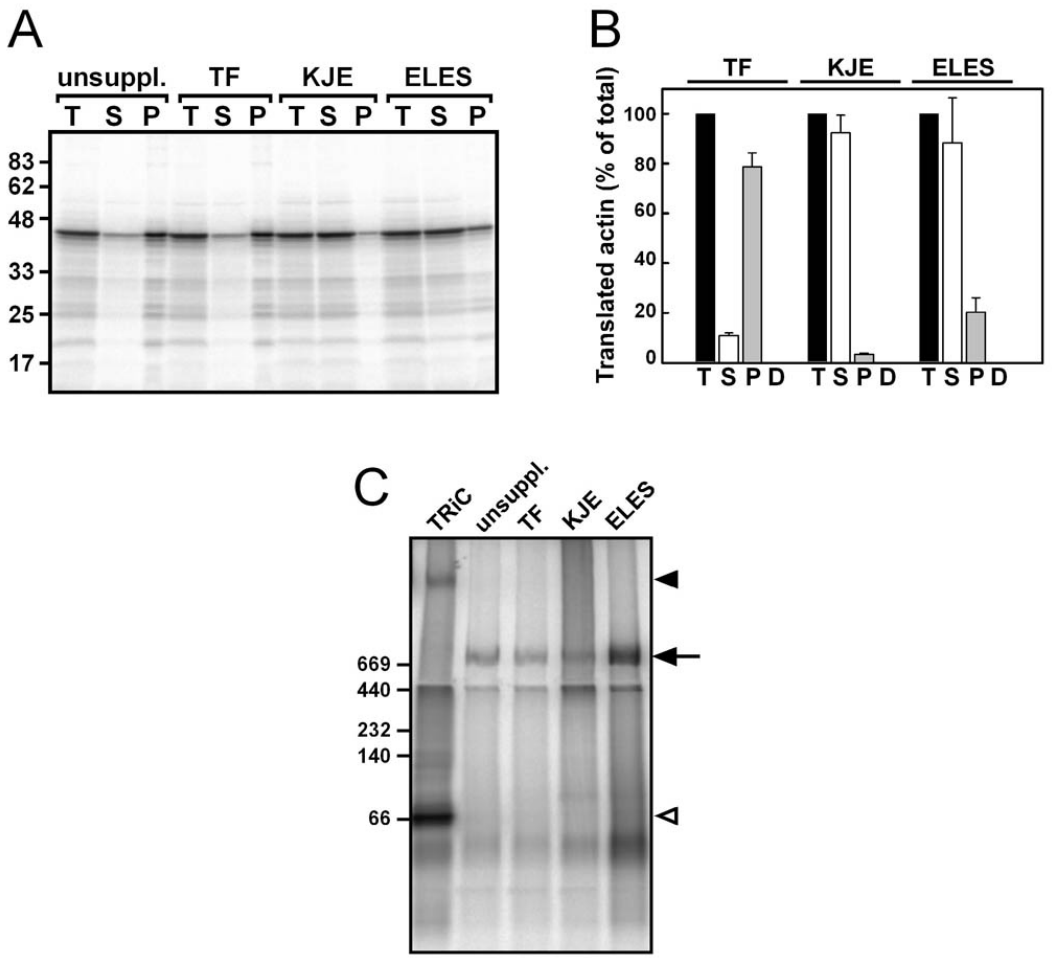

Figure 22: Supplementation of the S30 translation lysate with purified bacterial chaperones does not result in the production of native actin.

(A) SDS-PAGE of total (T), supernatant (S) and pellet (P) fractions of actin (42 kDa) produced in unsupplemented (unsuppl.) and trigger factor- (TF, 5 µM), DnaK/DnaJ/GrpE- (KJE, 10, 2, and 6 µM) or GroEL/GroES- (ELES, 1 and 2 µM) supplemented S30 lysate reactions. **(B)** Phosphoimaging quantitation of actin translations as shown in (A) as well as DNase I-bound native actin (D) as assessed in (C). **(C)** Native PAGE of actin synthesized in absence and presence of bacterial chaperones or TRiC, as indicated. After translations were stopped, supernatants of all reactions received DNase I. Symbols are as in Figure 20C.

Supplementation with ELES or KJE in the above mentioned concentrations resulted in ~90% of the synthesized actin remaining in the soluble fraction, whereas addition of TF did not improve actin solubility when compared to the unsupplemented reaction (~10%) (compare Figures 22A and 22B with Figure 20A and 20B). Higher chaperone concentrations did not lead to any further increase in actin solubility (data not shown). Next, actin present in the supernatants of these

chaperone-supplemented reactions was examined regarding the capability of forming a complex with DNase I as described above. In contrary to the production of native actin upon supplementation with TRiC, none of the bacterial chaperones tested were able to generate actin capable to bind to DNase I (Figure 22C).

3.2.4 Folding of actin assisted solely by TRiC occurs more slowly than folding in the eukaryotic cytosol

TRiC-mediated refolding of actin upon dilution from denaturant occurs with a half-time of ~15-30 min, which reflects the need for several cycles of actin binding and release from the chaperonin for the generation of native protein (Tian et al., 1995). In contrast, *de novo* folding of newly synthesized actin in the cytosol of wild-type eukaryotic cells is much faster, with half-times of ~1 min (Siegers et al., 1999). This finding suggests that actin translation and folding are normally efficiently coupled, and that actin leaves TRiC in a native or near-native state. This rapid folding process has been explained by the presence of a "folding compartment" in the eukaryotic cytosol, in which additional factors, such as PFD/GimC, sequester folding intermediates during TRiC-assisted folding and prevent their premature release into the crowded environment of the cytosol (Hartl and Hayer-Hartl, 2002). Indeed, when actin was synthesized in GimC-deficient yeast strains, the rate of actin folding was decrease 5-fold, with the overall yield of native actin being reduced by 40-50% (Siegers et al., 1999).

Since the bacterial S30 translation system lacks all of the factors normally present in the eukaryotic cytosol and *E. coli* chaperones are unable to mediate actin folding, this provided the opportunity to investigate the folding kinetics of newly translated actin assisted solely by TRiC. Therefore, the appearance over time of total translated actin (monitored by SDS-PAGE, as above) *versus* DNase I-binding actin (monitored by native PAGE, as above) was followed in a translation reaction supplemented with TRiC and [^{35}S]-Met (Figures 23A and 23B).

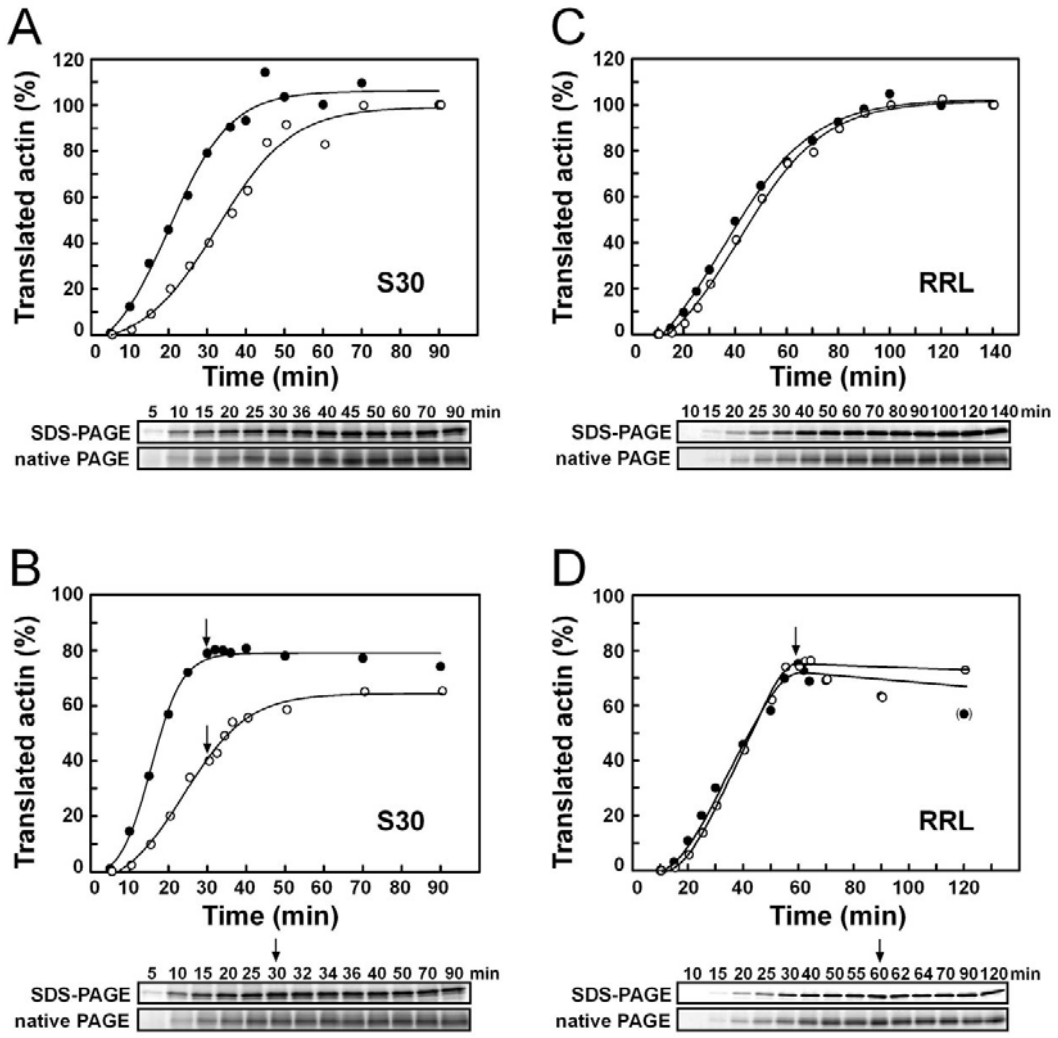

Figure 23: Folding of bacterially-translated actin assisted solely by TRiC occurs more slowly than actin folding in RRL.

Appearance of total (●) and DNase I-bound (○) actin in TRiC-supplemented bacterial S30 translation lysates (S30) **(A, B)** or unsupplemented reticulocyte lysates (RRL) **(C, D)** that received no treatment (A, C; final values set to 100%) or that received RNase A treatment to stop translation at the time point indicated by the arrow (B, D; point of RNase A addition set to the equivalent percentage value at the same time point in A and C, respectively). Lower panels: SDS-PAGE and native PAGE used for quantitation.

As can be observed, there is a delay of ~15 min in the appearance of native actin relative to full-length actin synthesized (Figure 23A). This finding suggests that translation is poorly coupled to TRiC-mediated folding in this system and that actin folds through a slow post-translational mechanism. If actin folding in the S30 lysate is not tightly coupled to translation, then addition of a translation inhibitor to an ongoing translation reaction should result in the accumulation of

native actin over the next few minutes after translation has stopped (for general information see Figure 14). Thus, RNase A was added to an ongoing reaction, supplemented with TRiC and [^{35}S]-Met as above. Subsequently, the appearance of native protein after translation termination was monitored over time (Figure 23B). Strikingly, whereas RNase A addition resulted in an immediate cession of translation, DNase I-binding actin continued to increase over the next minutes with a half-time of ~10-15 min. This result was in good agreement to the delay in actin folding observed in the untreated S30 reaction (Figure 23A). Thus, TRiC-assisted actin folding in the bacterial lysate occurs with similar kinetics resembling that of actin refolding upon dilution from denaturant (Tian et al., 1995).

The slow kinetics of actin folding relative to translation observed in the TRiC-supplemented bacterial lysate could be due to intrinsic properties of coupled transcription/translation lysates (such as general dilution of cytosolic factors, decreased crowding, *etc.*) or to a lack of specific factors that promote efficient actin folding. To investigate these possibilities, actin was translated in RRL and the kinetics of folding analyzed as described for TRiC-supplemented S30 reactions (Figure 23C). After a characteristic phase associated with transcription of the actin mRNA and ribosome loading, DNase I-binding actin was detectable shortly after the appearance of full-length actin, with a delay of only ~2-3 min. The fast folding kinetics observed were in good agreement to those reported for actin mRNA translation in RRL (Frydman and Hartl, 1996). If the majority of actin nascent chains are folding rapidly after their release from the ribosome, the addition of a translation inhibitor should lead to no further substantial increase of native actin after cessation of translation (for general information see Figure 14). Therefore, RNase A was added to an ongoing actin translation in RRL, similar to the one described above (Figure 23D). As expected, the accumulation of DNase I-binding actin stopped concurrently with translation, in sharp contrast to the result obtained with the bacterial lysate (Figure 23B). Taken together, these results suggest that, in the absence of additional factors, TRiC-mediated folding of newly translated actin is a slow process that necessitates several cycles of TRiC binding and release.

3.2.5 Bacterial S30-translated actin folded by TRiC readily polymerizes into filaments

A hallmark of actin that has reached its native state is its ability to polymerize into filaments (F-actin). Phalloidin, a bicyclic heptapeptide from the poisonous mushroom *Amanita phalloides*, binds specifically to F-actin and its fluorescent derivatives have been used extensively to visualize actin filaments *in vivo* and *in vitro* (Cooper, 1987). In order to find out whether actin that has been translated in the bacterial S30 lysate and assisted in its folding by TRiC is able to polymerize into filaments, products of a TRiC-supplemented actin translation reaction were stained with rhodamine-derivatized phalloidin (rPh) and examined by fluorescence microscopy (Figure 24A).

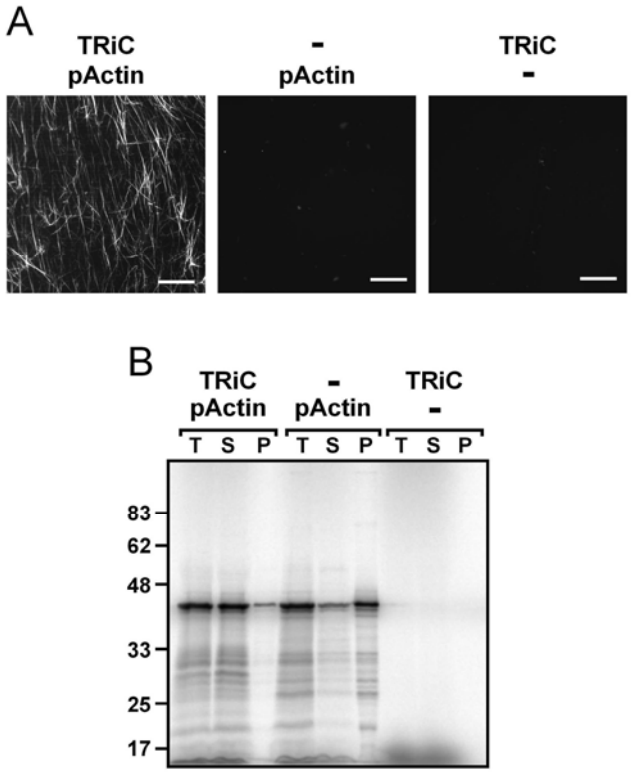

Figure 24: Bacterially-produced actin in the presence of TRiC readily polymerizes into filaments.

(A) Fluorescence microscopy of rhodamine-phalloidin binding actin filaments produced in bacterial S30 lysates containing a plasmid encoding actin (pActin) and/or supplemented with TRiC (TRiC), as indicated. Size bar = 20 µm. **(B)** SDS-PAGE of total (T), supernatant (S) and pellet (P) fractions of actin (42 kDa) produced in bacterial S30 lysates containing a plasmid encoding actin (pActin) and/or supplemented with TRiC (TRiC), as indicated.

Abundant rPh-binding structures of filamentous shape with diverse lengths and no evident branching or amorphous aggregation were visible. Thus, the observed structures are likely to represent *bona fide* rPh-binding F-actin since they were not observed in actin translation products of unsupplemented reactions (Figure 24A) (even though the amounts of actin synthesized were equivalent; Figure 24B), nor in TRiC-supplemented lysates devoid of the actin-encoding DNA plasmid (Figure 24A). Supplementation of actin S30 translation reactions with the bacterial chaperones ELES, KJE or TF at concentrations used in previous experiments (3.2.3) did not lead to the appearance of rPh-binding structures (data not shown).

The equilibrium between monomeric actin (G-actin) and polymerized actin (F-actin) is strongly favored towards F-actin at salt concentrations >50 mM K^+ or Na^+ and >2 mM Mg^{2+} (Pardee and Spudich, 1982). Therefore, it is plausible that in the translation lysates, which contain physiological salt concentrations, a considerable fraction of the actin polymerizes soon after it is released from TRiC as a native species. Since DNase I forms stable complexes with G-actin but not with F-actin (Hitchcock et al., 1976; Blikstad et al., 1978), the use of DNase I binding to quantitate the total amount of folded actin (G-actin + F-actin) under physiological salt concentrations may result in underestimation. If saturating quantities of rPh are used to bind F-actin, fluorescence can be used as a quantitative measure of the amount of filamentous actin present in the sample (Howard and Oresajo, 1985). To this end, the yield of F-actin present in the TRiC-supplemented reactions was estimated by measuring the amount of bound rPh. As phalloidin is known to bind with a stoichiometry of 1:1 to each F-actin protomer (Steinmetz et al., 1998), and ~4 μM actin is produced in a translation reaction, the product of an actin S30 translation reaction was incubated with 10 μM rPh. rPh bound to F-actin was separated from unbound material by gel filtration chromatography and fluorescence intensities of the individual fractions were measured (Figure 25). As a control, a similar experiment was performed upon translation of FL in an unsupplemented S30 translation reaction. Strikingly, since FL does not bind rPh, an increase of rPh-fluorescence in fractions eluting early from the gel filtration column (reflecting fractions containing high

molecular weight complexes) was only observed in the case of actin synthesized in presence of TRiC. Thus, the amount of F-actin produced in TRiC-supplemented translations was estimated to be ~1.6 µM, corresponding to ~40% of total actin synthesized.

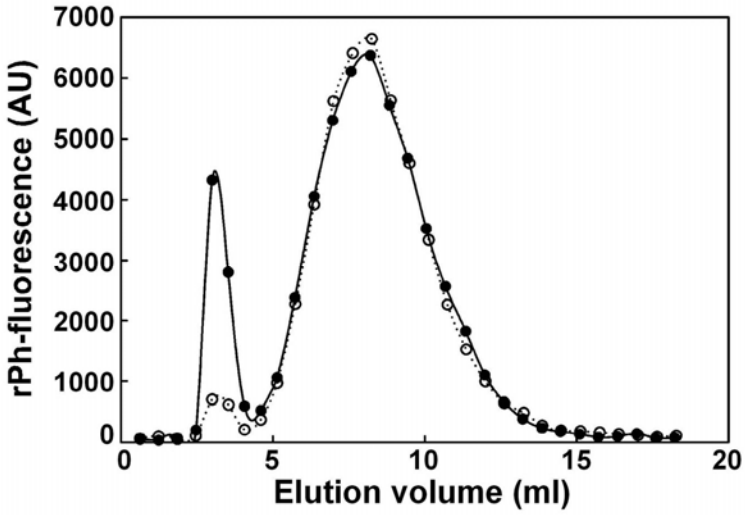

Figure 25: Quantiation of F-actin produced in a TRiC-supplemented S30 reaction.

Actin, translated in a TRiC-supplemented (●) and FL, translated in an unsupplemented bacterial lysate (○) and incubated with 10 µM rhodamine-phalloidin (rPh). Reactions were then passed through a Sephadex-G50 gel filtration column to separate rPh-labeled F-actin from unbound, free dye. Fractions were collected and rPh-fluorescence was measured at 540/572 nm (Excitation/Emission).

Notably, phalloidin is known to have a stabilizing function, and thus can prevent F-actin against depolymerization (Low and Wieland, 1974). In order to make certain that the amount of TRiC-folded actin, capable of binding to DNase I, remained unaffected upon rPh-treatment, actin labeling with rPh was additionally performed prior to DNase I incubation (Figure 26A). Importantly, the amount of DNase I-bound actin remained constant at a level of ~40-50%, irrespective of the time point of rPh treatment (compare Figures 26B and 20B). Thus, the overall percentage of newly synthesized, TRiC-folded actin in the bacterial system is ~80%, which corresponds to ~140 µg/ml (~3.2 µM) *per* hour.

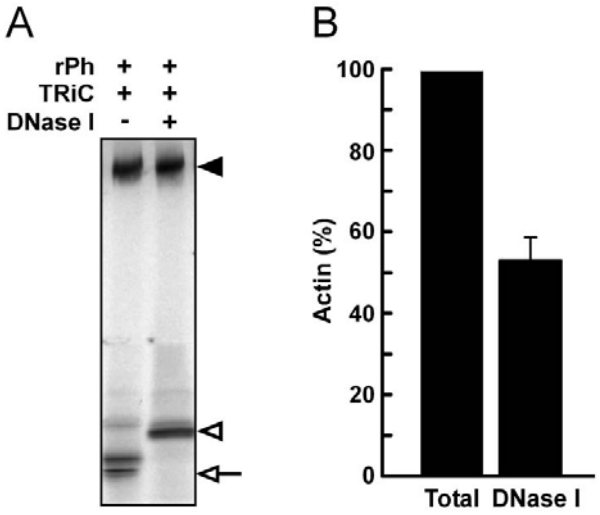

Figure 26: Incubation of actin with rPh does not affect DNase I binding efficieny.

(A) Native PAGE of actin synthesized in the presence of TRiC. Actin translation was stopped with RNAse A after 1 h and incubated with rPh (10 µM) before addition of DNase I to the supernatant, as indicated. Filled arrowhead: actin:TRiC complex; empty arrowhead: actin:DNase I complex; empty arrow: native actin. **(B)** Phosphoimaging quantitation of actin bound to DNase I (DNase I) as assessed in (A) relative to the amount of total actin synthesized (Total).

3.3 Role of TRiC in the folding of actin-fusion proteins

Despite a uniform size distribution of protein domains throughout all three kingdoms of life (Blake, 1985), the number of complex proteins combining multiple domains is proportionally larger in eukaryotes than in bacteria. In 1998, Netzer and Hartl proposed most eukaryotic multi-domain proteins to fold co-translationally in a domain-wise and conceivably Hsp70-assisted manner, but independent of the interaction with the TRiC chaperonin. In fact, it was suggested that TRiC is specialized for the post-translational completion of folding of modular proteins (including actin), which are constructed of discontiguous or structurally unstable sequence segments and therefore incapable of forming native tertiary structures during translation (Netzer and Hartl, 1998). Support for TRiC being involved in domain-wise protein folding mechanisms came from previous studies using pulse-chase experiments, where the chaperonin was shown to transiently associate with large substrate proteins, clearly exceeding the ~50 kDa size limit of the TRiC folding cavity (Ditzel et al.,

1998; Thulasiraman et al., 1999). Furthermore, cross-linking studies demonstrated that TRiC can interact co-translationally with actin nascent chains, soon after they emerge from the ribosomal exit site (McCallum et al., 2000; Etchells et al., 2005). These results strongly support a close association between the chaperonin and the translation machinery and strengthen the idea of TRiC being able to shield hydrophobic patches of discontiguously organized domains of modular proteins during synthesis (Netzer and Hartl, 1998). However, experimental evidence for a domain-wise mode of TRiC-mediated folding has not yet been provided.

In the following section, various actin-fusion proteins were generated and served as model multi-domain chaperonin substrates to elucidate the role of TRiC in domain-wise protein folding. Upon expression of the individual actin-fusions in *S. cerevisiae*, the folding state of actin within the fusion protein was examined by its capability to incorporate into yeast cytoskeletal structures, such as cortical patches and actin cables. Additionally, the actin-fusions were expressed in RRL and analyzed with regard to their specific binding to DNase I.

3.3.1 Actin-GFP fusions integrate into yeast actin cortical patches

Green fluorescent protein (GFP), a ~27 kDa single domain protein from the jellyfish *Aequorea victoria* (Prasher et al., 1992), is a frequently utilized fusion partner to analyze the intracellular localization of proteins in various cells types (Stearns, 1995; Simpson et al., 2000). Recently, several multi-domain GFP-fusion proteins were generated by domain recombination and demonstrated to fold with high efficiency upon expression in yeast (Chang et al., 2005). Based on this observation, modular proteins consisting of yeast actin, N- and/or C-terminally fused to different fluorescent proteins, were generated in order to investigate the capacity of TRiC to fold multi-domain proteins *in vivo* (Figure 27A). Depending on the number of attached fluorescent proteins, the actin fusion proteins varied in size between ~70-100 kDa and thus clearly exceeded the upper size limit of ~50 kDa, determined for group II chaperonin folding cavities (Ditzel et al., 1998). Individual domains between the fused proteins were connected by flexible linker regions as described previously (2.1.5.1; Chang et al., 2005). Upon recombinant expression of actin-GFP (AG) and GFP-actin (GA) in exponentially growing yeast

Δ*reg* cells (theses cells allow regulated protein expression from *GAL1*-controlled plasmids in presence of glucose) both fusion proteins displayed punctate, fluorescent cortical patches, asymmetrically localized to the bud and mother-bud neck (Figure 27B). Visualization of the actin cytoskeleton by rPh-staining demonstrated a co-localization of GFP- and rPh-labeled cortical patches, indicative for AG and GA being properly incorporated into the cellular actin cytoskeleton as well as actin having acquired its native state in both fusion variants. Co-localization of AG and GA with rPh-stained actin cables aligning along the mother-bud axis was not observed. Importantly, expression of AG and GA did not affect the actin distribution within the cells as the staining patterns with rPh were similar to those obtained for control cells harboring an empty plasmid or solely expressing actin or GFP, respectively.

In order to investigate whether TRiC is also able to fold actin when fused to both an N- and C-terminal fluorescent protein, an actin double-fusion was made. To this end, blue fluorescent protein (BFP: a GFP-variant with blue-shifted spectroscopic properties), whose fluorescence signal does not interfere with the detection of co-localized GFP- and rPh-labeled proteins *in vivo*, was N-terminally fused to the previously described AG, yielding the three-domain protein BAG (Figure 27A). Upon expression of BAG in Δ*reg* cells, the fluorescence signal resulting from the C-terminal GFP-moiety showed a diffuse cytosolic distribution, similar to that observed for GFP expression alone (Figure 27B). Incorporation of BAG in rPh-stained endogenous actin structures was not detectable.

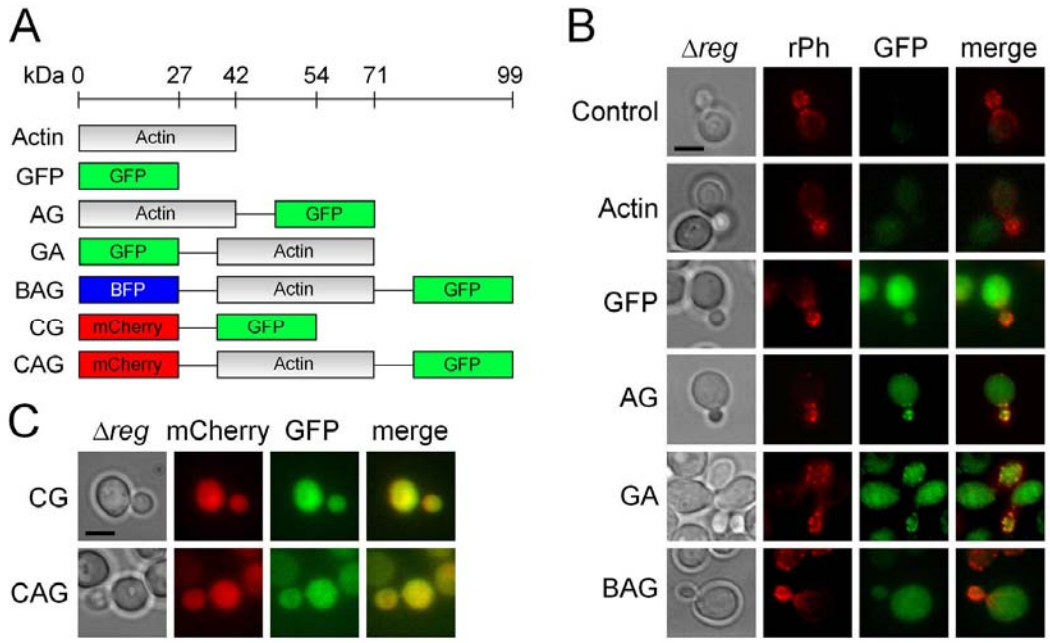

Figure 27: Expression of actin-fusion proteins in yeast.

(A) Actin-fusion proteins with the size (in kDa) of each protein being indicated on the scale depicted above the fusion constructs. **(B, C)** Fluorescence microscopy analysis of actin-fusions in fixed yeast Δ*reg* cells. **(B)** Cytoskeletal actin structures (cortical patches and actin cables) where visualized by staining with rhodamine-phalloidin (rPh). **(C)** Fusion-proteins containing both GFP and mCherry fluorescent proteins. Empty vector (Control), actin-GFP (AG), GFP-actin (GA), BFP-actin-GFP (BAG), mCherry-GFP (CG), mCherry-actin-GFP (CAG). Size bar = 4 µm.

To assess whether this effect is due to the multi-domain structure of BAG and accompanying steric hindrances during the process of F-actin assembly or whether it is an intrinsic problem caused by BFP, a second three-domain fusion was made. Therefore, BFP at the N-terminus of BAG was replaced by the equally sized and similarly folded red-fluorescent protein mCherry (monomeric Cherry: an improved DsRed-variant from *Discosoma* sp.) which was recently demonstrated to properly incorporate into cytoskeletal structures when fused to β-actin (Shaner et al., 2004). Expression of the newly made double-fusion CAG in Δ*reg* cells resulted in a diffuse cytosolic distribution of red and green fluorescence, similar to the GFP signal observed for BAG (Figure 27C). Essentially the same result was obtained upon expression of mCherry-GFP (CG), lacking the entire actin domain (Figure 27C). This supports the notion that, although both fluorescent protein domains in the actin-fusions are folded

correctly, CAG and BAG are not able to incorporate in preexisting cellular actin structures.

The *in vivo* expression of all actin-fusion proteins to their correct size was verified by western blot analyses. After cell lysis, equal amounts of yeast crude protein extracts were run on SDS-PAGE followed by immunoblotting with antibodies directed against GFP, actin (Act1p), and alcohol dehydrogenase (Adh1p), with the latter serving as an internal loading control (Figure 28). All fusion proteins were correctly expressed with GFP being part of their multi-domain structure. Furthermore, translation of the respective fusion proteins in RRL revealed the majority of synthesized protein to be in the soluble fraction (3.3.3).

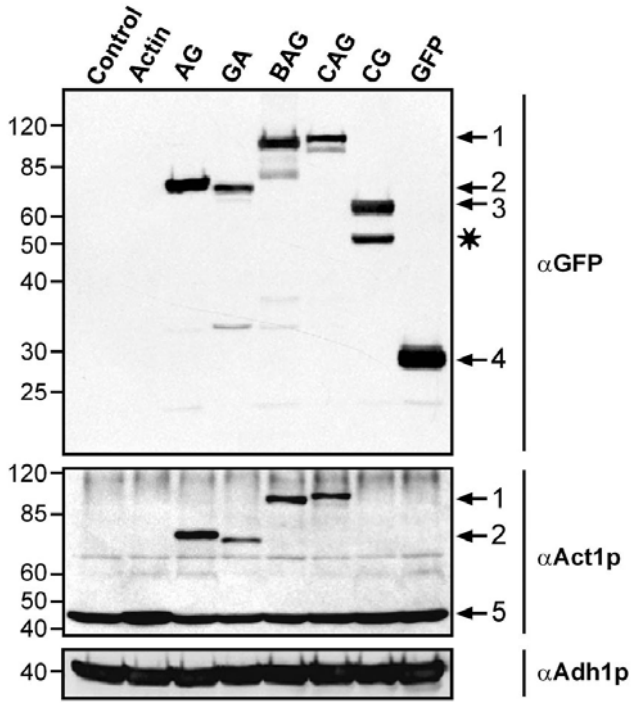

Figure 28: Western blot analyses of actin-fusion proteins upon expression in yeast.

Yeast Δ*reg* crude protein extracts of recombinantly expressed proteins, as indicated, were analyzed by SDS-PAGE and immunoblotting with antibodies directed against GFP (top), actin (Act1p, middle), and alcohol dehydrogenase (Adh1p, bottom), respectively. Numbers 1 to 5 indicate the position of equally sized proteins on the respective western blots: BAG and CAG (1), AG and GA (2), CG (3), GFP (4), actin (5). The band marked by an asterisk was not analyzed further. Abbreviations of the individual proteins are as in Figure 27.

3.3.2 Actin does not affect folding of GFP and mCherry in actin double-fusion proteins

In order to determine whether actin located between two fluorescence partners in a multi-domain protein imposes any constraints on their folding, *in vitro* fluorescence studies were performed. CAG was overexpressed in yeast and enriched to a semi-pure state by affinity purification (His-tag) and gel filtration (Figure 29A; 2.3.3.4). Additionally, CAG and CG (lacking the actin domain), were translated in cell-free wheat germ lysate (WG; Figure 29A) in order to reveal possible differences in the folding of multi-domain actin-fusions *in vitro* and *in vivo*. Notably, protein synthesis performed in the WG system is significantly more efficient than in RRL. Furthermore, the thus produced proteins are directly applicable to fluorescence analyses as WG does not contain hemoglobin, the iron-containing protein of red blood cells interfering with fluorescence measurements. The fluorescence emission spectra acquired for CAG (enriched from yeast) revealed an approximately 9-fold higher GFP-fluorescence intensity when compared to the signal obtained for mCherry (Figure 29B, top panel). Essentially the same ratios of GFP/mCherry-fluorescence were measured in the soluble fractions of CAG and CG upon expression in WG (Figure 29B and 29C). These findings suggest that mCherry and GFP, N- and C-terminally fused to actin, are able to fold with similar efficiencies upon expression *in vivo* and *in vitro*. Thus, folding of the individual fluorescent proteins in CAG seems to occur independently and unimpaired by the folding state of actin. Furthermore, these results are in accordance to the previously reported *in vivo* fluorescence data (Figure 27).

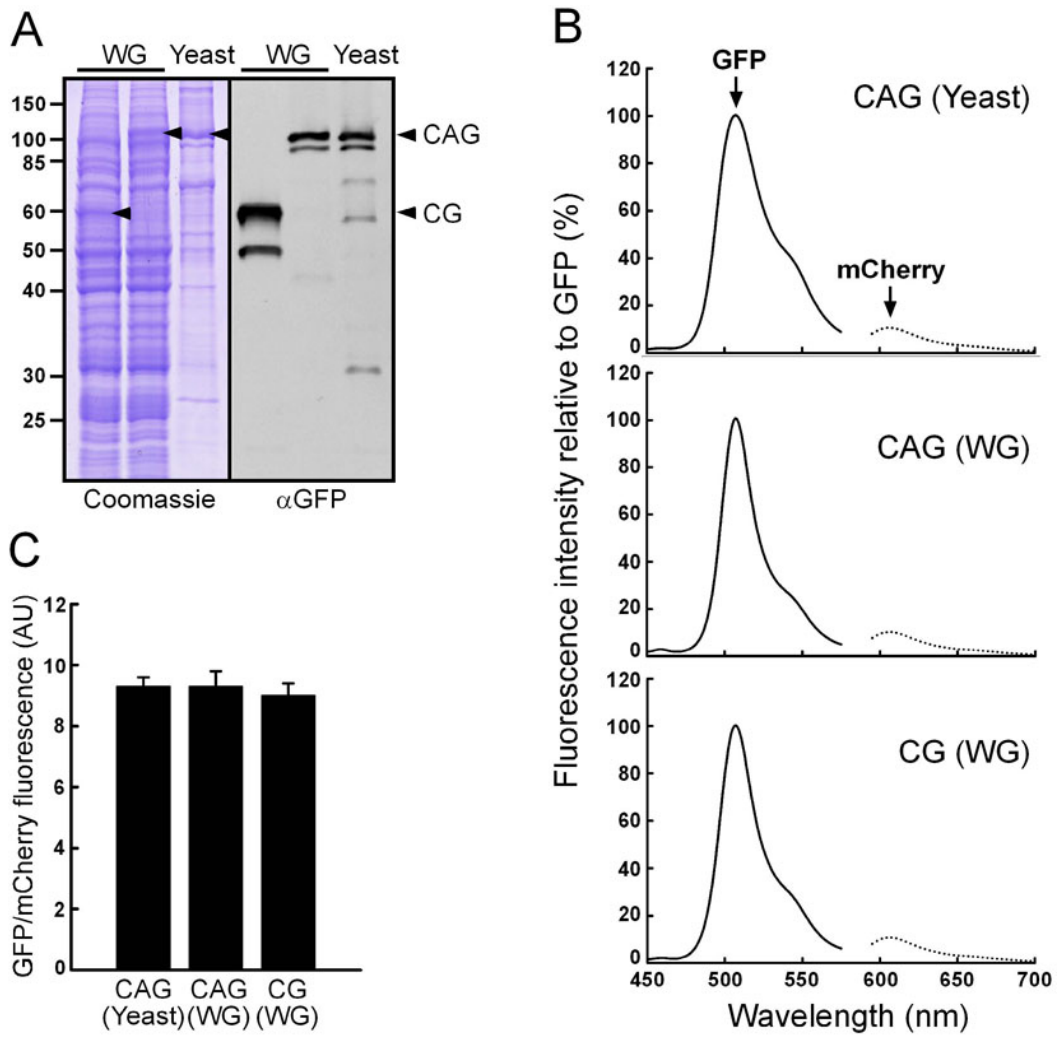

Figure 29: Actin does not affect fluorescence intensities of GFP and mCherry in the double-fusion CAG.

(A) SDS-PAGE (left) and Western blot analysis directed against GFP (right) of enriched CAG upon expression in yeast (Yeast) as well as samples of the soluble lysate fraction of CAG and CG upon expression in wheat germ lysates (WG). Full-length fusion proteins are indicated by arrowheads. **(B)** Combined fluorescence emission spectra of GFP (excited at 397 nm, solid line) and mCherry (excited at 585 nm, dotted line) acquired from CAG and CG upon expression in yeast (Yeast) or wheat germ lysates (WG), as indicated. **(C)** Ratios of GFP/mCherry-fluorescence intensities as assessed in (B), obtained at their fluorescence maxima at 506 nm and 606 nm, respectively.

3.3.3 TRiC is capable of assisting domain-wise protein folding

Next, the ability of TRiC to facilitate the folding of discrete domains of large multi-domain actin-fusion proteins was investigated *in vitro*. To this end, the already existing actin fusion constructs (Figure 27A) were subcloned in *in vitro* expression vectors suitable for T7-promoter driven protein expression (Figure 30A). In addition to that, BAG variants containing a TEV-(Tobacco Etch Virus)-protease cleavage site in the linker connecting BFP and actin (referred to as BTAG and BTAG-G150P, respectively) were made. This allowed the specific protein processing upon translation, and subsequent evaluation of the folding state of actin in the remaining AG-fusion by binding to DNase I (see below). To assess whether actin can reach its native state when embedded between two fusion partners is of particular interest, since only AG and GA have been shown to properly integrate into yeast cortical patches upon expression *in vivo* (Figure 27B).

In vitro translation reactions of individual actin-fusions were performed in RRL supplemented with [^{35}S]-Met, as described (2.3.4). Examination of the translation products by SDS-PAGE analysis revealed all fusions to appear almost exclusively in the soluble fraction (Figure 30B). Since the folding cavity of group II chaperonins was reported to have an upper size limit of ~50 kDa (Ditzel et al., 1998), the ability of TRiC to interact with actin-fusion proteins ranging between ~70-100 kDa (thus, too large for complete encapsulation) was analyzed. Therefore, samples of total RRL translation products were run on native PAGE and the resulting complexes analyzed by phosphoimaging (Figure 30C). TRiC was found to interact with all fusions containing actin as part of their protein composition, irrespective of the actin position within the molecule. As expected, complex formation between TRiC and BG (BFP-GFP), lacking the actin domain, was not observed. BTAG-G150P, a BTAG variant with the highly conserved glycine-150 in actin being mutated to proline (1.3.4) did not display any abnormalities with regard to solubility and TRiC binding when compared to other fusion proteins (Figures 30B and 30C). Since this particular point-mutation was recently reported to cause impaired actin folding due to protein arrest on the

TRiC chaperonin (McCormack et al., 2001), BTAG-G150P was utilized as a control fusion-protein for subsequent *in vitro* experiments.

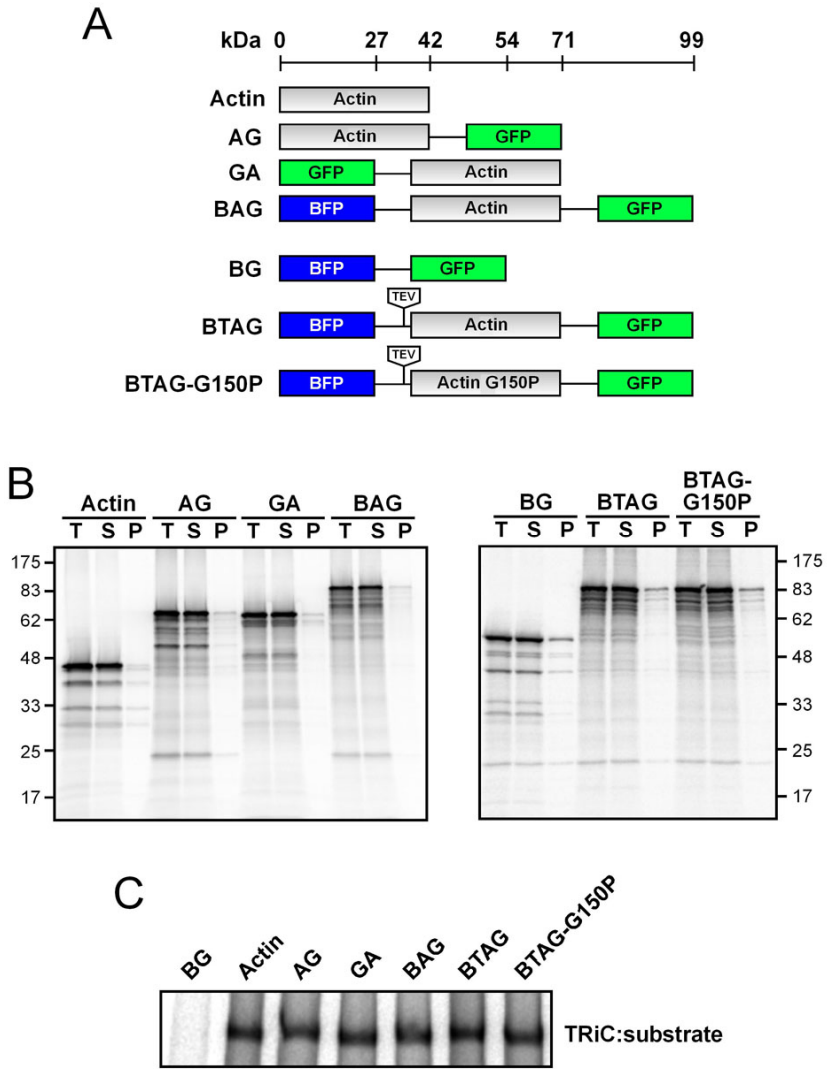

Figure 30: Actin-fusions expressed in RRL are soluble and interact with TRiC.

A) Actin-fusion constructs for *in vitro* expression in RRL with the size (in kDa) of each protein being indicated on the scale depicted above the fusion constructs. **(B)** SDS-PAGE of total (T), supernatant (S) and pellet (P) fractions of actin-fusions translated in RRL, as indicated. **(C)** Native PAGE of total protein samples from translation reactions as performed in (B) showing TRiC:substrate complexes (TRiC:substrate). actin-GFP (AG), GFP-actin (GA), BFP-actin-GFP (BAG), BFP-GFP (BG), BAG containing a TEV-protease cleavage site in the linker region between BFP and actin (BTAG), BTAG with actin amino acid 150 being mutated from glycine to proline (BTAG-G150P).

If the eukaryotic chaperonin TRiC is indeed able to fold large modular proteins in a domain-wise manner, one would expect that TEV-cleavage of BTAG

and BTAG-G150P, upon translation in RRL, results in stable AG-fragments able to bind to DNase I. To ensure that actin had acquired its native state in the context of the fusion protein, TRiC function had to be efficiently abolished prior to protease treatment. Actin folding in desalted RRL was previously demonstrated to be dependent on the addition of hydrolyzable ATP (Frydman and Hartl, 1996). In analogy, refolding of denatured radiolabeled actin in untreated, ATP-containing RRL resulted in the production of native actin (Figure 31, lane 6) as evidenced by the characteristic mobility shift on native PAGE after addition of DNase I (Figure 31, lane 7). Similar results were obtained when actin was refolded in presence of purified TRiC (Figure 31, lanes 1-3; also see Figure 18) or upon *de novo* synthesis of actin in untreated RRL (Figure 31, lanes 8-9). Treatment of RRL with apyrase for 2 min prior to actin refolding efficiently inhibited TRiC function and did not lead to the formation of native actin (Figure 31, lanes 4-5).

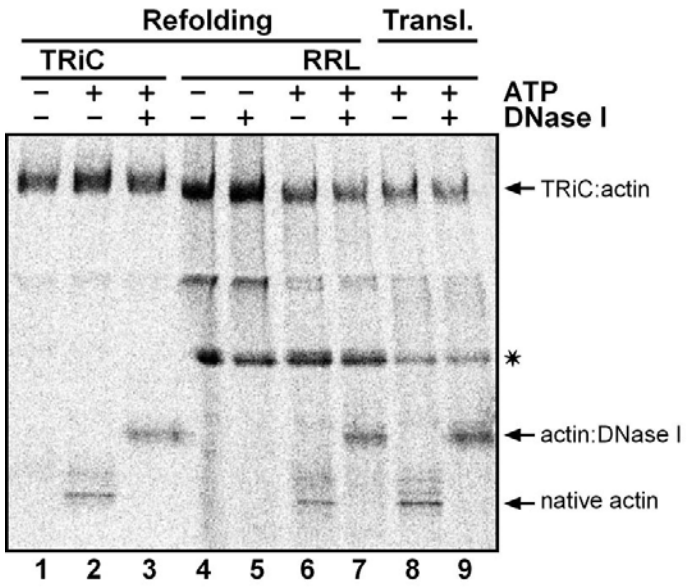

Figure 31: Depletion of ATP in RRL efficiently inhibits TRiC-mediated actin folding.

Native PAGE of actin refolding experiments performed with purified TRiC (lanes 1-3) or in rabbit reticulocyte lysate (RRL, lanes 4-7). Reactions were conducted in presence or absence of ATP and upon completion additionally received DNase I, as indicated. Lanes 8-9: actin synthesized in RRL as described (2.3.4). Bands marked with an asterisk, probably representing actin bound to PFD, were not analyzed further.

Based on these results, translation reactions of yeast actin as well as AG and GA fusion proteins were carried out in RRL for 90 min. Upon depletion of ATP by treatment with apyrase for 2 min, folded actin was precipitated with DNase I-Sepharose beads for 2 h in the cold. In every case tested, substantial amounts of radiolabeled material specifically associated with DNase I as analyzed by SDS-PAGE and phosphoimaging (Figure 32A). Thus, TRiC is able to meditate folding of newly translated actin even when the actin molecule is N- or C-terminally fused to GFP and hence is lager than the determined capacity of the chaperonin cavity (~71 kDa compared to ~50 kDa of the chaperonin cavity). Importantly, this result is consistent with the proper incorporation of AG and GA into actin cortical patches upon expression in yeast (Figure 27B). Next, the ability of TRiC to accomplish folding of actin when bilaterally fused to two fluorescent proteins was investigated. To this end, similar experiments to the ones described above were performed with actin double-fusion proteins (Figure 32B). In addition to treatment with apyrase, the translation reactions were subjected to TEV-protease cleavage for 30 min at 30 °C. As expected, cleavage only occurred in BTAG and BTAG-G150P containing a TEV-site in the linker between BFP and actin, liberating BFP from the remaining AG-fragment (Figure 32B: compare lanes 1, 3, 5, and 7 with lanes 9-12, respectively). Upon incubation with DNase I-beads, similar amounts of BG and AG-G150P (resulting from BTAG-G150P) relative to the input material were precipitated (Figure 32B and 32C). Since BG does not contain actin, this was considered the background level of non-specific DNase I binding. Strikingly, complex formation with DNase I was ~7-fold more efficient for AG (originating from BTAG) than for AG-G150P containing an actin-mutant with impaired folding properties. Interestingly, even though the AG-fragment of cleaved BTAG efficiently bound to DNase I, uncleaved BAG (Figure 32B, lane 4: arrow) did not show DNase I binding above background level (Figure 32C). Together, TRiC is not only able to facilitate the folding of AG and GA, with actin being accessible at least from one side of the protein, but also mediates the domain-wise folding of actin double-fusions, with actin embedded between two fluorescent partners.

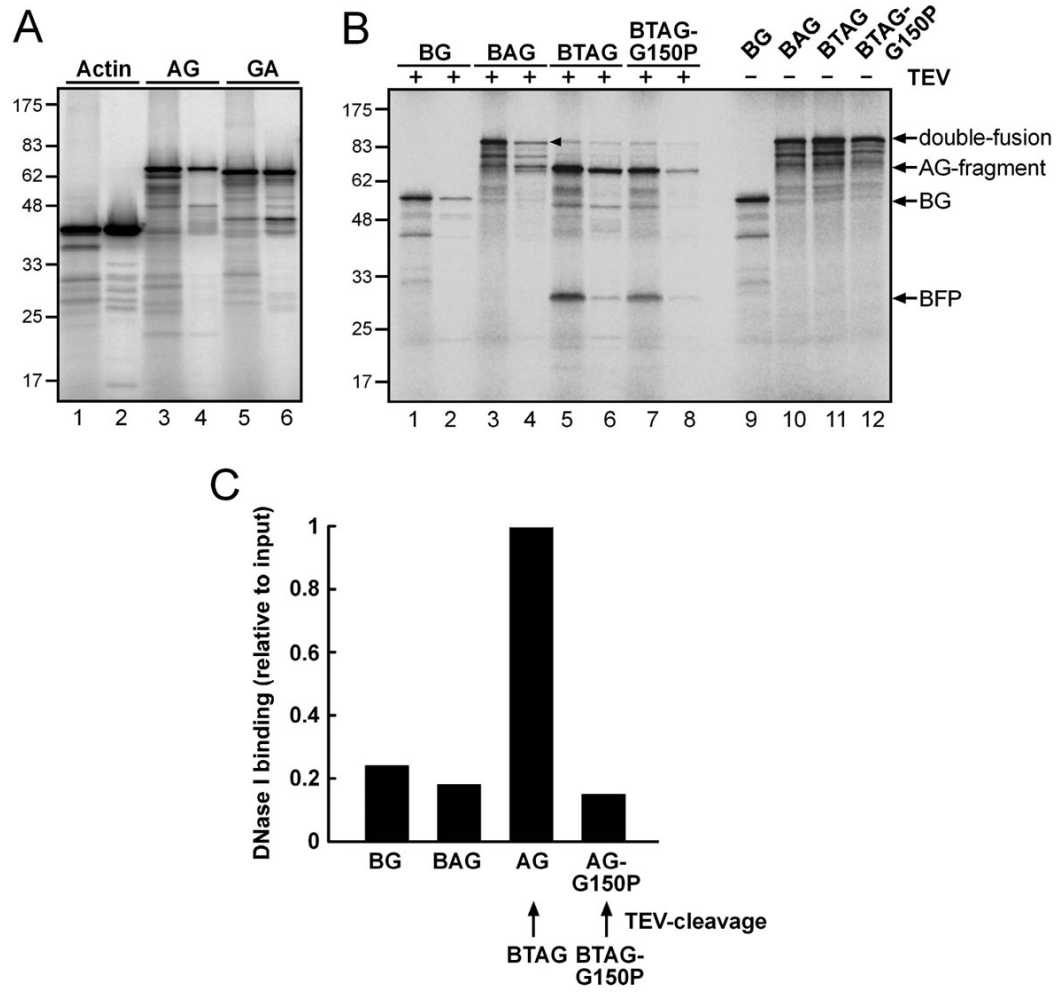

Figure 32: TRiC is able to facilitate domain-wise folding of actin-fusion proteins.

(A, B) DNase I-precipitations of actin-containing fusion proteins upon *de novo* synthesis in RRL and subsequent apyrase treatment, analyzed by SDS-PAGE and phosphoimaging. **(A)** Input (10% of total; odd numbers) and eluate fractions from DNase I-beads (even numbers). **(B)** Prior to DNase I-precipitation, reactions were additionally subjected to TEV-protease treatment, as indicated. Lanes 1-8: input (10% of total; odd numbers) and eluate fractions from DNase I-beads (even numbers). Lanes 9-12: untreated total protein fractions. **(C)** Phosphoimaging quantitation of DNase I-precipitates as assessed in (B: lanes 2, 4, 6 and 8); band used for quantitation of BAG (lane 4) is indicated by an arrowhead. Abbreviations of the individual proteins are as in Figure 30.

In view of these observations and the inability of BAG to properly integrate into actin cortical patches (Figure 27B), the folding state of actin within BTAG and BTAG-G150P was further investigated *in vivo*. Upon protein expression in yeast Δ*reg* cells to similar levels, cell lysis under native conditions was performed in presence of cycloheximide and apyrase in order to inhibit

protein synthesis and TRiC function, respectively (2.4.6). Treatment with TEV-protease (30 min at 30 °C) and subsequent DNase I-precipitation of the cleavage products for 2 h in the cold revealed a ~5-fold higher binding efficiency of AG, originating from BTAG, than for AG-G150P containing the actin mutant protein (Figure 33).

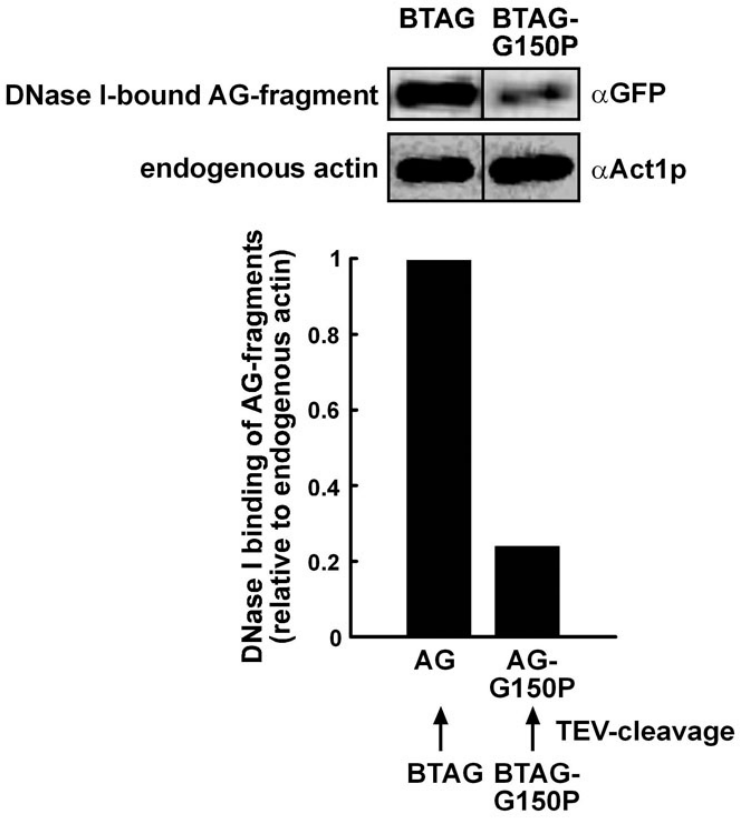

Figure 33: TRiC facilitates the folding of multi-domain proteins *in vivo*.

BTAG and BTAG-G150P were expressed to similar levels in yeast Δ*reg* cells. Following cell lysis in presence of cycloheximide and apyrase, the crude extracts were treated with TEV-protease and the resulting AG-fragments precipitated by DNase I-Sepharose beads. Upper panel: DNase I-bound AG-fragments (top) and endogenous yeast actin (bottom) analyzed by immunoblotting against GFP and yeast actin (Act1p), respectively. Lower panel: Quantitation of AG-fragments upon TEV-cleavage and precipitation by DNase I-beads as assessed by immunoblotting.

As the *in vivo* experiment perfectly matched the data obtained *in vitro* (see above), TRiC was assumed to indeed facilitate the domain-wise folding of multi-domain fusion proteins, too large for complete encapsulation in the chaperonin cavity.

4 Discussion

In this work, the role of molecular chaperones in the folding of eukaryotic multi-domain proteins was investigated upon translation in cell-free translation systems. Protein expression in a chaperone-diminished *E. coli* lysate allowed a detailed analysis of how chaperone intervention during *de novo* synthesis affects the mechanism of protein folding and its coupling to translation. In the case of FL, supplementation of the bacterial lysate with purified TF and the Hsp70 chaperone system KJE not only affected the efficiency but also the mechanism of *de novo* folding.

Furthermore, the absence of eukaryotic chaperones in the *E. coli* lysate provided the possibility to determine the minimum requirements for the efficient production of native actin upon *de novo* synthesis. Formation of correctly folded actin was assayed in the absence and presence of the above mentioned *E. coli* chaperones as well as ELES or the eukaryotic chaperonin TRiC. Importantly, TRiC was found to be necessary and sufficient for the folding of actin without further manipulations.

Additionally, using multi-domain proteins, the previously suggested role of TRiC in domain-wise folding of complex modular proteins was investigated. In yeast, the expression of actin fused to various fluorescent proteins not only allowed the exact location of these proteins within the cell, but also the detection of any incorporation into pre-existing actin structures. The formation of native actin within the fusion-proteins upon expression *in vivo* and in eukaryotic cell-free translation systems was verified by its ability to bind to DNase I.

4.1 TF and DnaK affect the efficiency and mechanism of *de novo* protein folding in the bacterial cytosol

The Gram-negative bacterium *E. coli* is the most extensively used prokaryotic organism for the recombinant expression of proteins for research and biotechnology. Unfortunately, overproduction of heterologous (eukaryotic

multi-domain) proteins in the bacterial cytosol is often accompanied by misfolding and subsequent segregation of non-native intermediates into insoluble aggregates, known as inclusion bodies (Marston, 1986; Baneyx and Mujacic, 2004). Although inclusion bodies mainly consist of highly concentrated and almost pure protein, hence simplifying purification, *in vitro* refolding yields of complex modular proteins are usually very low (Marston, 1986; Jaenicke, 1987). A frequently used approach to improve the solubility of heterologous aggregation-prone proteins in *E. coli* involves the overexpression of molecular chaperones implicated in *de novo* protein folding. Since in many cases the "yield-limiting" step for the generation of native protein is folding, rather than synthesis, the beneficial effects of increased chaperone concentrations like that of TF, KJE as well as ELES were demonstrated multiple times (Caspers et al., 1994; Dale et al., 1994; Thomas and Baneyx, 1996; Nishihara et al., 2000; Baneyx and Palumbo, 2003). On the other hand, *E. coli* cells lacking both TF and KJE (Δ*tig*Δ*dnaKdnaJ*) display fundamental defects in cytosolic protein folding (Genevaux et al., 2004). Notably, deletion of GroEL and/or its cofactor GroES is lethal since both protein complexes are absolutely essential for bacterial growth (Fayet et al., 1989).

4.1.1 The bacterial cytosol does not support efficient folding of eukaryotic multi-domain proteins

In order to investigate the effect of bacterial chaperones on the folding of eukaryotic multi-domain proteins, FL was expressed in a bacterial S30 lysate. Whereas the *in vivo* concentrations of TF, DnaK, and GroEL under standard growth conditions are ~40 μM, ~50 μM, and ~3 μM, respectively (Lill et al., 1988; Hesterkamp and Bukau, 1998; Hartl and Hayer-Hartl, 2002), the chaperone concentrations in this lysate were determined to by ~0.5 μM for both TF and DnaK, and ~0.1 μM for GroEL (Agashe et al., 2004). Hence, this lysate represents a dilute cytosol, drastically depleted of bacterial chaperones.

Refolding of fully denatured FL in the absence of chaperones is known to be an extremely slow process (equilibrium is reached only after days). This phenomenon is attributed to kinetically trapped folding intermediates imposed

by intramolecular misfolding (Herbst et al., 1998; Frydman et al., 1999). In contrast, FL refolding in the presence of the Hsp70 system occurs with a half-time of ~10-15 min and with approximately 80% efficiency (Szabo et al., 1994). To assess whether the residual amounts of bacterial chaperones in this system are able to support protein folding *in vitro*, refolding experiments of chemically denatured FL were performed in the S30 lysate (Figure 11). Efficient refolding (up to ~80-90%) was only seen when the lysate was supplemented with purified components of the bacterial Hsp70 chaperone system KJE, irrespective of the presence of TF. Since neither the unsupplemented nor the TF-supplemented lysate could restore FL activity above background level (~10%), refolding of FL was demonstrated to depend solely on the presence of KJE as described previously (Schroder et al., 1993; Szabo et al., 1994). Refolding experiments in the presence of ELES were not performed, as the bacterial chaperonin does not support FL folding *in vitro* (Frydman et al., 1992). Given these findings, the S30 lysate was considered to be a dilute bacterial cytosol preparation, functionally depleted of endogenous chaperones.

As shown initially, FL expression in *E. coli* and *S. cervisiae* resulted in dramatic differences regarding protein solubility and enzyme activity (Figure 10). Whereas in yeast, FL was almost exclusively soluble and active, its solubility in *E. coli* was only ~40% with most of the protein being inactive due to intramolecular misfolding and/or interchain aggregation. This observation is astonishing, since the bacterial cytosol contains high amounts of KJE (see above), demonstrated to be the only chaperones necessary and sufficient for FL refolding *in vitro* (Figure 11). Together, these findings strongly suggest that the chaperone interaction of FL nascent chains during *de novo* folding differs considerably from that required for efficient refolding of FL out of denaturant.

To elucidate the phenomenon of why eukaryotic multi-domain proteins fold inefficiently in the bacterial cytosol, FL was translated in cell-free lysates of eukaryotic (RRL) and bacterial (S30) origin. In accordance to the data obtained in yeast, folding of FL in RRL occurred with ~60% efficiency and essentially all the protein was recovered in the soluble fraction (Figure 10). Further, comparing the kinetics of translation and folding revealed that FL enzyme activity appeared

virtually concurrently with the production of full-length chains (Figure 13A), indicative of a co-translational folding mechanism. This observation was in good agreement to the co-translational folding of the N-terminal domain of FL during synthesis, and the rapid formation of native protein upon chain release from the ribosome (Frydman et al., 1994; Kolb et al., 1994; Frydman et al., 1999). Thus, efficient folding of multi-domain proteins in the eukaryotic cytosol may be facilitated by a mechanism of sequential, co-translational domain folding, similar to that observed for the artificial two-domain protein Ras-DHFR (Netzer and Hartl, 1997). Moreover, the eukaryotic Hsp70 system was suggested to play a critical role in stabilizing nascent chains of multi-domain proteins at early times of translation in order to prevent intramolecular misfolding and protein aggregation (Frydman et al., 1994). Unexpectedly, co-translational folding of FL was also observed in the unsupplemented S30 lysate (Figure 13A). However, under these conditions, the folding yield was very low (~5% compared to ~60% in RRL) and only ~45% of the protein was recovered in the soluble fraction (Figure 10). This supports the notion that successful folding of complex eukaryotic proteins in the bacterial cytosol not only depends on the applied mechanism but also on the availability of suitable chaperones promoting their effective folding.

Although supplementing the lysate with bacterial chaperones improved the solubility of newly translated FL considerably, an increase in specific activity was only observed when TF was added alone or in combination with KJE. Moreover, the beneficial effect of TF on FL activity was demonstrated to strongly depend on the residual amounts of DnaK in the lysate, as the specific activity did not increase when DnaK levels were reduced further by immunodepletion (Agashe et al., 2004). These findings suggest that, in order to increase the folding efficiency of newly translated FL, TF and KJE have to cooperate, whereas refolding of denatured FL in the same lysate only depends on KJE. Further, given a refolding efficiency of ~80-90% in presence of KJE (Figure 11), and a recovery of only ~20% of active enzyme upon translation in the TF/KJE-supplemented lysate (3.1.2), TF seems to function inefficiently in stabilizing FL nascent chains in a conformation competent for folding by KJE. Together, the folding yield of newly

translated FL appears to be critically dependent on the ability of bacterial chaperones in order to prevent misfolding events in elongating chains as soon as they emerge from ribosomal tunnel. The validity of this assumption becomes obvious when looking at the expression of bacterial β-galactosidase (β-gal; a tetrameric complex with five domains per subunit (Jacobson et al., 1994)) in the same chaperone supplemented lysate. In that case, translation in the presence of TF and KJE resulted in ~90% soluble and active protein (Agashe et al., 2004). This strongly indicates that β-gal utilizes the *E. coli* chaperone system with high efficiency, whereas TF and KJE seem to be incompatible with the co-translational mechanism observed for FL folding in the eukaryotic cytosol.

4.1.2 Post-translational folding improves protein solubility and folding yield

FL folding in both *in vitro* systems, RRL and the unsupplemented S30 lysate, occurs rapidly and via a co-translational folding mechanism (Figure 13A). However, the tight coupling of translation and folding is only highly efficient in the eukaryotic lysate (~60%, compared to ~5% in the bacterial lysate; Figure 10), where FL folding is assisted by the mammalian Hsp70 system (Frydman et al., 1994). Strikingly, supplementing the S30 lysate with purified TF increased the amount of active FL 2 to 3-fold and concurrently imposed a significant deceleration in the kinetics of FL folding without affecting the actual speed of translation (Figures 12B and 13B). The delay in FL folding relative to protein synthesis was even more pronounced when the system was supplemented with TF and KJE together. Under these conditions, the folding yield was approximately 4-fold higher compared to FL translation in the unsupplemented lysate, indicative for a functional cooperation between TF and KJE in the S30 lysate. More generally, these findings suggest that in the presence of TF and KJE, *de novo* folding of FL is shifted from a rapid but inefficient folding pathway to a post-translational folding regime increasing both solubility and enzyme activity (Figures 12B and 13). However, with only ~20% of the protein being native, compared to ~60% or ~100% upon FL synthesis in RRL or yeast cells,

respectively, folding in the chaperone supplemented S30 lysate is much less efficient than in the eukaryotic cytosol (Figure 10).

Although previous data demonstrated that TF and KJE need to cooperate in order to improve the folding efficiency of FL in the bacterial lysate (3.1.2), their time of action during *de novo* folding remains unknown. Therefore, protein translations of ongoing FL reactions were terminated with RNase A and the appearance of FL enzyme activity was followed over time. In accordance to the TF/KJE-imposed delay in FL folding (Figure 13B), FL translation in the presence of these chaperones caused a more than 2-fold increase in enzyme activity upon inhibition of translation (Figure 15) Notably, the kinetics of activity increase were identical to that of KJE-mediated FL refolding out of denaturant (Figures 11 and 15). Since this post-translational folding phase was only observed when both chaperones were present from the beginning of the translation reaction, a functional cooperation between TF and KJE had to occur co-translationally (Figure 15). Thereby, TF binding to the large subunit of translating ribosome constitutes a prerequisite for its productive interaction with elongating nascent chains as post-translational FL activity was not observed with a triple-mutant form of TF, $TF_{FRK/AAA}$, which does not bind to the ribosome (Kramer et al., 2002). Post-translational folding was also abolished upon depletion of ATP in the system, arguing for the important role of the ATP-regulated bacterial Hsp70 system in FL folding. Additionally, control experiments releasing ribosomal stalled FL nascent chains into unsupplemented or TF/KJE-supplemented lysate demonstrated that TF and KJE do not delay the completion of FL folding upon protein release from the ribosome, but instead cause a genuine switch in the folding mechanism (Agashe et al., 2004). Together, these findings suggest that the co-translational action of both TF and KJE during *de novo* synthesis of FL is essential for enforcing post-translational folding, accompanied by an increase in protein solubility and the amount of active enzyme synthesized. Interestingly, the default-pathway of both β-gal folding and assembly in active tetramers in the unsupplemented S30 lysate was shown to be co-translational with an efficiency of about 25% (Agashe et al., 2004). Further, addition of TF and KJE, separately or together, markedly delayed folding relative

to translation, thereby improving β-gal activity up to ~75% and ~100%, respectively. Thus, in contrast to the combined action required in order to delay FL folding, TF and KJE seem to have overlapping functions in the folding and assembly process of β-gal. Moreover, as refolding of denatured β-gal in the chaperone supplemented lysate occurred with only ~10% efficiency, *de novo* folding of the bacterial multi-domain protein was suggested to be critically dependent on the co-translational activity of TF and KJE (Agashe et al., 2004).

4.1.3 How do TF and KJE delay protein folding?

A possible mechanism of how the combined action of TF and DnaK, which both recognize similar hydrophobic regions in newly synthesized proteins (Rudiger et al., 1997; Patzelt et al., 2001), could cause delayed folding in the bacterial cytosol was suggested in the work of Agashe et al. (2004). By conducting recruitment experiments of radiolabeled TF to translating ribosomes, the number of recruited TF molecules was shown to correlate well with the size of the translated protein and/or differences in the occurrence of hydrophobic peptide regions, recognized by the chaperone (Patzelt et al., 2001). Furthermore, TF was suggested to delay folding and misfolding of nascent chains by a dynamic interaction cycle in which the initially ribosome bound TF leaves its docking site at the 50S subunit and maintains contact with the elongating polypeptide chain, thereby providing room for a new TF molecule to dock onto the then vacant ribosome. Importantly, the mechanism proposed above was recently confirmed and described in more detail (Kaiser et al., 2006). By using fluorescence spectroscopy, TF function was monitored on translating ribosomes in real-time. As TF does not form long-lived complexes with newly synthesized substrate proteins (Hesterkamp et al., 1996; Maier et al., 2003; Kaiser et al., 2006), retention of the folding competence in protein regions, distantly located from the ribosome, may thus require the engagement of DnaK, whose chaperone function is independent of the ribosome. Since several high affinity DnaK-binding sites were determined in each structural domain of both FL and β-gal (Agashe et al., 2004) and DnaK binding/rebinding to non-native proteins occurs within seconds (Pierpaoli et al., 1997), rapid co-translational domain folding in each protein

would require the coordinated release of multiple DnaK molecules for which there is so far no experimental evidence. Considering the translation speed to be ~5-10 times faster in bacteria (~20 amino acids *per* second) when compared to the eukaryotic system (Bremer and Dennis, 1996), the functional cooperation between TF and KJE might be optimized for stabilizing nascent chains of complex modular architecture in a state competent for efficient post-translational folding. Interference by TF with the post-translational completion of folding is supposedly not a problem, since TF-nascent chain complexes are only formed subsequent to TF binding at the ribosome (Kaiser et al., 2006).

4.1.4 Default folding *versus* chaperone-assisted folding

Based on the *in vitro* data obtained for FL folding in the bacterial and eukaryotic cell lysates in this study, and the body of work generated with a second model protein (β-gal) in the same lysates as well as in living cells (*E. coli* and *S. cerevisiae*) (Agashe et al., 2004), a model explaining the role of TF and DnaK in determining both the mechanism and yield of protein folding in the bacterial cytosol was suggested (Figure 34). In the absence of TF and KJE, a default co-translational pathway produces a small proportion of native or native-like domain structures which complete folding rapidly after chains are released from the ribosome (Figure 34, (1)); the majority of nascent polypeptides misfold due to intermolecular misfolding or interchain aggregation (Figure 34, (2)). TF and KJE delay any folding (or misfolding) events, until the chain is released from the ribosome (Figure 34, (3)). The capacity of the chaperones to prevent folding is sufficient for bacterial proteins of average size, but is limited for long nascent chains. For proteins such as FL, the chaperone-imposed delay in folding would result in a high proportion of misfolded molecules (Figure 34, (6)). Large bacterial proteins such as β-gal, on the other hand, are adapted to this chaperone mechanism and could initiate productive folding co-translationally (Figure 34, (4)). Following nascent chain release from the ribosome, post-translational folding would be completed by KJE through ATP-dependent binding and release cycles (Figure 34, (7)), or upon protein transfer to downstream chaperones such as GroEL. In this scheme, the inherent propensity

of a protein to undergo intramolecular misfolding (kinetic trapping), either co- or post-translationally, would determine the yield of the folding process. Inefficient folding (and aggregation) would occur for those eukaryotic proteins (Figure 34, (6, 8)) that are highly dependent on a mechanism of timely co-translational domain folding in order to avoid kinetic traps. Such a pathway is actively supported by the chaperones in the eukaryotic cytosol (Figure 34, (5)) (Frydman et al., 1994).

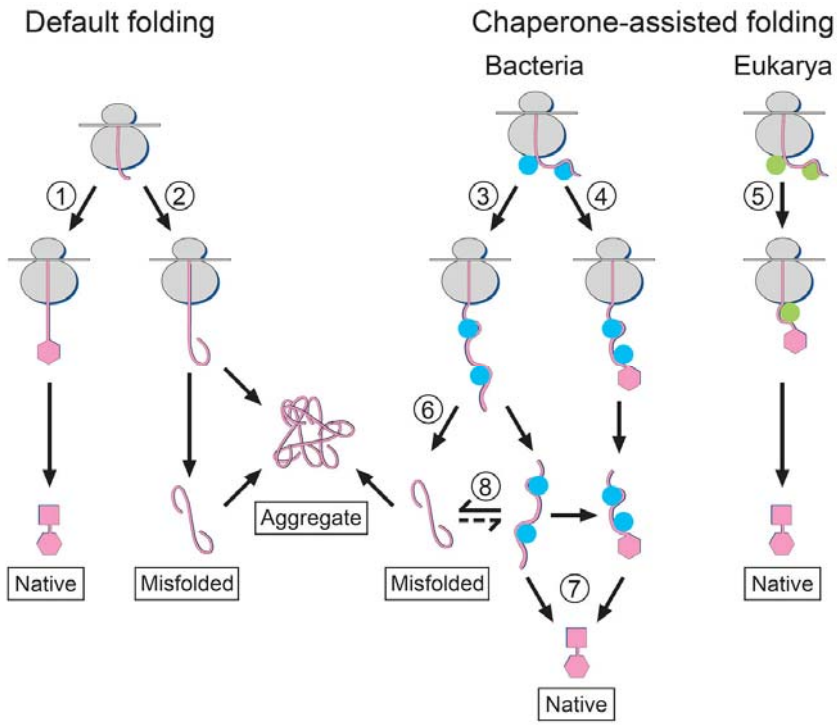

Figure 34: Effects of nascent chain-binding chaperones on the folding of multi-domain proteins, a working model.

The translating polypeptide chain is shown in pink with folded domains represented by hexagons and squares. Bacterial chaperones are given in blue and eukaryotic chaperones in green. Left: Default-pathway of co-translational domain folding (1) or misfolding (2) during rapid elongation in bacteria in the absence of nascent chain-binding chaperones. Right: Chaperone-assisted post-translational (3) or delayed co-translational folding (4) in bacteria, and efficient chaperone-assisted co-translational folding in the eukaryotic cytosol (5). Co-translational misfolding of proteins such as FL in the presence of bacterial chaperones (6). Folding (7) and misfolding (8) through post-translational chaperone cycling in the bacterial cytosol.

More generally, since TF only exists in bacteria which, on average, have smaller and fewer multi-domain proteins than eukaryotes (Netzer and Hartl, 1997), this ribosome associated chaperone may reflect an evolutionarily ancient principle of assisted folding. On the other hand, the efficient co-translational domain folding, as it occurs in the eukaryotic cytosol, may have contributed to the evolution of the variety of complex modular proteins characteristic of eukaryotic cells (Netzer and Hartl, 1997).

4.2 TRiC function is compatible with the bacterial translation machinery

In the *E. coli* cytosol, the majority of proteins (>60%) consist of only a single folding unit (up to ~300 amino acids). It has been suggested that these proteins can fold rapidly and without further assistance upon release from the ribosome (Hartl and Hayer-Hartl, 2002). In contrast, larger bacterial proteins consisting of several domains (such as β-gal) are strongly dependent on the productive interaction of molecular chaperones in order to avoid intramolecular misfolding and/or aggregation (4.1.1). Although the bacterial chaperone machinery is highly effective in folding endogenous proteins, overexpression of modular eukaryotic proteins in the same systems often leads to misfolding and aggregation (Baneyx and Mujacic, 2004). The low folding yield of FL, for example, was shown to result from a reduced compatibility with bacterial chaperones (4.1). However, misfolding of actin in the bacterial cytosol is due to the lack of the eukaryotic chaperonin TRiC, the only chaperone able to direct actin to its native state (Tian et al., 1995).

4.2.1 TRiC promotes efficient *de novo* folding of actin

From its discovery, TRiC has been reported to be a molecular chaperone for actin and tubulin folding in the eukaryotic cytosol (Gao et al., 1992; Lewis et al., 1992; Yaffe et al., 1992). Many protocols for its purification have been described and the sources have varied from RRL (Gao et al., 1992; Yaffe et al., 1992; Norcum, 1996; Cowan, 1998) to bovine and mouse testis (Frydman et al., 1992; Liou and Willison, 1997; Ferreyra and Frydman, 2000), to guinea-pig and

rat brain (Roobol and Carden, 1993), to yeast (Miklos et al., 1994) as well as to different cell lines (Lewis et al., 1992; Roobol et al., 1995; Liou and Willison, 1997). Due to the complexity associated with expression, correct folding and proper assembly of the eight different TRiC subunits, attempts to obtain functionally active chaperonin complexes upon recombinant co-expression of all subunits have been unsuccessful so far. For this part of the work, TRiC was purified from bovine testis, where its expression is known to be highly upregulated during spermatogenesis (Willison et al., 1990). The purification was performed according to the protocol of Ferreyra and Frydman (Ferreyra and Frydman, 2000) with additional modifications as described in detail in the material and methods section (2.3.3.1). In brief, to avoid any adverse effects upon TRiC activity, the ammonium sulfate precipitation which applies high physical stress to the protein complex was omitted. Furthermore, the number of chromatographic steps was reduced to four, instead of five in the published protocol. Importantly, these modifications neither affected the overall yield of purified TRiC (~8 mg *per* 100 g testis) nor its activity and the ability to refold chemically denatured actin had a similar efficiency (~50%) to that reported previously (Gao et al., 1992; Ferreyra and Frydman, 2000) (Figures 16 and 18).

Given the combination of purified and functional TRiC and a highly productive bacterial *in vitro* translation system, which did not contain eukaryotic chaperones, the effect of TRiC on the behavior of actin folding during *de novo* synthesis in a bacterial lysate was analyzed in detail. In accordance to actin being sequestered into inclusion bodies upon expression in *E. coli* (Frankel et al., 1991) and TRiC being the only chaperone known to support efficient actin folding *in vivo* and *in vitro* (Tian et al., 1995), actin synthesis in the unsupplemented lysate resulted in ~90% of the protein found in the insoluble fraction (Figure 20A and 20B). Approximately ~10% of translated actin remained soluble, probably as a result of transient binding to residual bacterial chaperones present in the lysate (Figure 20C). On the other hand, when actin translations were performed in presence of purified TRiC (5 μM), ~80% of total synthesized protein appeared in the soluble faction (Figure 20). By taking advantage of the fact that only native monomeric actin (G-actin) forms a stable binary complex with DNase I

(Lazarides and Lindberg, 1974), approximately half of the soluble actin was demonstrated to exist as actin monomers with a correctly folded three-dimensional structure. Strikingly, as will be discussed later (4.2.2), the remainder of soluble protein was also native, but had already polymerized into actin filaments (F-actin) which are incapable of DNase I-binding (Hitchcock et al., 1976). Together, these findings clearly indicate that a bacterial translation system, functionally depleted of endogenous chaperones (3.1.2), is compatible with TRiC-assisted folding of a eukaryotic protein. Further, TRiC was demonstrated to be the only chaperone necessary and sufficient for the folding of substantial amounts of native actin (~140 µg/ml) without any further manipulation. More generally, since the bacterial cytosol did not contain any eukaryotic chaperones, the S30 lysate might thus constitute an ideal system to analyze the detailed mechanism of TRiC-mediated protein folding.

In view of the chaperone-impoverished S30 lysate and the effect on protein solubility/activity of FL observed upon chaperone supplementation (Figure 12B), actin was translated in the presence of individual bacterial chaperones. Although actin overexpression in *E. coli* cells results in the formation of inclusion bodies (Frankel et al., 1991), its *de novo* synthesis in the KJE or ELES supplemented S30 lysate yielded almost completely soluble protein (Figures 22A and 22B). However, the thus produced actin was not native as it did not form a stable complex with DNase I (Figure 22C). On the other hand, lysate supplementation with TF neither affected actin solubility nor its folding when compared to the unsupplemented lysate. In the past, recombinant protein expression in bacterial hosts was demonstrated to be able to exceed >50% of total cellular protein (Baneyx and Mujacic, 2004). Thus, massive overexpression of actin in *E. coli* cells is likely to overwhelm the chaperone capacity of the KJE and ELES system. As a logical consequence, actin chains without access to the beneficial effects of chaperone binding might be susceptible to aggregation and directed into inclusion bodies. Hence, it would be interesting to know whether low level expression of actin in *E. coli* could increase its solubility. Assuming an *in vivo* concentration of DnaK and GroEL (under standard growth conditions) of ~50 µM and ~3 µM, respectively (Hartl and Hayer-Hartl, 2002), a similar amount

of actin chains (~50 µM, corresponding to ~0.8 mg/ml) could principally be maintained in a soluble state.

4.2.2 Coexistence of G-actin and *bona fide* F-actin in the bacterial lysate

Actin constitutes the major component of the thin filaments of muscle cells and of the cytoskeleton of nonmuscle cells, taking part in a multitude of biological processes (Pollard et al., 2000). To accomplish these diverse set of functions inside the cell, actin molecules underlie a permanent turnover of polymerization into paired-helical F-actin microfilaments and dissociation into monomeric G-actin (Moseley and Goode, 2006). Under physiological salt concentrations, as observed *in vivo* and in cell-free translation systems, the equilibrium of this process is shifted towards F-actin formation (Pardee and Spudich, 1982). The critical G-actin concentration at which association and dissociation reactions are balanced at the fast growing end of the actin filaments (also called the "barbed end" or "(+)-end") was determined to be ~0.1 µM (>12-fold lower than that of the slow growing end; also called the "pointed end" or "(-)-end") (Wegner and Isenberg, 1983).

The amount of soluble actin translated in the TRiC-supplemented S30 lysate is approximately 3.2 µM, hence clearly exceeding the critical G-actin concentration (Figures 19 and 20). Since only half of the soluble actin (~1.6 µM) formed a stable complex with DNase I (Figure 20), the remainder was assumed to be readily polymerized into filamentous F-actin which does not bind to DNase I (Hitchcock et al., 1976). Indeed, staining of actin translation products with rPh, which tightly and specifically binds to F-actin (but not to G-actin) (Estes et al., 1981; Vandekerckhove et al., 1985), revealed substantial amounts of filamentous shaped structures of diverse lengths and without evident branching (Figure 24A). Strikingly, these structures were only observed in TRiC-supplemented actin translations but not upon reaction supplementation with any of the bacterial chaperones. Thus, for the first time, supplementation of a cell-free bacterial translation lysate with the eukaryotic chaperonin TRiC could be demonstrated to be capable of producing sufficient amounts of *de novo* folded actin in order to

promote polymerization into *bona fide* F-actin filaments. Furthermore, as rPh binds at a stoichiometry of 1:1 to each F-actin protomer (Steinmetz et al., 1998), fluorescence was used as a measure to quantitate the amount of filamentous actin present in the sample (Howard and Oresajo, 1985; Cooper, 1987). It turned out that in the TRiC-supplemented reaction approximately 1.6 µM of the soluble actin had polymerized into filamentous F-actin. These finding correlated well with the previously determined 3.2 µM of soluble actin present in the system whereof ~1.6 µM could be shown to exist as monomeric G-actin (evidenced by binding to DNase I; Figure 20). Notably, phalloidin is well known to stabilize F-actin against depolymerization by preventing monomer dissociation at both the barbed and pointed ends of the filament (Estes et al., 1981). Thus, incubation of the actin translation product with rPh could potentially shift the equilibrium from G-actin towards actin filaments and therefore lead to a decrease in DNase I-binding material. Importantly, when TRiC-folded actin was incubated with rPh prior to DNase I treatment, the amount DNase I-bound actin was not affected and remained constant at a level similar to that observed for an untreated reaction (compare Figures 20 and 26). Hence, rPh addition to the translation product does not shift the equilibrium between F- and G-actin towards a decrease of monomeric actin. In summary, supplementation of the bacterial lysate with purified TRiC is sufficient to generate ~140 µg/ml (~3.2 µM) *per* hour of correctly folded actin, detectable either as monomers or actin filaments.

4.2.3 Actin translation in the S30 lysate is poorly coupled to TRiC-mediated folding

The lack of eukaryotic chaperones in the bacterial lysate provided the possibility to investigate the kinetics of actin in *de novo* folding solely assisted by the TRiC chaperonin in more detail (Figure 23). By comparing the kinetics of translation and folding in presence of TRiC, native actin appeared with a delay of ~15 min relative to full-length actin synthesized (Figure 23A). This finding correlates well with the slow kinetics of TRiC-assisted actin refolding upon dilution from denaturant ($t_{½}$ ~15-30 min) and thus may reflect a similar folding

pathway, which necessitates multiple cycles of binding and release from the chaperonin until actin acquires its native conformation (Gao et al., 1992; Tian et al., 1995). In contrast, *de novo* folding of actin in the eukaryotic cytosol is a rapid process tightly coupled to translation (Siegers et al., 1999). There, newly synthesized actin chains transit efficiently from the ribosome into the TRiC chaperonin and fold into their native structure with a half time of ~1 min upon synthesis. In accordance to these observations, native actin was detectable within 2-3 min after the appearance of full-length actin upon translation in RRL (Figure 23C; Frydman and Hartl, 1996). It should be mentioned that due to its discontiguous sub-domain architecture (Figure 9A; Kabsch et al., 1990), actin can attain its native state only once its complete sequence has emerged from the ribosome. However, the rapid folding process in the eukaryotic cytosol has been explained by the existence of an integrated "folding compartment", constituted by TRiC and the jellyfish-shaped chaperone PFD, in which actin nascent chains are allowed to fold unimpaired and sequestered from the crowded cellular environment (Siegers et al., 1999; Hartl and Hayer-Hartl, 2002). Although biochemical and genetic analyses revealed PFD to be dispensable for efficient TRiC-substrate interactions (Figure 20; Rommelaere et al., 1999; Siegers et al., 1999), deletion of individual PFD genes caused a significant decrease in actin folding rates as well as the release of non-native actin chains into the bulk cytosol (Siegers et al., 1999). Furthermore, the co-translational action of PFD may allow actin nascent chains to be delivered to TRiC in a restricted set of particular conformations that the chaperonin is able to productively assist in folding. Since the bacterial lysate does not contain any of the eukaryotic nascent chain binding proteins, the delayed actin folding in the chaperone-supplemented lysate may be due to the inappropriate delivery of actin to TRiC. Consequently, if actin binding occurs in an unfavorable conformation relative to the subunit topology of the chaperonin ring, TRiC may have to release and re-bind actin repeatedly until the correct regions of the protein contact the appropriate chaperonin subunits. In agreement with this concept are the observations that in cryo-EM reconstructions or upon cross-linking of TRiC to actin nascent chains, specific chaperonin subunits appear to bind defined regions of the actin protein (Llorca et al., 2000;

Etchells et al., 2005). The significant amount of actin folding observed upon translation termination in the bacterial lysate may thus reflect a need for actin chains to occupy TRiC for a prolonged period during folding and/or the requirement of actin for multiple rounds of chaperone binding and release, as mentioned above. Together, *de novo* actin folding in the bacterial lysate solely assisted by TRiC is efficient but occurs *via* a slow post-translational mechanism poorly coupled to translation (Figures 23A and 23B). In sharp contrast, termination of protein synthesis in the eukaryotic lysate did not lead to any further increase in the amount of DNase I-bound actin (Figure 23D), validating the tight interconnection between folding and translation (Frydman and Hartl, 1996; Siegers et al., 1999). Additionally, folding compartmentation and the proposed "proofreading" function of PFD in the eukaryotic cytosol (Siegers et al., 1999) may reduce the need of actin cycles on and off the chaperonin to a minimum (possibly to only one cycle!) and prevent premature release of incompletely folded actin molecules that would otherwise be susceptible to aggregation, degradation and/or improper interactions with other components of the cytosol. However, the exact mechanism of how protein folding occurs in the eukaryotic cytosol remains to be elucidated.

4.2.4 Implications for the cell-free protein synthesis of eukaryotic proteins

To date, the production of sufficient amounts of mutant forms of actin for biochemical and structural analysis is very limited. Purification of biochemical amounts of mutant actins from eukaryotic systems amenable to recombinant protein expression, such as *S. cerevisiae*, has been described for mutants that are compatible with cell viability (Kron et al., 1992). Expression of actin-mutants carrying more drastic mutations, such as sub-domain substitutions with parts of the prokaryotic actin homologue MreB (Carballido-Lopez, 2006), results in cellular toxicity and/or aggregation of the expressed protein in yeast (C. M. Kaiser and J. M. Barral, unpublished observations). The system described here, however, may circumvent these limitations and allow robust production of actin mutants for their subsequent characterization. Similar to actin, the

cytoskeletal protein tubulin is a major substrate of TRiC (Yaffe et al., 1992; Melki et al., 1993). Unlike actin, however, tubulin folding and polymerization into microtubules requires several cytosolic cofactors in addition to TRiC (Cowan and Lewis, 2001). Experiments, similar to those reported here for actin, may allow the assessment of the minimal requirements for *de novo* folding and assembly of tubulin.

The compatibility between a bacterial translation system and a eukaryotic chaperone, as described for actin and TRiC, may represent a more general solution for the efficient production of correctly folded eukaryotic proteins that otherwise misfold or lead to cellular toxicity upon recombinant expression.

4.3 TRiC-mediated folding of actin fusion proteins too large for entire encapsulation in the chaperonin cavity

The evolution of eukaryotes is characterized by an enormous increase in the diversity and structural complexity of proteins. Recent comparative studies of the proteomes from different organisms revealed that approximately two-thirds of eukaryotic proteins consist of two or more domains (Apic et al., 2001; Ekman et al., 2005). This observation was explained by the evolution of complex genomes where random gene fusion events led to the generation of modular polypeptides with novel functions (Kummerfeld and Teichmann, 2005). Previous work has demonstrated that during translation on eukaryotic ribosomes, modular proteins fold extremely efficient by sequential and co-translational folding of their individual domains (Netzer and Hartl, 1997). However, modular proteins whose domains are constructed of discontiguous sequence segments, including actin, are unable to form native tertiary structures co-translationally. Folding of these proteins was suggested to depend strongly on the shielding function provided by the TRiC cavity (Netzer and Hartl, 1998). Whether TRiC-assisted folding requires the entire encapsulation of the substrate protein inside the folding cage (Meyer et al., 2003) or whether the chaperonin also facilitates sequential and domain-wise folding of modular proteins which cannot be accommodated as a whole and would therefore partially extend through a gap in

the apical domains (Frydman et al., 1994; Ditzel et al., 1998; Thulasiraman et al., 1999), remained to be elucidated.

4.3.1 Localization of actin fusion proteins in yeast

The yeast actin cytoskeleton consists of two types of F-actin containing structures: cortical patches, which are localized to sites of cell surface growth; and cables, running through the cytoplasm along the mother-bud axis. Visualization of these filamentous actin structures was accomplished in fixed cells using fluorescently labeled phalloidin or actin antibodies, respectively (Adams and Pringle, 1984; Kilmartin and Adams, 1984; Novick and Botstein, 1985). In recent years, the generation of recombinant fusion proteins consisting of actin or actin-binding proteins and GFP provided the opportunity to perform live cell image analyses, revealing both actin structures to be motile and highly dynamic (Doyle and Botstein, 1996; Carlsson et al., 2002; Yang and Pon, 2002). Concurrently, these findings deomonstrated that actin fused to GFP is able to acquire its native three-dimensional conformation since it readily integrates into F-actin structures (Doyle and Botstein, 1996). Furthermore, by fusing GFP to either side of a robustly folding protein Chang et al. recently showed that expression of these proteins in *S. cerevisiae* resulted in correctly folded domains, corroborating the enhanced capacity of the eukaryotic system for co-translational folding (Chang et al., 2005).

Based on these observations, actin fusion proteins, varying in size and position of the attached fluorescent proteins, were generated and their folding ability and proper integration into the yeast actin cytoskeleton investigated (Figure 27). Expression of the actin variants AG and GA in exponentially growing yeast cells produced a robust GFP-fluorescence signal that localized exclusively to actin cortical patches and had no obvious effect on cell growth or the overall organization of the actin cytoskeleton (Figure 27B). The appropriate integration of AG and GA into cortical patches was additionally confirmed by the subsequent visualization of F-actin containing cellular structures using rPh. Strikingly, the GFP signal of both fusion proteins co-localized with rPh-stained patches, asymmetrically situated in the bud and at the mother-bud neck, but was

not detectable in cables aligning along the mother-bud axis. These findings are in good agreement to the data obtained upon live cell image analyses of yeast cells expressing C-terminally GFP-tagged actin (Doyle and Botstein, 1996). There, AG was demonstrated to properly assemble into cortical patches, indicative of actin having acquired its native state, unimpaired by supposable constraints associated with the consecutive folding of the GFP moiety. Furthermore, similar to the work presented here, AG incorporation in actin cables was not detectable.

Interestingly, expression of the ~100 kDa sized actin double fusion proteins did not result in the localization of these proteins to any actin cytoskeletal structures. Instead, the fluorescence signal of both mCherry and GFP in CAG showed a diffuse cytosolic distribution, comparable to that obtained for the expression of GFP alone (Figures 27B and 27C). In contrast to AG and GA, the bilateral occupation of actin with fluorescent proteins might lead to sterical hindrances which possibly interfere with the assembly process of G-actin into actin filaments. This hypothesis is further supported by the actin crystal structure, in which both the N- and C-terminus are located in close proximity in subdomain 1 of the small domain (Kabsch et al., 1990). Hence, fusion of a second fluorescent protein to actin may not only hinder interactions among actin monomers in order to from F-actin, but may also affect the association with actin binding proteins, such as the Arp2/3 complex and profilin (Mockrin and Korn, 1980; Mullins et al., 1998), which are involved in the formation of cortical patches or the acceleration of nucleotide exchange on G-actin, respectively. Importantly, full-length expression of all actin fusion proteins investigated was confirmed by western blot analysis (Figure 28). Therefore, fluorescence solely resulting from mCherry or GFP upon proteolytical cleavage from the double fusion and/or premature translation termination after synthesis of the N-terminal fluorescent partner is considered to be unlikely.

Together, these results suggest that actin fused to GFP is capable of folding into its native state, as demonstrated by the localization to cortical patches, regardless of its actual position within the fusion protein. Expression of the large multi-domain actin double fusion proteins, however, did not result in the integration of these proteins into yeast cytoskeletal structures. Nevertheless,

since mCherry and GFP were shown to be correctly folded in CAG, assessed by their fluorescence signal (Figures 27C and 29), actin in between these proteins is likely to be also native. The exact folding state of actin in various fusion proteins will be discussed in detail in the following section.

4.3.2 Domain-wise folding in the eukaryotic cytosol

GFP fluorescence was recently utilized as a reliable indicator to monitor folding of proteins to which it was recombinantly fused (Waldo et al., 1999; Chang et al., 2005). *In vitro* refolding as well as *de novo* folding experiments of GFP fusion proteins in *E. coli* and *S. cerevisiae* suggested that, if the GFP domain is not able to acquire its β-barrel structure within a time-frame compatible with the synthesis of the partner domain, it may interfere with the folding of the latter (Chang et al., 2005). Notably, in contrast to the bacterial cytosol, folding of modular GFP-fusions in yeast was highly efficient. This phenomenon was explained by the existence of a sequential and co-translational folding mechanism in the eukaryotic cytosol (Netzer and Hartl, 1997), thus, reducing the interference between domains during folding.

Since actin folding is strictly dependent on the chaperonin TRiC, and correctly folded fluorescent proteins are assessable by monitoring their characteristic fluorescence, fusion of these proteins to actin provided an ideal means to investigate a suggested role of TRiC in domain-wise protein folding (Frydman et al., 1994; Thulasiraman et al., 1999). First evidence for TRiC supporting such a mechanism came from the observation that AG and GA properly integrated into yeast cortical patches (Figure 27B). Furthermore, upon *in vitro* translation in RRL, both proteins formed a stable complex with DNase I (Figure 32A), indicative of correctly folded actin. As AG and GA exceed the upper size limit of the chaperonin cavity by ~20 kDa (Ditzel et al., 1998), it might well be that only the actin domain is enclosed inside the folding cage, while the GFP-moiety remains outside during folding. Such an action is mechanistically conceivable, as group II chaperonins lack a GroES-like cofactor and lid closure proceeds through the conversion of flexible, solvent exposed apical protrusions

into an ordered arrangement of β-strands following an iris-like mechanism (Llorca et al., 2001).

In the case of AG and GA, TRiC could in principle interact with actin from at least one side of the fusion protein. To investigate whether the chaperonin was also able to facilitate actin folding when both termini of the protein were occupied by fluorescent fusion partners, the double-fusions BAG, BTAG, and BTAG-G150P were translated in RRL. Upon protein synthesis and subsequent inhibition of TRiC function by depletion of ATP (Figure 31), the translation products were subjected to TEV protease treatment. Thereby, BTAG and BTAG-G150P, containing a TEV-cleavage site in the linker region between BFP and actin, efficiently released their N-terminal BFP-moiety (Figures 32B and 32C). Subsequently, the folding state of actin in the resulting truncations AG and AG-G150P as well as full-length BAG was monitored by its ability to form a stable complex with DNase I. In accordance to the inability of actin double-fusions to properly integrate into cortical patches *in vivo* (Figure 27; 4.3.1), DNase I-binding of unprocessed BAG occurred only at background levels, similar to those observed for the control protein BG (Figure 32C). These findings suggest that either TRiC is simply not able to fold actin when embedded between two proteins or that both fusion partners restrain actin in DNase I-binding due to steric hindrance in a defined actin region, known as the DNase I binding-loop (residues 39-51 in actin subdomain 2). An answer to these speculations was provided by the result obtained for AG, originating from the double-fusion BTAG. Upon secession of BFP from BTAG, AG was freed from steric hindrances and bound to DNase I with 5-fold higher efficiency when compared to BAG (Figures 32B and 32C). In contrast, AG-G150P, containing an actin mutant with impaired folding properties, did not bind to DNase I above background level (Figure 32C). Thus, actin in BTAG must have acquired its native state prior to protease treatment, as TRiC function and therefore folding was abolished by depletion of ATP before TEV cleavage. Essentially the same result was obtained when BTAG and BTAG-G150P were expressed in yeast Δ*reg* cells (Figure 33). In turn, the amount of AG (originating from BTAG) precipitated by DNase I-bead was ~5-fold higher compared to AG-G150P originating from BTAG-G150P.

Together, these data strongly support the notion that TRiC is indeed able to assist in the domain-wise folding of large multi-domain proteins which cannot be accommodated in the chaperonin cavity as a whole.

4.3.3 Model for TRiC-assisted folding of large modular proteins

Lately, ATP-induced lid closure and subsequent confinement of actin inside TRiC was proposed to be essential for the production of native actin (Meyer et al., 2003). However, TRiC-mediated folding of large modular proteins was suggested to occur in a domain-wise manner outside of the cavity, by a mechanism which does not require encapsulation of the whole substrate protein (Thulasiraman et al., 1999; Spiess et al., 2004; Young et al., 2004). The exact *modus operandi* of how and when TRiC interacts with its putative substrate proteins and which additional chaperones might be involved in this process is still controversial (Farr et al., 1997; Siegers et al., 1999; Etchells et al., 2005).

In this work, various actin fusion proteins were utilized to investigate the possibility of TRiC being able to efficiently bind to and fold actin when fused to either an N-/C-terminal fusion partner or both. The data obtained are summarized in a working model, illustrating how TRiC might facilitate the *de novo* folding of multi-domain proteins during protein synthesis in the eukaryotic cytosol (Figure 35). Considering an artificial three-domain protein, such as BAG, only the intermediate actin domain would require TRiC for folding. Thus, folding of the N- and C-terminal fluorescent proteins is likely to occur spontaneously during translation and without further assistance of chaperones (Figure 35, (1), (2), and (6)). On the other hand, proteins consisting of discontiguous or structurally unstable protein domains, such as actin, are strongly dependent on the productive interaction with TRiC and can only fold, once their sequence has completely emerged from the ribosome (Netzer and Hartl, 1998). In principle, TRiC binding to the growing actin chain in BAG is virtually feasible at two stages. Firstly, co-translationally (Figure 35, (5)), as suggested by recent cross-linking studies (McCallum et al., 2000; Etchells et al., 2005), while the remainder of the fusion protein is still synthesized. Secondly, post-translationally (Figure 35, (3)), upon completion of synthesis and

subsequent transfer of BAG to the chaperonin. The latter might be accomplished by a so-called "folding compartment", closely coupled to the translation machinery (Siegers et al., 1999). However, the final conversion of actin into its native state is considered to occur by the sole encapsulation of the actin domain, while the rest of the BAG fusion remains outside and extends through a gap in the apical domains (Figure 35, (3) and (5)). This assumption is consistent with the determined size of the folding cavity of group II chaperonins which can only accommodate proteins with less than 50 kDa (Ditzel et al., 1998).

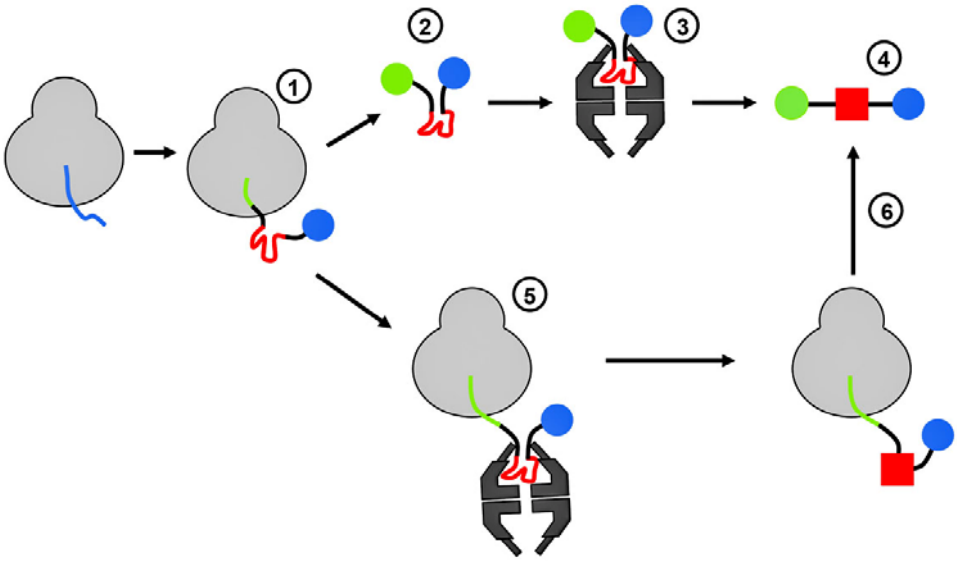

Figure 35: TRiC-mediated domain-wise protein folding in the eukaryotic cytosol, a working model.

The individual domains of the translating polypeptide chain are shown in blue (BFP), red (actin), and green (GFP), with the folded domains represented by circles and squares. The ribosome and TRiC are represented in gray and black, respectively. For reasons of simplicity, ribosome-associated and cytosolic chaperones were omitted. (1, 2) Upon translation, the N- and C-terminal domains fold spontaneously and without assistance of chaperones. (3, 4) Specific encapsulation and post-translational folding of the TRiC-dependent actin domain, while BFP and GFP remain outside of the chaperonin. (5) During translation, TRiC interacts co-translationally with the intermediate actin domain and facilitates its folding. (6) Upon chain release from the chaperonin and completion of protein synthesis, folding of the C-terminal GFP-moiety occurs spontaneously.

Interestingly, the above mentioned model bears a striking resemblance to the degradation of proteins facilitated by the 20S proteasome (Pickart and Cohen, 2004). In analogy to the enclosure of protein domains for TRiC-assisted

folding, the multi-chambered proteasome complex uses a similar mechanism to catalyze the endoproteolytical cleavage of disordered polypeptide loops embedded between stable proteins segments (Liu et al., 2003).

4.4 Perspective

At present, the genomes of many organisms have been sequenced. Following this success, the detailed characterization of previously unknown proteins requires a highly efficient and reliable protein expression system able to generate versatile native proteins. Since chemical protein synthesis is not practicable for the production of long polypeptides, and *in vivo* expression is only applicable to proteins that do not affect host cell physiology, cell-free translation systems overcoming both limitations are becoming increasingly popular (Spirin, 2004; Endo and Sawasaki, 2006). Up to now, *in vitro* protein synthesis systems are available from several organisms (Jackson et al., 2004).

In this study, cell-free translation systems have proven to be an ideal tool for addressing a multitude of highly interesting aspects in the field of biochemistry and biotechnology. Besides the insights gained into existing differences in the coupling of translation and folding of multi-domain proteins in the bacterial and eukaryotic cytosol, TRiC was found to be able to facilitate domain-wise folding of large modular proteins which do not entirely fit into the folding cavity. Additionally, the compatibility between bacterial translation systems and eukaryotic chaperones, as described for actin and TRiC, may provide a more general solution for the efficient production of correctly folded eukaryotic proteins (Baneyx and Mujacic, 2004).

Notably, in parallel to this work, first promising attempts were made to utilize cell-free translation systems to determine the structure of large oligomeric complexes. Following subunit synthesis and *in vitro* assembly, the multi-subunit complexes were subjected to cryo-EM microscopy analysis without preceding purification. In the future, such a strategy may prove especially useful in gaining fast access to medium resolution structures of short lived or semi-stable macromolecular assemblies.

5 References

Adams, A.E. and Pringle, J.R. (1984) Relationship of actin and tubulin distribution to bud growth in wild-type and morphogenetic-mutant Saccharomyces cerevisiae. *J Cell Biol*, **98**, 934-945.

Adams, A.E. and Pringle, J.R. (1991) Staining of actin with fluorochrome-conjugated phalloidin. *Methods Enzymol*, **194**, 729-731.

Agashe, V.R., Guha, S., Chang, H.C., Genevaux, P., Hayer-Hartl, M., Stemp, M., Georgopoulos, C., Hartl, F.U. and Barral, J.M. (2004) Function of trigger factor and DnaK in multidomain protein folding: increase in yield at the expense of folding speed. *Cell*, **117**, 199-209.

Agashe, V.R. and Hartl, F.U. (2000) Roles of molecular chaperones in cytoplasmic protein folding. *Semin Cell Dev Biol*, **11**, 15-25.

Amaral, M.D. (2004) CFTR and chaperones: processing and degradation. *J Mol Neurosci*, **23**, 41-48.

Anfinsen, C.B. (1973) Principles that govern the folding of protein chains. *Science*, **181**, 223-230.

Apic, G., Gough, J. and Teichmann, S.A. (2001) Domain combinations in archaeal, eubacterial and eukaryotic proteomes. *J Mol Biol*, **310**, 311-325.

Baldwin, R.L. (1989) How does protein folding get started? *Trends Biochem Sci*, **14**, 291-294.

Baldwin, R.L. (1995) The nature of protein folding pathways: the classical versus the new view. *J Biomol NMR*, **5**, 103-109.

Baneyx, F. (1999) Recombinant protein expression in Escherichia coli. *Curr Opin Biotechnol*, **10**, 411-421.

Baneyx, F. and Mujacic, M. (2004) Recombinant protein folding and misfolding in Escherichia coli. *Nat Biotechnol*, **22**, 1399-1408.

Baneyx, F. and Palumbo, J.L. (2003) Improving heterologous protein folding via molecular chaperone and foldase co-expression. *Methods Mol Biol*, **205**, 171-197.

Baram, D., Pyetan, E., Sittner, A., Auerbach-Nevo, T., Bashan, A. and Yonath, A. (2005) Structure of trigger factor binding domain in biologically homologous complex with eubacterial ribosome reveals its chaperone action. *Proc Natl Acad Sci U S A*, **102**, 12017-12022.

Barral, J.M., Broadley, S.A., Schaffar, G. and Hartl, F.U. (2004) Roles of molecular chaperones in protein misfolding diseases. *Semin Cell Dev Biol*, **15**, 17-29.

Blake, C.C. (1985) Exons and the evolution of proteins. *Int Rev Cytol*, **93**, 149-185.

Blikstad, I., Markey, F., Carlsson, L., Persson, T. and Lindberg, U. (1978) Selective assay of monomeric and filamentous actin in cell extracts, using inhibition of deoxyribonuclease I. *Cell*, **15**, 935-943.

Bradford, M.M. (1976) A rapid and sensitive method for the quantitation of microgram quantities of protein utilizing the principle of protein-dye binding. *Anal Biochem*, **72**, 248-254.

Braig, K., Otwinowski, Z., Hegde, R., Boisvert, D.C., Joachimiak, A., Horwich, A.L. and Sigler, P.B. (1994) The crystal structure of the bacterial chaperonin GroEL at 2.8 A. *Nature*, **371**, 578-586.

Bremer, H. and Dennis, P.P. (1996) Modulation of chemical composition and other parameters of the cell by growth rate. In Neidhardt, F.C. (ed.), *Escherichia Coli and Salmonella: Cellular and Molecular Biology*. ASM Press, Washington, D.C., pp. 1553-1569.

Bryngelson, J.D., Onuchic, J.N., Socci, N.D. and Wolynes, P.G. (1995) Funnels, pathways, and the energy landscape of protein folding: a synthesis. *Proteins*, **21**, 167-195.

Buchberger, A., Schroder, H., Hesterkamp, T., Schonfeld, H.J. and Bukau, B. (1996) Substrate shuttling between the DnaK and GroEL systems indicates a chaperone network promoting protein folding. *J Mol Biol*, **261**, 328-333.

Buchner, J. (1996) Supervising the fold: functional principles of molecular chaperones. *Faseb J*, **10**, 10-19.

Bukau, B., Deuerling, E., Pfund, C. and Craig, E.A. (2000) Getting newly synthesized proteins into shape. *Cell*, **101**, 119-122.

Bukau, B. and Horwich, A.L. (1998) The Hsp70 and Hsp60 chaperone machines. *Cell*, **92**, 351-366.

Bukau, B. and Walker, G.C. (1989) Cellular defects caused by deletion of the Escherichia coli dnaK gene indicate roles for heat shock protein in normal metabolism. *J Bacteriol*, **171**, 2337-2346.

Camasses, A., Bogdanova, A., Shevchenko, A. and Zachariae, W. (2003) The CCT chaperonin promotes activation of the anaphase-promoting complex through the generation of functional Cdc20. *Mol Cell*, **12**, 87-100.

Carballido-Lopez, R. (2006) The bacterial actin-like cytoskeleton. *Microbiol Mol Biol Rev*, **70**, 888-909.

Carlsson, A.E., Shah, A.D., Elking, D., Karpova, T.S. and Cooper, J.A. (2002) Quantitative analysis of actin patch movement in yeast. *Biophys J*, **82**, 2333-2343.

Carrascosa, J.L., Llorca, O. and Valpuesta, J.M. (2001) Structural comparison of prokaryotic and eukaryotic chaperonins. *Micron*, **32**, 43-50.

Caspers, P., Stieger, M. and Burn, P. (1994) Overproduction of bacterial chaperones improves the solubility of recombinant protein tyrosine kinases in Escherichia coli. *Cell Mol Biol (Noisy-le-grand)*, **40**, 635-644.

Chang, H.C., Kaiser, C.M., Hartl, F.U. and Barral, J.M. (2005) De novo folding of GFP fusion proteins: high efficiency in eukaryotes but not in bacteria. *J Mol Biol*, **353**, 397-409.

Chaudhuri, T.K., Farr, G.W., Fenton, W.A., Rospert, S. and Horwich, A.L. (2001) GroEL/GroES-mediated folding of a protein too large to be encapsulated. *Cell*, **107**, 235-246.

Chen, L. and Sigler, P.B. (1999) The crystal structure of a GroEL/peptide complex: plasticity as a basis for substrate diversity. *Cell*, **99**, 757-768.

Chen, X., Sullivan, D.S. and Huffaker, T.C. (1994) Two yeast genes with similarity to TCP-1 are required for microtubule and actin function in vivo. *Proc Natl Acad Sci U S A*, **91**, 9111-9115.

Chiti, F. and Dobson, C.M. (2006) Protein misfolding, functional amyloid, and human disease. *Annu Rev Biochem*, **75**, 333-366.

Conti, E., Franks, N.P. and Brick, P. (1996) Crystal structure of firefly luciferase throws light on a superfamily of adenylate-forming enzymes. *Structure*, **4**, 287-298.

Cooper, J.A. (1987) Effects of cytochalasin and phalloidin on actin. *J Cell Biol*, **105**, 1473-1478.

Cowan, N.J. (1998) Mammalian cytosolic chaperonin. *Methods Enzymol*, **290**, 230-241.

Cowan, N.J. and Lewis, S.A. (2001) Type II chaperonins, prefoldin, and the tubulin-specific chaperones. *Adv Protein Chem*, **59**, 73-104.

Coyle, J.E., Jaeger, J., Gross, M., Robinson, C.V. and Radford, S.E. (1997) Structural and mechanistic consequences of polypeptide binding by GroEL. *Fold Des*, **2**, R93-104.

Craig, E.A., Gambill, B.D. and Nelson, R.J. (1993) Heat shock proteins: molecular chaperones of protein biogenesis. *Microbiol Rev*, **57**, 402-414.

Crooke, E. and Wickner, W. (1987) Trigger factor: a soluble protein that folds pro-OmpA into a membrane-assembly-competent form. *Proc Natl Acad Sci U S A*, **84**, 5216-5220.

Daggett, V. and Fersht, A.R. (2003) Is there a unifying mechanism for protein folding? *Trends Biochem Sci*, **28**, 18-25.

Dale, G.E., Schonfeld, H.J., Langen, H. and Stieger, M. (1994) Increased solubility of trimethoprim-resistant type S1 DHFR from Staphylococcus aureus in Escherichia coli cells overproducing the chaperonins GroEL and GroES. *Protein Eng*, **7**, 925-931.

Deuerling, E., Patzelt, H., Vorderwulbecke, S., Rauch, T., Kramer, G., Schaffitzel, E., Mogk, A., Schulze-Specking, A., Langen, H. and Bukau, B. (2003) Trigger Factor and DnaK possess overlapping substrate pools and binding specificities. *Mol Microbiol*, **47**, 1317-1328.

Deuerling, E., Schulze-Specking, A., Tomoyasu, T., Mogk, A. and Bukau, B. (1999) Trigger factor and DnaK cooperate in folding of newly synthesized proteins. *Nature*, **400**, 693-696.

Dill, K.A. and Chan, H.S. (1997) From Levinthal to pathways to funnels. *Nat Struct Biol*, **4**, 10-19.

Dinner, A.R., Sali, A., Smith, L.J., Dobson, C.M. and Karplus, M. (2000) Understanding protein folding via free-energy surfaces from theory and experiment. *Trends Biochem Sci*, **25**, 331-339.

Ditzel, L., Lowe, J., Stock, D., Stetter, K.O., Huber, H., Huber, R. and Steinbacher, S. (1998) Crystal structure of the thermosome, the archaeal chaperonin and homolog of CCT. *Cell*, **93**, 125-138.

Dobrzynski, J.K., Sternlicht, M.L., Farr, G.W. and Sternlicht, H. (1996) Newly-synthesized beta-tubulin demonstrates domain-specific interactions with the cytosolic chaperonin. *Biochemistry*, **35**, 15870-15882.

Dobson, C.M. (1999) Protein misfolding, evolution and disease. *Trends Biochem Sci*, **24**, 329-332.

Dobson, C.M. (2004) Principles of protein folding, misfolding and aggregation. *Semin Cell Dev Biol*, **15**, 3-16.

Dobson, C.M., Sali, A. and Karplus, M. (1998) Protein folding: a perspective from theory and experiment. *Angew Chem Int Ed Engl*, **37**, 868-893.

Doyle, T. and Botstein, D. (1996) Movement of yeast cortical actin cytoskeleton visualized in vivo. *Proc Natl Acad Sci U S A*, **93**, 3886-3891.

Ekman, D., Bjorklund, A.K., Frey-Skott, J. and Elofsson, A. (2005) Multi-domain proteins in the three kingdoms of life: orphan domains and other unassigned regions. *J Mol Biol*, **348**, 231-243.

Ellis, J. (1987) Proteins as molecular chaperones. *Nature*, **328**, 378-379.

Ellis, J. (2001) Macromolecular crowding: an important but neglected aspect of the intracellular environment. *Current Opinion in Structural Biology*, **11**, 114-119.

Ellis, R.J. (2006) Protein folding: inside the cage. *Nature*, **442**, 360-362.

Ellis, R.J. and Hart, F.U. (2000) Folding and binding: problems with proteins. *Curr Opin Struct Biol*, **10**, 13-15.

Ellis, R.J. and Hartl, F.U. (1996) Protein folding in the cell: competing models of chaperonin function. *Faseb J*, **10**, 20-26.

Ellis, R.J. and Hartl, F.U. (1999) Principles of protein folding in the cellular environment. *Curr Opin Struct Biol*, **9**, 102-110.

Ellis, R.J. and Hemmingsen, S.M. (1989) Molecular chaperones: proteins essential for the biogenesis of some macromolecular structures. *Trends Biochem Sci*, **14**, 339-342.

Endo, Y. and Sawasaki, T. (2006) Cell-free expression systems for eukaryotic protein production. *Curr Opin Biotechnol*, **17**, 373-380.

Estes, J.E., Selden, L.A. and Gershman, L.C. (1981) Mechanism of action of phalloidin on the polymerization of muscle actin. *Biochemistry*, **20**, 708-712.

Etchells, S.A., Meyer, A.S., Yam, A.Y., Roobol, A., Miao, Y., Shao, Y., Carden, M.J., Skach, W.R., Frydman, J. and Johnson, A.E. (2005) The cotranslational contacts between ribosome-bound nascent polypeptides and the subunits of the hetero-oligomeric chaperonin TRiC probed by photocross-linking. *J Biol Chem*, **280**, 28118-28126.

Evans, I.H. (1996) *Yeast Protocols*. Humana Press, Totowa, New Jersey.

Ewalt, K.L., Hendrick, J.P., Houry, W.A. and Hartl, F.U. (1997) In vivo observation of polypeptide flux through the bacterial chaperonin system. *Cell*, **90**, 491-500.

Farr, G.W., Scharl, E.C., Schumacher, R.J., Sondek, S. and Horwich, A.L. (1997) Chaperonin-mediated folding in the eukaryotic cytosol proceeds through rounds of release of native and nonnative forms. *Cell*, **89**, 927-937.

Fayet, O., Ziegelhoffer, T. and Georgopoulos, C. (1989) The groES and groEL heat shock gene products of Escherichia coli are essential for bacterial growth at all temperatures. *Journal of Bacteriology*, **171**, 1379-1385.

Feldman, D.E., Spiess, C., Howard, D.E. and Frydman, J. (2003) Tumorigenic mutations in VHL disrupt folding in vivo by interfering with chaperonin binding. *Mol Cell*, **12**, 1213-1224.

Feldman, D.E., Thulasiraman, V., Ferreyra, R.G. and Frydman, J. (1999) Formation of the VHL-elongin BC tumor suppressor complex is mediated by the chaperonin TRiC. *Mol Cell*, **4**, 1051-1061.

Ferbitz, L., Maier, T., Patzelt, H., Bukau, B., Deuerling, E. and Ban, N. (2004) Trigger factor in complex with the ribosome forms a molecular cradle for nascent proteins. *Nature*, **431**, 590-596.

Ferreyra, R.G. and Frydman, J. (2000) Purification of the cytosolic chaperonin TRiC from bovine testis. *Methods Mol Biol*, **140**, 153-160.

Fersht, A.R. (1997) Nucleation mechanisms in protein folding. *Curr Opin Struct Biol*, **7**, 3-9.

Fersht, A.R. and Daggett, V. (2002) Protein folding and unfolding at atomic resolution. *Cell*, **108**, 573-582.

Flaherty, K.M., McKay, D.B., Kabsch, W. and Holmes, K.C. (1991) Similarity of the three-dimensional structures of actin and the ATPase fragment of a 70-kDa heat shock cognate protein. *Proc Natl Acad Sci U S A*, **88**, 5041-5045.

Flynn, G.C., Pohl, J., Flocco, M.T. and Rothman, J.E. (1991) Peptide-binding specificity of the molecular chaperone BiP. *Nature*, **353**, 726-730.

Frankel, S., Condeelis, J. and Leinwand, L. (1990) Expression of actin in Escherichia coli. Aggregation, solubilization, and functional analysis. *J Biol Chem*, **265**, 17980-17987.

Frankel, S., Sohn, R. and Leinwand, L. (1991) The use of sarkosyl in generating soluble protein after bacterial expression. *Proc Natl Acad Sci U S A*, **88**, 1192-1196.

Freedman, R.B., Hirst, T.R. and Tuite, M.F. (1994) Protein disulphide isomerase: building bridges in protein folding. *Trends Biochem Sci*, **19**, 331-336.

Frydman, J. (2001) Folding of newly translated proteins in vivo: the role of molecular chaperones. *Annu Rev Biochem*, **70**, 603-647.

Frydman, J., Erdjument-Bromage, H., Tempst, P. and Hartl, F.U. (1999) Co-translational domain folding as the structural basis for the rapid de novo folding of firefly luciferase. *Nat Struct Biol*, **6**, 697-705.

Frydman, J. and Hartl, F.U. (1996) Principles of chaperone-assisted protein folding: differences between in vitro and in vivo mechanisms. *Science*, **272**, 1497-1502.

Frydman, J., Nimmesgern, E., Erdjument-Bromage, H., Wall, J.S., Tempst, P. and Hartl, F.U. (1992) Function in protein folding of TRiC, a cytosolic ring complex containing TCP-1 and structurally related subunits. *Embo J*, **11**, 4767-4778.

Frydman, J., Nimmesgern, E., Ohtsuka, K. and Hartl, F.U. (1994) Folding of nascent polypeptide chains in a high molecular mass assembly with molecular chaperones. *Nature*, **370**, 111-117.

Gao, Y., Thomas, J.O., Chow, R.L., Lee, G.H. and Cowan, N.J. (1992) A cytoplasmic chaperonin that catalyzes beta-actin folding. *Cell*, **69**, 1043-1050.

Geissler, S., Siegers, K. and Schiebel, E. (1998) A novel protein complex promoting formation of functional alpha- and gamma-tubulin. *Embo J*, **17**, 952-966.

Genevaux, P., Keppel, F., Schwager, F., Langendijk-Genevaux, P.S., Hartl, F.U. and Georgopoulos, C. (2004) In vivo analysis of the overlapping functions of DnaK and trigger factor. *EMBO Rep*, **5**, 195-200.

Gething, M.J. and Sambrook, J. (1992) Protein folding in the cell. *Nature*, **355**, 33-45.

Gietz, D., St Jean, A., Woods, R.A. and Schiestl, R.H. (1992) Improved method for high efficiency transformation of intact yeast cells. *Nucleic Acids Res*, **20**, 1425.

Gill, S.C. and von Hippel, P.H. (1989) Calculation of protein extinction coefficients from amino acid sequence data. *Anal Biochem*, **182**, 319-326.

Gomez-Puertas, P., Martin-Benito, J., Carrascosa, J.L., Willison, K.R. and Valpuesta, J.M. (2004) The substrate recognition mechanisms in chaperonins. *J Mol Recognit*, **17**, 85-94.

Gutsche, I., Essen, L.O. and Baumeister, W. (1999) Group II chaperonins: new TRiC(k)s and turns of a protein folding machine. *J Mol Biol*, **293**, 295-312.

Hansen, W.J., Cowan, N.J. and Welch, W.J. (1999) Prefoldin-nascent chain complexes in the folding of cytoskeletal proteins. *J Cell Biol*, **145**, 265-277.

Harrison, C.J., Hayer-Hartl, M., Di Liberto, M., Hartl, F. and Kuriyan, J. (1997) Crystal structure of the nucleotide exchange factor GrpE bound to the ATPase domain of the molecular chaperone DnaK. *Science*, **276**, 431-435.

Hartl, F.U. (1996) Molecular chaperones in cellular protein folding. *Nature*, **381**, 571-579.

Hartl, F.U. and Hayer-Hartl, M. (2002) Molecular chaperones in the cytosol: from nascent chain to folded protein. *Science*, **295**, 1852-1858.

Hayer-Hartl, M.K., Ewbank, J.J., Creighton, T.E. and Hartl, F.U. (1994) Conformational specificity of the chaperonin GroEL for the compact folding intermediates of alpha-lactalbumin. *Embo J*, **13**, 3192-3202.

Hayer-Hartl, M.K., Martin, J. and Hartl, F.U. (1995) Asymmetrical interaction of GroEL and GroES in the ATPase cycle of assisted protein folding. *Science*, **269**, 836-841.

Hayer-Hartl, M.K., Weber, F. and Hartl, F.U. (1996) Mechanism of chaperonin action: GroES binding and release can drive GroEL-mediated protein folding in the absence of ATP hydrolysis. *Embo J*, **15**, 6111-6121.

Heim, R., Prasher, D.C. and Tsien, R.Y. (1994) Wavelength mutations and posttranslational autoxidation of green fluorescent protein. *Proc Natl Acad Sci U S A*, **91**, 12501-12504.

Heller, M., John, M., Coles, M., Bosch, G., Baumeister, W. and Kessler, H. (2004) NMR studies on the substrate-binding domains of the thermosome: structural plasticity in the protrusion region. *J Mol Biol*, **336**, 717-729.

Hemmingsen, S.M., Woolford, C., van der Vies, S.M., Tilly, K., Dennis, D.T., Georgopoulos, C.P., Hendrix, R.W. and Ellis, R.J. (1988) Homologous plant and bacterial proteins chaperone oligomeric protein assembly. *Nature*, **333**, 330-334.

Herbst, R., Gast, K. and Seckler, R. (1998) Folding of firefly (Photinus pyralis) luciferase: aggregation and reactivation of unfolding intermediates. *Biochemistry*, **37**, 6586-6597.

Hesterkamp, T. and Bukau, B. (1996) Identification of the prolyl isomerase domain of Escherichia coli trigger factor. *FEBS Lett*, **385**, 67-71.

Hesterkamp, T. and Bukau, B. (1998) Role of the DnaK and HscA homologs of Hsp70 chaperones in protein folding in E.coli. *Embo J*, **17**, 4818-4828.

Hesterkamp, T., Deuerling, E. and Bukau, B. (1997) The amino-terminal 118 amino acids of Escherichia coli trigger factor constitute a domain that is necessary and sufficient for binding to ribosomes. *J Biol Chem*, **272**, 21865-21871.

Hesterkamp, T., Hauser, S., Lutcke, H. and Bukau, B. (1996) Escherichia coli trigger factor is a prolyl isomerase that associates with nascent polypeptide chains. *Proc Natl Acad Sci U S A*, **93**, 4437-4441.

Hitchcock, S.E., Carisson, L. and Lindberg, U. (1976) Depolymerization of F-actin by deoxyribonuclease I. *Cell*, **7**, 531-542.

Ho, Y., Gruhler, A., Heilbut, A., Bader, G.D., Moore, L., Adams, S.L., Millar, A., Taylor, P., Bennett, K., Boutilier, K., Yang, L., Wolting, C., Donaldson, I., Schandorff, S., Shewnarane, J., Vo, M., Taggart, J., Goudreault, M., Muskat, B., Alfarano, C., Dewar, D., Lin, Z., Michalickova, K., Willems, A.R., Sassi, H., Nielsen, P.A., Rasmussen, K.J., Andersen, J.R., Johansen, L.E., Hansen, L.H., Jespersen, H., Podtelejnikov, A., Nielsen, E., Crawford, J., Poulsen, V., Sorensen, B.D., Matthiesen, J., Hendrickson, R.C., Gleeson, F., Pawson, T., Moran, M.F., Durocher, D., Mann, M., Hogue, C.W., Figeys, D. and Tyers, M. (2002) Systematic identification of protein complexes in Saccharomyces cerevisiae by mass spectrometry. *Nature*, **415**, 180-183.

Hoffmann, A., Merz, F., Rutkowska, A., Zachmann-Brand, B., Deuerling, E. and Bukau, B. (2006) Trigger factor forms a protective shield for nascent polypeptides at the ribosome. *J Biol Chem*, **281**, 6539-6545.

Hohfeld, J., Minami, Y. and Hartl, F.U. (1995) Hip, a novel cochaperone involved in the eukaryotic Hsc70/Hsp40 reaction cycle. *Cell*, **83**, 589-598.

Houry, W.A., Frishman, D., Eckerskorn, C., Lottspeich, F. and Hartl, F.U. (1999) Identification of in vivo substrates of the chaperonin GroEL. *Nature*, **402**, 147-154.

Howard, T.H. and Oresajo, C.O. (1985) A method for quantifying F-actin in chemotactic peptide activated neutrophils: study of the effect of tBOC peptide. *Cell Motil*, **5**, 545-557.

Hunt, J.F., Weaver, A.J., Landry, S.J., Gierasch, L. and Deisenhofer, J. (1996) The crystal structure of the GroES co-chaperonin at 2.8 A resolution. *Nature*, **379**, 37-45.

Hynes, G.M. and Willison, K.R. (2000) Individual subunits of the eukaryotic cytosolic chaperonin mediate interactions with binding sites located on subdomains of beta-actin. *J Biol Chem*, **275**, 18985-18994.

Iizuka, R., So, S., Inobe, T., Yoshida, T., Zako, T., Kuwajima, K. and Yohda, M. (2004) Role of the helical protrusion in the conformational change and

molecular chaperone activity of the archaeal group II chaperonin. *J Biol Chem*, **279**, 18834-18839.

Jackson, A.M., Boutell, J., Cooley, N. and He, M. (2004) Cell-free protein synthesis for proteomics. *Brief Funct Genomic Proteomic*, **2**, 308-319.

Jackson, S.E. and Fersht, A.R. (1991) Folding of chymotrypsin inhibitor 2. 1. Evidence for a two-state transition. *Biochemistry*, **30**, 10428-10435.

Jacobson, R.H., Zhang, X.J., DuBose, R.F. and Matthews, B.W. (1994) Three-dimensional structure of beta-galactosidase from E. coli. *Nature*, **369**, 761-766.

Jaenicke, R. (1987) Folding and association of proteins. *Prog Biophys Mol Biol*, **49**, 117-237.

Jaenicke, R. (1991) Protein folding: local structures, domains, subunits, and assemblies. *Biochemistry*, **30**, 3147-3161.

Jordan, R. and McMacken, R. (1995) Modulation of the ATPase activity of the molecular chaperone DnaK by peptides and the DnaJ and GrpE heat shock proteins. *J Biol Chem*, **270**, 4563-4569.

Kabsch, W., Mannherz, H.G., Suck, D., Pai, E.F. and Holmes, K.C. (1990) Atomic structure of the actin:DNase I complex. *Nature*, **347**, 37-44.

Kafri, G., Willison, K.R. and Horovitz, A. (2001) Nested allosteric interactions in the cytoplasmic chaperonin containing TCP-1. *Protein Sci*, **10**, 445-449.

Kaiser, C.M., Chang, H.C., Agashe, V.R., Lakshmipathy, S.K., Etchells, S.A., Hayer-Hartl, M., Hartl, F.U. and Barral, J.M. (2006) Real-time observation of trigger factor function on translating ribosomes. *Nature*, **444**, 455-460.

Karplus, M. and Weaver, D.L. (1976) Protein-folding dynamics. *Nature*, **260**, 404-406.

Kauzmann, W. (1959) Some factors in the interpretation of protein denaturation. *Adv Protein Chem*, **14**, 1-63.

Kerner, M.J., Naylor, D.J., Ishihama, Y., Maier, T., Chang, H.C., Stines, A.P., Georgopoulos, C., Frishman, D., Hayer-Hartl, M., Mann, M. and Hartl, F.U. (2005) Proteome-wide analysis of chaperonin-dependent protein folding in Escherichia coli. *Cell*, **122**, 209-220.

Kilmartin, J.V. and Adams, A.E. (1984) Structural rearrangements of tubulin and actin during the cell cycle of the yeast Saccharomyces. *J Cell Biol*, **98**, 922-933.

Kim, P.S. and Baldwin, R.L. (1982) Specific intermediates in the folding reactions of small proteins and the mechanism of protein folding. *Annu Rev Biochem*, **51**, 459-489.

Kim, P.S. and Baldwin, R.L. (1990) Intermediates in the folding reactions of small proteins. *Annu Rev Biochem*, **59**, 631-660.

Kim, S., Willison, K.R. and Horwich, A.L. (1994) Cystosolic chaperonin subunits have a conserved ATPase domain but diverged polypeptide-binding domains. *Trends Biochem Sci*, **19**, 543-548.

Klumpp, M., Baumeister, W. and Essen, L.O. (1997) Structure of the substrate binding domain of the thermosome, an archaeal group II chaperonin. *Cell*, **91**, 263-270.

Kolb, V.A., Makeyev, E.V. and Spirin, A.S. (1994) Folding of firefly luciferase during translation in a cell-free system. *Embo J*, **13**, 3631-3637.

Kramer, G., Patzelt, H., Rauch, T., Kurz, T.A., Vorderwulbecke, S., Bukau, B. and Deuerling, E. (2004a) Trigger factor peptidyl-prolyl cis/trans isomerase activity is not essential for the folding of cytosolic proteins in Escherichia coli. *J Biol Chem*, **279**, 14165-14170.

Kramer, G., Rauch, T., Rist, W., Vorderwulbecke, S., Patzelt, H., Schulze-Specking, A., Ban, N., Deuerling, E. and Bukau, B. (2002) L23 protein functions as a chaperone docking site on the ribosome. *Nature*, **419**, 171-174.

Kramer, G., Rutkowska, A., Wegrzyn, R.D., Patzelt, H., Kurz, T.A., Merz, F., Rauch, T., Vorderwulbecke, S., Deuerling, E. and Bukau, B. (2004b) Functional dissection of Escherichia coli trigger factor: unraveling the function of individual domains. *J Bacteriol*, **186**, 3777-3784.

Kron, S.J., Drubin, D.G., Botstein, D. and Spudich, J.A. (1992) Yeast actin filaments display ATP-dependent sliding movement over surfaces coated with rabbit muscle myosin. *Proc Natl Acad Sci U S A*, **89**, 4466-4470.

Kubota, H., Hynes, G.M., Kerr, S.M. and Willison, K.R. (1997) Tissue-specific subunit of the mouse cytosolic chaperonin-containing TCP-1. *FEBS Lett*, **402**, 53-56.

Kummerfeld, S.K. and Teichmann, S.A. (2005) Relative rates of gene fusion and fission in multi-domain proteins. *Trends Genet*, **21**, 25-30.

Laemmli, U.K. (1970) Cleavage of structural proteins during the assembly of the head of bacteriophage T4. *Nature*, **227**, 680-685.

Lakshmipathy, S.K., Tomic, S., Kaiser, C.M., Chang, H.C., Genevaux, P., Georgopoulos, C., Barral, J.M., Johnson, A.E., Hartl, F.U. and Etchells, S.A. (2007) Identification of nascent chain interaction sites on trigger factor. *J Biol Chem*.

Langer, T., Lu, C., Echols, H., Flanagan, J., Hayer, M.K. and Hartl, F.U. (1992a) Successive action of DnaK, DnaJ and GroEL along the pathway of chaperone-mediated protein folding. *Nature*, **356**, 683-689.

Langer, T., Pfeifer, G., Martin, J., Baumeister, W. and Hartl, F.U. (1992b) Chaperonin-mediated protein folding: GroES binds to one end of the GroEL cylinder, which accommodates the protein substrate within its central cavity. *Embo J*, **11**, 4757-4765.

Laskey, R.A., Honda, B.M., Mills, A.D. and Finch, J.T. (1978) Nucleosomes are assembled by an acidic protein which binds histones and transfers them to DNA. *Nature*, **275**, 416-420.

Lazarides, E. and Lindberg, U. (1974) Actin is the naturally occurring inhibitor of deoxyribonuclease I. *Proc Natl Acad Sci U S A*, **71**, 4742-4746.

Levinthal, C. (1969) How to Fold Graciously. In DeBrunner, J.T.P. and Munck, E. (eds.), *Mossbauer Spectroscopy in Biological Systems: Proceedings of a meeting held at Allerton House*. University of Illinois Press, Illinois, pp. pp. 22-24.

Lewis, S.A., Tian, G., Vainberg, I.E. and Cowan, N.J. (1996) Chaperonin-mediated folding of actin and tubulin. *J Cell Biol*, **132**, 1-4.

Lewis, V.A., Hynes, G.M., Zheng, D., Saibil, H. and Willison, K. (1992) T-complex polypeptide-1 is a subunit of a heteromeric particle in the eukaryotic cytosol. *Nature*, **358**, 249-252.

Lill, R., Crooke, E., Guthrie, B. and Wickner, W. (1988) The "trigger factor cycle" includes ribosomes, presecretory proteins, and the plasma membrane. *Cell*, **54**, 1013-1018.

Lin, P. and Sherman, F. (1997) The unique hetero-oligomeric nature of the subunits in the catalytic cooperativity of the yeast Cct chaperonin complex. *Proc Natl Acad Sci U S A*, **94**, 10780-10785.

Lin, Z. and Rye, H.S. (2006) GroEL-mediated protein folding: making the impossible, possible. *Crit Rev Biochem Mol Biol*, **41**, 211-239.

Lindquist, S. (1986) The heat-shock response. *Annu Rev Biochem*, **55**, 1151-1191.

Lindquist, S. and Craig, E.A. (1988) The heat-shock proteins. *Annu Rev Genet*, **22**, 631-677.

Liou, A.K. and Willison, K.R. (1997) Elucidation of the subunit orientation in CCT (chaperonin containing TCP1) from the subunit composition of CCT micro-complexes. *Embo J*, **16**, 4311-4316.

Liu, C.W., Corboy, M.J., DeMartino, G.N. and Thomas, P.J. (2003) Endoproteolytic activity of the proteasome. *Science*, **299**, 408-411.

Llorca, O., Martin-Benito, J., Grantham, J., Ritco-Vonsovici, M., Willison, K.R., Carrascosa, J.L. and Valpuesta, J.M. (2001) The 'sequential allosteric ring' mechanism in the eukaryotic chaperonin-assisted folding of actin and tubulin. *Embo J*, **20**, 4065-4075.

Llorca, O., Martin-Benito, J., Ritco-Vonsovici, M., Grantham, J., Hynes, G.M., Willison, K.R., Carrascosa, J.L. and Valpuesta, J.M. (2000) Eukaryotic chaperonin CCT stabilizes actin and tubulin folding intermediates in open quasi-native conformations. *Embo J*, **19**, 5971-5979.

Llorca, O., McCormack, E.A., Hynes, G., Grantham, J., Cordell, J., Carrascosa, J.L., Willison, K.R., Fernandez, J.J. and Valpuesta, J.M. (1999a) Eukaryotic type II chaperonin CCT interacts with actin through specific subunits. *Nature*, **402**, 693-696.

Llorca, O., Smyth, M.G., Carrascosa, J.L., Willison, K.R., Radermacher, M., Steinbacher, S. and Valpuesta, J.M. (1999b) 3D reconstruction of the ATP-bound form of CCT reveals the asymmetric folding conformation of a type II chaperonin. *Nat Struct Biol*, **6**, 639-642.

Lomas, D.A. and Carrell, R.W. (2002) Serpinopathies and the conformational dementias. *Nat Rev Genet*, **3**, 759-768.

Low, I. and Wieland, T. (1974) The interaction of phalloidin. Some of its derivatives, and of other cyclic peptides with muscle actin as studied by viscosimetry. *FEBS Lett*, **44**, 340-343.

Maier, R., Eckert, B., Scholz, C., Lilie, H. and Schmid, F.X. (2003) Interaction of trigger factor with the ribosome. *J Mol Biol*, **326**, 585-592.

Marston, F.A. (1986) The purification of eukaryotic polypeptides synthesized in Escherichia coli. *Biochem J*, **240**, 1-12.

Martin, J., Mayhew, M., Langer, T. and Hartl, F.U. (1993) The reaction cycle of GroEL and GroES in chaperonin-assisted protein folding. *Nature*, **366**, 228-233.

Mayer, M.P., Schroder, H., Rudiger, S., Paal, K., Laufen, T. and Bukau, B. (2000) Multistep mechanism of substrate binding determines chaperone activity of Hsp70. *Nat Struct Biol*, **7**, 586-593.

Mayor, U., Johnson, C.M., Daggett, V. and Fersht, A.R. (2000) Protein folding and unfolding in microseconds to nanoseconds by experiment and simulation. *Proc Natl Acad Sci U S A*, **97**, 13518-13522.

McCallum, C.D., Do, H., Johnson, A.E. and Frydman, J. (2000) The interaction of the chaperonin tailless complex polypeptide 1 (TCP1) ring complex (TRiC) with ribosome-bound nascent chains examined using photo-cross-linking. *J Cell Biol*, **149**, 591-602.

McCormack, E.A., Llorca, O., Carrascosa, J.L., Valpuesta, J.M. and Willison, K.R. (2001) Point mutations in a hinge linking the small and large domains of beta-actin result in trapped folding intermediates bound to cytosolic chaperonin CCT. *J Struct Biol*, **135**, 198-204.

McNew, J.A. and Goodman, J.M. (1996) The targeting and assembly of peroxisomal proteins: some old rules do not apply. *Trends Biochem Sci*, **21**, 54-58.

Melki, R. and Cowan, N.J. (1994) Facilitated folding of actins and tubulins occurs via a nucleotide-dependent interaction between cytoplasmic chaperonin and distinctive folding intermediates. *Mol Cell Biol*, **14**, 2895-2904.

Melki, R., Vainberg, I.E., Chow, R.L. and Cowan, N.J. (1993) Chaperonin-mediated folding of vertebrate actin-related protein and gamma-tubulin. *J Cell Biol*, **122**, 1301-1310.

Merz, F., Hoffmann, A., Rutkowska, A., Zachmann-Brand, B., Bukau, B. and Deuerling, E. (2006) The C-terminal domain of Escherichia coli trigger factor represents the central module of its chaperone activity. *J Biol Chem*, **281**, 31963-31971.

Meyer, A.S., Gillespie, J.R., Walther, D., Millet, I.S., Doniach, S. and Frydman, J. (2003) Closing the folding chamber of the eukaryotic chaperonin requires the transition state of ATP hydrolysis. *Cell*, **113**, 369-381.

Miklos, D., Caplan, S., Mertens, D., Hynes, G., Pitluk, Z., Kashi, Y., Harrison-Lavoie, K., Stevenson, S., Brown, C., Barrell, B. and et al. (1994) Primary structure and function of a second essential member of the heterooligomeric TCP1 chaperonin complex of yeast, TCP1 beta. *Proc Natl Acad Sci U S A*, **91**, 2743-2747.

Miller, E.J., Meyer, A.S. and Frydman, J. (2006) Modeling of possible subunit arrangements in the eukaryotic chaperonin TRiC. *Protein Sci*, **15**, 1522-1526.

Minton, A.P. (2000) Implications of macromolecular crowding for protein assembly. *Curr Opin Struct Biol*, **10**, 34-39.

Minton, A.P. (2001) The influence of macromolecular crowding and macromolecular confinement on biochemical reactions in physiological media. *J Biol Chem*, **276**, 10577-10580.

Mockrin, S.C. and Korn, E.D. (1980) Acanthamoeba profilin interacts with G-actin to increase the rate of exchange of actin-bound adenosine 5'-triphosphate. *Biochemistry*, **19**, 5359-5362.

Morimoto, R.I. (1998) Regulation of the heat shock transcriptional response: cross talk between a family of heat shock factors, molecular chaperones, and negative regulators. *Genes Dev*, **12**, 3788-3796.

Moseley, J.B. and Goode, B.L. (2006) The yeast actin cytoskeleton: from cellular function to biochemical mechanism. *Microbiol Mol Biol Rev*, **70**, 605-645.

Mullins, R.D., Heuser, J.A. and Pollard, T.D. (1998) The interaction of Arp2/3 complex with actin: nucleation, high affinity pointed end capping, and formation of branching networks of filaments. *Proc Natl Acad Sci U S A*, **95**, 6181-6186.

Naylor, D.J. and Hartl, F.U. (2001) Contribution of molecular chaperones to protein folding in the cytoplasm of prokaryotic and eukaryotic cells. *Biochem Soc Symp*, 45-68.

Netzer, W.J. and Hartl, F.U. (1997) Recombination of protein domains facilitated by co-translational folding in eukaryotes. *Nature*, **388**, 343-349.

Netzer, W.J. and Hartl, F.U. (1998) Protein folding in the cytosol: chaperonin-dependent and -independent mechanisms. *Trends Biochem Sci*, **23**, 68-73.

Nirenberg, M.W. and Matthaei, J.H. (1961) The dependence of cell-free protein synthesis in E. coli upon naturally occurring or synthetic polyribonucleotides. *Proc Natl Acad Sci U S A*, **47**, 1588-1602.

Nishihara, K., Kanemori, M., Yanagi, H. and Yura, T. (2000) Overexpression of trigger factor prevents aggregation of recombinant proteins in Escherichia coli. *Appl Environ Microbiol*, **66**, 884-889.

Nishimura, A., Morita, M., Nishimura, Y. and Sugino, Y. (1990) A rapid and highly efficient method for preparation of competent Escherichia coli cells. *Nucleic Acids Res*, **18**, 6169.

Nitsch, M., Walz, J., Typke, D., Klumpp, M., Essen, L.O. and Baumeister, W. (1998) Group II chaperonin in an open conformation examined by electron tomography. *Nat Struct Biol*, **5**, 855-857.

Norcum, M.T. (1996) Novel isolation method and structural stability of a eukaryotic chaperonin: the TCP-1 ring complex from rabbit reticulocytes. *Protein Sci*, **5**, 1366-1375.

Novick, P. and Botstein, D. (1985) Phenotypic analysis of temperature-sensitive yeast actin mutants. *Cell*, **40**, 405-416.

Onuchic, J.N. and Wolynes, P.G. (2004) Theory of protein folding. *Curr Opin Struct Biol*, **14**, 70-75.

Onuchic, J.N., Wolynes, P.G., Luthey-Schulten, Z. and Socci, N.D. (1995) Toward an outline of the topography of a realistic protein-folding funnel. *Proc Natl Acad Sci U S A*, **92**, 3626-3630.

Otzen, D.E., Itzhaki, L.S., elMasry, N.F., Jackson, S.E. and Fersht, A.R. (1994) Structure of the transition state for the folding/unfolding of the barley chymotrypsin inhibitor 2 and its implications for mechanisms of protein folding. *Proc Natl Acad Sci U S A*, **91**, 10422-10425.

Pappenberger, G., Wilsher, J.A., Roe, S.M., Counsell, D.J., Willison, K.R. and Pearl, L.H. (2002) Crystal structure of the CCTgamma apical domain: implications for substrate binding to the eukaryotic cytosolic chaperonin. *J Mol Biol*, **318**, 1367-1379.

Pardee, J.D. and Spudich, J.A. (1982) Purification of muscle actin. *Methods Enzymol*, **85 Pt B**, 164-181.

Patzelt, H., Kramer, G., Rauch, T., Schonfeld, H.J., Bukau, B. and Deuerling, E. (2002) Three-state equilibrium of Escherichia coli trigger factor. *Biol Chem*, **383**, 1611-1619.

Patzelt, H., Rudiger, S., Brehmer, D., Kramer, G., Vorderwulbecke, S., Schaffitzel, E., Waitz, A., Hesterkamp, T., Dong, L., Schneider-Mergener, J., Bukau, B. and Deuerling, E. (2001) Binding specificity of Escherichia coli trigger factor. *Proc Natl Acad Sci U S A*, **98**, 14244-14249.

Pickart, C.M. and Cohen, R.E. (2004) Proteasomes and their kin: proteases in the machine age. *Nat Rev Mol Cell Biol*, **5**, 177-187.

Pierpaoli, E.V., Sandmeier, E., Baici, A., Schonfeld, H.J., Gisler, S. and Christen, P. (1997) The power stroke of the DnaK/DnaJ/GrpE molecular chaperone system. *J Mol Biol*, **269**, 757-768.

Pollard, T.D., Blanchoin, L. and Mullins, R.D. (2000) Molecular mechanisms controlling actin filament dynamics in nonmuscle cells. *Annu Rev Biophys Biomol Struct*, **29**, 545-576.

Prasher, D.C., Eckenrode, V.K., Ward, W.W., Prendergast, F.G. and Cormier, M.J. (1992) Primary structure of the Aequorea victoria green-fluorescent protein. *Gene*, **111**, 229-233.

Ptitsyn, O.B. (1987) Protein folding: hypotheses and experiments. *J Protein Chem*, **6**, 273–293.

Ptitsyn, O.B. and Rashin, A.A. (1975) A model of myoglobin self-organization. *Biophys Chem*, **3**, 1-20.

Ramachandran, G.N. and Sasisekharan, V. (1968) Conformation of polypeptides and proteins. *Adv Protein Chem*, **23**, 283-438.

Rommelaere, H., De Neve, M., Melki, R., Vandekerckhove, J. and Ampe, C. (1999) The cytosolic class II chaperonin CCT recognizes delineated hydrophobic sequences in its target proteins. *Biochemistry*, **38**, 3246-3257.

Roobol, A. and Carden, M.J. (1993) Identification of chaperonin particles in mammalian brain cytosol and of T-complex polypeptide 1 as one of their components. *J Neurochem*, **60**, 2327-2330.

Roobol, A., Holmes, F.E., Hayes, N.V., Baines, A.J. and Carden, M.J. (1995) Cytoplasmic chaperonin complexes enter neurites developing in vitro and differ in subunit composition within single cells. *J Cell Sci*, **108 (Pt 4)**, 1477-1488.

Rudiger, S., Germeroth, L., Schneider-Mergener, J. and Bukau, B. (1997) Substrate specificity of the DnaK chaperone determined by screening cellulose-bound peptide libraries. *Embo J*, **16**, 1501-1507.

Rudiger, S., Schneider-Mergener, J. and Bukau, B. (2001) Its substrate specificity characterizes the DnaJ co-chaperone as a scanning factor for the DnaK chaperone. *Embo J*, **20**, 1042-1050.

Sambrook, J., Fritsch, E.F. and Maniatis, T. (1989) *Molecular Cloning*. Cold Spring Harbor Press, Cold Spring Harbor, NY.

Schagger, H. and von Jagow, G. (1991) Blue native electrophoresis for isolation of membrane protein complexes in enzymatically active form. *Anal Biochem*, **199**, 223-231.

Schechter, A.N., Chen, R.F. and Anfinsen, C.B. (1970) Kinetics of folding of staphylococcal nuclease. *Science*, **167**, 886-887.

Schellman, J.A. (1955) The stability of hydrogen-bonded peptide structures in aqueous solution. *C R Trav Lab Carlsberg [Chim]*, **29**, 230-259.

Schlunzen, F., Wilson, D.N., Tian, P., Harms, J.M., McInnes, S.J., Hansen, H.A., Albrecht, R., Buerger, J., Wilbanks, S.M. and Fucini, P. (2005) The binding mode of the trigger factor on the ribosome: implications for protein folding and SRP interaction. *Structure*, **13**, 1685-1694.

Schmid, F.X., Mayr, L.M., Mucke, M. and Schonbrunner, E.R. (1993) Prolyl isomerases: role in protein folding. *Adv Protein Chem*, **44**, 25-66.

Scholz, C., Stoller, G., Zarnt, T., Fischer, G. and Schmid, F.X. (1997) Cooperation of enzymatic and chaperone functions of trigger factor in the catalysis of protein folding. *Embo J*, **16**, 54-58.

Schroder, H., Langer, T., Hartl, F.U. and Bukau, B. (1993) DnaK, DnaJ and GrpE form a cellular chaperone machinery capable of repairing heat-induced protein damage. *Embo J*, **12**, 4137-4144.

Schultz, C.P. (2000) Illuminating folding intermediates. *Nat Struct Biol*, **7**, 7-10.

Shaner, N.C., Campbell, R.E., Steinbach, P.A., Giepmans, B.N., Palmer, A.E. and Tsien, R.Y. (2004) Improved monomeric red, orange and yellow fluorescent proteins derived from Discosoma sp. red fluorescent protein. *Nat Biotechnol*, **22**, 1567-1572.

Siegers, K., Bolter, B., Schwarz, J.P., Bottcher, U.M., Guha, S. and Hartl, F.U. (2003) TRiC/CCT cooperates with different upstream chaperones in the folding of distinct protein classes. *Embo J*, **22**, 5230-5240.

Siegers, K., Waldmann, T., Leroux, M.R., Grein, K., Shevchenko, A., Schiebel, E. and Hartl, F.U. (1999) Compartmentation of protein folding in vivo: sequestration of non-native polypeptide by the chaperonin-GimC system. *Embo J*, **18**, 75-84.

Siegert, R., Leroux, M.R., Scheufler, C., Hartl, F.U. and Moarefi, I. (2000) Structure of the molecular chaperone prefoldin: unique interaction of multiple coiled coil tentacles with unfolded proteins. *Cell*, **103**, 621-632.

Sigler, P.B., Xu, Z., Rye, H.S., Burston, S.G., Fenton, W.A. and Horwich, A.L. (1998) Structure and function in GroEL-mediated protein folding. *Annu Rev Biochem*, **67**, 581-608.

Sikorski, R.S. and Hieter, P. (1989) A system of shuttle vectors and yeast host strains designed for efficient manipulation of DNA in Saccharomyces cerevisiae. *Genetics*, **122**, 19-27.

Simpson, J.C., Wellenreuther, R., Poustka, A., Pepperkok, R. and Wiemann, S. (2000) Systematic subcellular localization of novel proteins identified by large-scale cDNA sequencing. *EMBO Rep*, **1**, 287-292.

Slavotinek, A.M., Stone, E.M., Mykytyn, K., Heckenlively, J.R., Green, J.S., Heon, E., Musarella, M.A., Parfrey, P.S., Sheffield, V.C. and Biesecker, L.G. (2000) Mutations in MKKS cause Bardet-Biedl syndrome. *Nat Genet*, **26**, 15-16.

Smith, T.F., Gaitatzes, C., Saxena, K. and Neer, E.J. (1999) The WD repeat: a common architecture for diverse functions. *Trends Biochem Sci*, **24**, 181-185.

Spiess, C., Meyer, A.S., Reissmann, S. and Frydman, J. (2004) Mechanism of the eukaryotic chaperonin: protein folding in the chamber of secrets. *Trends Cell Biol*, **14**, 598-604.

Spiess, C., Miller, E.J., McClellan, A.J. and Frydman, J. (2006) Identification of the TRiC/CCT Substrate Binding Sites Uncovers the Function of Subunit Diversity in Eukaryotic Chaperonins. *Mol Cell*, **24**, 25-37.

Spirin, A.S. (2004) High-throughput cell-free systems for synthesis of functionally active proteins. *Trends Biotechnol*, **22**, 538-545.

Stearns, T. (1995) Green fluorescent protein. The green revolution. *Curr Biol*, **5**, 262-264.

Steinmetz, M.O., Stoffler, D., Muller, S.A., Jahn, W., Wolpensinger, B., Goldie, K.N., Engel, A., Faulstich, H. and Aebi, U. (1998) Evaluating atomic models of F-actin with an undecagold-tagged phalloidin derivative. *J Mol Biol*, **276**, 1-6.

Stone, D.L., Slavotinek, A., Bouffard, G.G., Banerjee-Basu, S., Baxevanis, A.D., Barr, M. and Biesecker, L.G. (2000) Mutation of a gene encoding a putative chaperonin causes McKusick-Kaufman syndrome. *Nat Genet*, **25**, 79-82.

Sunde, M. and Blake, C. (1997) The structure of amyloid fibrils by electron microscopy and X-ray diffraction. *Adv Protein Chem*, **50**, 123-159.

Szabo, A., Langer, T., Schroder, H., Flanagan, J., Bukau, B. and Hartl, F.U. (1994) The ATP hydrolysis-dependent reaction cycle of the Escherichia coli Hsp70 system DnaK, DnaJ, and GrpE. *Proc Natl Acad Sci U S A*, **91**, 10345-10349.

Tanford, C. (1962) Contribution of Hydrophobic Interactions to the Stability of the Globular Conformation of Proteins. *J. Am. Chem. Soc.*, **84**, 4240 - 4247.

Terada, K., Kanazawa, M., Bukau, B. and Mori, M. (1997) The human DnaJ homologue dj2 facilitates mitochondrial protein import and luciferase refolding. *J Cell Biol*, **139**, 1089-1095.

Teter, S.A., Houry, W.A., Ang, D., Tradler, T., Rockabrand, D., Fischer, G., Blum, P., Georgopoulos, C. and Hartl, F.U. (1999) Polypeptide flux through bacterial Hsp70: DnaK cooperates with trigger factor in chaperoning nascent chains. *Cell*, **97**, 755-765.

Thomas, J.G. and Baneyx, F. (1996) Protein misfolding and inclusion body formation in recombinant Escherichia coli cells overexpressing Heat-shock proteins. *J Biol Chem*, **271**, 11141-11147.

Thomas, P.J., Qu, B.H. and Pedersen, P.L. (1995) Defective protein folding as a basis of human disease. *Trends Biochem Sci*, **20**, 456-459.

Thulasiraman, V., Yang, C.F. and Frydman, J. (1999) In vivo newly translated polypeptides are sequestered in a protected folding environment. *Embo J*, **18**, 85-95.

Tian, G., Vainberg, I.E., Tap, W.D., Lewis, S.A. and Cowan, N.J. (1995) Specificity in chaperonin-mediated protein folding. *Nature*, **375**, 250-253.

Tomic, S., Johnson, A.E., Hartl, F.U. and Etchells, S.A. (2006) Exploring the capacity of trigger factor to function as a shield for ribosome bound polypeptide chains. *FEBS Lett*, **580**, 72-76.

Ullers, R.S., Luirink, J., Harms, N., Schwager, F., Georgopoulos, C. and Genevaux, P. (2004) SecB is a bona fide generalized chaperone in Escherichia coli. *Proc Natl Acad Sci U S A*, **101**, 7583-7588.

Ursic, D., Sedbrook, J.C., Himmel, K.L. and Culbertson, M.R. (1994) The essential yeast Tcp1 protein affects actin and microtubules. *Mol Biol Cell*, **5**, 1065-1080.

Vainberg, I.E., Lewis, S.A., Rommelaere, H., Ampe, C., Vandekerckhove, J., Klein, H.L. and Cowan, N.J. (1998) Prefoldin, a chaperone that delivers unfolded proteins to cytosolic chaperonin. *Cell*, **93**, 863-873.

Valent, Q.A., de Gier, J.W., von Heijne, G., Kendall, D.A., ten Hagen-Jongman, C.M., Oudega, B. and Luirink, J. (1997) Nascent membrane and presecretory proteins synthesized in Escherichia coli associate with signal recognition particle and trigger factor. *Mol Microbiol*, **25**, 53-64.

Valent, Q.A., Kendall, D.A., High, S., Kusters, R., Oudega, B. and Luirink, J. (1995) Early events in preprotein recognition in E. coli: interaction of SRP and trigger factor with nascent polypeptides. *Embo J*, **14**, 5494-5505.

Vandekerckhove, J., Deboben, A., Nassal, M. and Wieland, T. (1985) The phalloidin binding site of F-actin. *Embo J*, **4**, 2815-2818.

Vendruscolo, M. and Dobson, C.M. (2005) Towards complete descriptions of the free-energy landscapes of proteins. *Philos Transact A Math Phys Eng Sci*, **363**, 433-450; discussion 450-432.

Vorderwulbecke, S., Kramer, G., Merz, F., Kurz, T.A., Rauch, T., Zachmann-Brand, B., Bukau, B. and Deuerling, E. (2004) Low temperature or GroEL/ES overproduction permits growth of Escherichia coli cells lacking trigger factor and DnaK. *FEBS Lett*, **559**, 181-187.

Waldo, G.S., Standish, B.M., Berendzen, J. and Terwilliger, T.C. (1999) Rapid protein-folding assay using green fluorescent protein. *Nat Biotechnol*, **17**, 691-695.

Wegner, A. and Isenberg, G. (1983) 12-fold difference between the critical monomer concentrations of the two ends of actin filaments in physiological salt conditions. *Proc Natl Acad Sci U S A*, **80**, 4922-4925.

Wetlaufer, D.B. (1973) Nucleation, rapid folding, and globular intrachain regions in proteins. *Proc Natl Acad Sci U S A*, **70**, 697-701.

Willison, K.R., Hynes, G., Davies, P., Goldsborough, A. and Lewis, V.A. (1990) Expression of three t-complex genes, Tcp-1, D17Leh117c3, and D17Leh66, in purified murine spermatogenic cell populations. *Genet Res*, **56**, 193-201.

Wolynes, P.G., Onuchic, J.N. and Thirumalai, D. (1995) Navigating the folding routes. *Science*, **267**, 1619-1620.

Won, K.A., Schumacher, R.J., Farr, G.W., Horwich, A.L. and Reed, S.I. (1998) Maturation of human cyclin E requires the function of eukaryotic chaperonin CCT. *Mol Cell Biol*, **18**, 7584-7589.

Xu, Z., Horwich, A.L. and Sigler, P.B. (1997) The crystal structure of the asymmetric GroEL-GroES-(ADP)7 chaperonin complex. *Nature*, **388**, 741-750.

Yaffe, M.B., Farr, G.W., Miklos, D., Horwich, A.L., Sternlicht, M.L. and Sternlicht, H. (1992) TCP1 complex is a molecular chaperone in tubulin biogenesis. *Nature*, **358**, 245-248.

Yang, H.C. and Pon, L.A. (2002) Actin cable dynamics in budding yeast. *Proc Natl Acad Sci U S A*, **99**, 751-756.

Young, J.C., Agashe, V.R., Siegers, K. and Hartl, F.U. (2004) Pathways of chaperone-mediated protein folding in the cytosol. *Nat Rev Mol Cell Biol*, **5**, 781-791.

Zhu, X., Zhao, X., Burkholder, W.F., Gragerov, A., Ogata, C.M., Gottesman, M.E. and Hendrickson, W.A. (1996) Structural analysis of substrate binding by the molecular chaperone DnaK. *Science*, **272**, 1606-1614.

Zimmerman, S.B. and Minton, A.P. (1993) Macromolecular crowding: biochemical, biophysical, and physiological consequences. *Annu Rev Biophys Biomol Struct*, **22**, 27-65.

Zimmerman, S.B. and Trach, S.O. (1991) Estimation of macromolecule concentrations and excluded volume effects for the cytoplasm of Escherichia coli. *Journal of Molecular Biology*, **222**, 599-620.

Zylicz, M., Yamamoto, T., McKittrick, N., Sell, S. and Georgopoulos, C. (1985) Purification and properties of the dnaJ replication protein of Escherichia coli. *J Biol Chem*, **260**, 7591-7598.

6 Abbreviations

Units are expressed according to the international system of units (SI), including outside units accepted for use with the SI. Amino acids are abbreviated with their one or three letter symbols.

ADP	adenosine 5'-diphosphate
AG	actin-GFP fusion protein (→ GFP)
ATP	adenosine 5'-triphosphate
AU	arbitrary unit
bp	base pair
BAG	BFP-actin-GFP fusion protein (→ BFP; → GFP)
BFP	blue fluorescent protein
BG	BFP-GFP fusion protein (→ BFP; → GFP)
β-gal	β-galactosidase
BTAG	BAG containing a TEV-cleavage site (→ BAG; → TEV)
CAG	mCherry-actin-GFP fusion protein (→ GFP)
Cα	alpha carbon atom
CCT	chaperonin containing TCP1 (→ TRiC)
CDTA	*trans*-1,2-diaminocyclohexane-*N,N,N',N'*-tetraacetic acid
CECF	continuous exchange cell-free
CG	mCherry-GFP fusion protein (→ GFP)
CIP	calf intestinal alkaline phosphatase
cryo-EM	cryoelectron microscopy
C-terminus	carboxy-terminus
Da	Dalton
DMSO	dimethylsulfoxid
DNA	deoxyribonucleic acid
DNase I	deoxyribonuclease I
dNTP	didesoxy-nucleoside triphosphate
DTT	dithiothreitol
E	GrpE (bacterial nucleotide exchange factor of DnaK; → K)
ECL	enhance chemiluminescence
E. coli	*Escherichia coli*
EDTA	ethylenediaminetetraacetic acid
EGTA	glycol-bis(2-aminoethylether)-*N,N,N',N'*-tetraacetic acid

EL	GroEL (bacterial Hsp60 chaperonin)
ES	GroES (bacterial Hsp10 co-chaperonin)
F-actin	filamentous actin
FL	firefly luciferase
FPLC	fast performance liquid chromatography
g	acceleration of gravity, 9.81 m/s^2
GA	GFP-actin fusion protein (→ GFP)
G-actin	monomeric actin
GdnHCl	guanidinium hydrochloride
GFP	green fluorescent protein
GimC	genes involved in microtubule biogenesis complex (→ PFD)
HEPES	N-(2-hydroxyethyl)piperazine-N'-2-ethanesulfonic acid
HMW	high molecular weight
HRP	horseradish peroxidase
Hsp	heat shock proteins
HU	high urea
HY	high yield
IB	inclusion body
IPTG	isopropyl-β-D-1-thiogalactopyranoside
J	DnaJ (bacterial Hsp40 chaperone)
K	DnaK (bacterial Hsp70 chaperone)
KJE	DnaK, DnaJ, and GrpE (→ E; → J; → K)
LB	Luria Bertani
LMW	low molecular weight
mCherry	monomeric Cherry
MOPS	3-(N-morpholino)propanesulfonic acid
MW	molecular weight
MWCO	MW cut-off (→ MW)
mRNA	messenger RNA
NAC	nascent chain-associated complex
Ni-NTA	nickel-nitrilotriacetic acid
N-terminus	amino-terminus
OD	optical density
PAGE	polyacrylamide gel electrophoresis
PBS	phosphate-buffered saline
PCR	polymerase chain reaction
PDI	protein disulfide isomerase
PEG	polyethylene glycol
PFD	prefoldin (→ GimC)

pH	reverse logarithm of relative hydrogen proton (H^+) concentration
Pi	inorganic phosphate
PMSF	phenylmethylsulfonyl fluoride
PPIase	peptidyl-prolyl *cis/trans* isomerase
PK	Proteinase K
RAC	ribosome-associate complex
RNA	ribonucleic acid
RNase A	ribonuclease A
rPh	rhodamine-phalloidin
RRL	rabbit reticulocyte lysate
RT	room temperature
RTS	rapid translation system
[^{35}S]	sulfur isotope
S30	soluble cell lysate fraction when centrifuged at 30,000 *g*
SC	synthetic complete
S. cerevisiae	*Saccharomyces cerevisiae*
SDS	sodiumdodecylsulfate
sHsp	small heat shock protein
TAE	Tris-acetate-EDTA (→ EDTA; → Tris)
TBS	Tris-buffered saline (→ Tris)
TBS-T	TBS containing Tween20 (→ TBS; → Tween20)
TCA	trichloroacetic acid
TE	Tris-EDTA (→ EDTA; → Tris)
TEMED	*N,N,N',N'*-tetramethylethylenediamine
TEV	Tobacco Etch Virus
TF	trigger factor
$TF_{FRK/AAA}$	TF with residues $_{44}$FRK$_{46}$ replaced by alanines (→ TF)
TNT	coupled transcription and translation
TRiC	TCP1 ring complex (→ CCT)
Tris	tris(hydroxymethyl)aminomethane
TritonX-100	octyl phenol ethoxylate
Tween20	polyoxyethylen-sorbitan-monolaurate
UV/VIS	ultraviolet/visible
VHL	Von Hippel-Lindau tumor suppressor protein
v/v	volume/volume
WG	wheat germ
w/v	weight/volume
YPD	medium containing yeast extract, peptone, and dextrose